Charles University

Faculty of Science

Study programme: Biology

Branch of study: Genetics, molecular biology and virology

Bc. Helena Caisová

Analysis of serological cross-reactivity between antibodies against BK polyomavirus variants

Analýza zkřížené sérologické reaktivity protilátek proti variantám BK polyomaviru

DIPLOMA THESIS

Supervisor: RNDr. Lenka Horníková, Ph.D.

Prague 2023

Svoluji k zapůjčení své diplomové práce ke studijním účelům a prosím, aby byla vedena přesná evidence vypůjčovatelů. Převzaté údaje je vypůjčovatel povinen řádně citovat.

Prohlašuji, že jsem tuto diplomovou práci vypracovala samostatně a výhradně s použitím citovaných pramenů, literatury a dalších odborných zdrojů. Tato práce ani její podstatná část nebyla předložena k získání jiného nebo stejného akademického titulu.

V Praze, dne ....

Podpis autora

Děkuji své vedoucí diplomové práce RNDr. Lence Horníkové, Ph.D. za vlídné přijetí do laboratoře a také za pozitivní přístup, klid a vstřícnost, kterými mne provázela nejen při experimetnální práci. Také velmi děkuji svým konzultantkám RNDr. Haně Španielové, Ph.D. a Mgr. et Mgr. Alžbětě Hejtmánkové za předání cenných rad a zkušeností na počátku i v průběhu celého mého studia. Srdečné děkuji patří i Mgr. Janě Váňové, a to jak za zaučení v laboratoři, tak za životní inspiraci. Dále děkuji doc. RNDr. Jitce Forstové, CSc. a všem členům laboratoře za příjemnou atmosféru a za poskytnutí potřebného materiálu. Na závěr bych chtěla vyjádřit velké díky mé rodině a přátelům, kteří mi byli podporou po celou dobu mého studia, zejména Davidovi Vokrouhlickému za trpělivost a technickou pomoc.

Tento diplomový projekt vznikl v letech 2020-2023 za podpory Univerzity Karlovy (GA UK, číslo projektu: 1294120).

Abstrakt: BK polyomavirus (BKPyV), který asymptomaticky infikuje zhruba 80 % lidské populace, se může reaktivovat u imunosuprimovaných pacientů po transplantaci ledviny a způsobit nefropatii. V evropské populaci kolují nejčastěji dva subtypy BKPyV, BKPyV-I a BKPyV-IV, které se chovají jako odlišné sérotypy. Ukazuje se, že recipienti, kteří přijímají ledvinu od dárce pozitivního na jiný BKPyV subtyp, mají větší riziko odmítnutí štěpu. Jen pomocí sérologického testu ELISA ale nelze rozhodnout, zda je pacient infikován subtypem BKPyV-I či BKPyV-IV, jelikož protilátková odpověď proti těmto dvěma subtypům je zkřížená. Tato práce si kladla za cíl identifikovat epitopy na hlavním antigenním proteinu VP1, které jsou zodpovědné za vazbu křížově reagujících a/nebo subtypově specifických protilátek. Identifikace takových epitopů by mohla dále vést ke zlepšení pretransplantační diagnostiky a lepšímu managementu pacientů po transplantaci. Proto byly připraveny dva typy antigenů složené z VP1 proteinu subtypu BKPyV-IV se zavedenými mutacemi charakteristickými pro BKPyV-I v DE a EF smyčce VP1, které byly otestovány pomocí kompetiční eseje na panelu lidských sér. Výsledky ukázaly, že oblast DE smyčky je imunogenní epitop, který váže specifické protilátky pro subtyp I. Naopak mutace v EF smyčce porušily epitop, který je obecně rozeznávaný protilátkami.

Dalším cílem této práce bylo také zjistit, zda se mutace ve VP1 podílí na zhoršeném průběhu patologie, která je asociovaná s BKPyV. Bioinformatickou analýzou VP1 sekvencí (n = 505) pocházejících od pacientů s různým stupněm patologie, se podařilo ukázat, že by subtyp BKPyV-IV mohl být spojen s menším rizikem vzniku patologie. Dále byly také identifikovány místa ve VP1 proteinu, na které působí pozitivní selekce. Pozitivně selektované aminokyselinové mutace byly zastoupeny rovnoměrně ve všech pacientských skupinách, a proto pravděpodobně nesouvisí s rozvojem patologie na populační úrovni.

Klíčová slova: BK polyomavirus, BKPyV-I, BKPyV-IV, sérologie, ELISA, transplantace ledvin

Abstract: BK polyomavirus (BKPyV), which asymptomatically infects about 80 % of the human population, can reactivate in immunosuppressed patients after kidney transplantation and cause nephropathy. In the European population, there are predominantly two BKPyV subtypes, BKPyV-I and BKPyV-IV, which behave as different serotypes. Recipients who receive a kidney from a donor positive for a different subtype are at a greater risk of graft rejection. So far, it is impossible to distinguish between these two subtypes using a serological ELISA test as serum antibodies against these two subtypes cross-react. This work aimed to identify epitopes on the major antigenic protein VP1, which are responsible for the binding of cross-reacting and/or subtype-specific antibodies. The identification of such epitopes could further lead to improvement in pre-transplant diagnostics and better management of patients after transplantation. Therefore, two types of antigens composed of the VP1 protein of the BKPyV-IV subtype with introduced mutations characteristic of BKPyV-I in the DE and EF loops of VP1 were prepared and tested using an antigen competition assay with a panel of human sera. The results showed that the DE loop region is an immunogenic epitope that binds specific antibodies for BKPyV subtype I. Conversely, a mutation in the EF loop disrupted the epitope recognized by antibodies in general.

This work also aimed to investigate the impact of VP1 mutations on pathology associated with BKPyV. Using bioinformatic analysis of VP1 sequences (n = 505), which originated from patients with different clinical statuses, it was shown that the BKPyV-IV subtype could be associated with a lower risk of disease progression. Furthermore, sites in the VP1 protein affected by positive selection were also identified. However, mutated amino acids at these sites were represented equally in all patient groups and are, therefore, probably not related to the development of pathology at the population level.

Keywords: BK polyomavirus, BKPyV-I, BKPyV-IV, serology, ELISA, kidney transplantation

Contents

List of frequently used abbreviations

ACA	antigen competition assay
BKPyV	BK polyomavirus
BKPyV-IV-DEmut	pseudovirion BKV-IV with mutated DE loop
BKPyV-IV-EFmut	pseudovirion BKV-IV with mutated EF loop
BKPyVAN	BK polyomavirus-associated nephropathy
ELISA	enzyme-linked immunosorbent assay
EGFP	enhanced green fluorescent protein
EM	electron microscopy
GST	glutathione S-transferase
JCPyV	JC polyomavirus
Ktx	kidney transplant
MPyV	mouse polyomavirus
MCPyV	Merkel cell polyomavirus
NAb	neutralizing antibody
NCBI	National Center for Biotechnology Information
NCCR	non-coding control region
PsV	pseudovirion
PyV	polyomavirus
RCF	relative centrifugal force
SDS-PAGE	sodium dodecyl sulphate–polyacrylamide gel electrophoresis
VLP	virus-like particle
VP1, 2, 3	viral protein 1, 2, 3

Introduction

Serological studies indicate that nearly 80% of the human population is seropositive for BK polyomavirus (BKPyV). This virus usually causes a common childhood infection with minimal clinical implications. Later during human life, BKPyV remains clinically silent and persists in the kidneys. However, it can reactivate in times of immunological impairment, causing nephropathy mainly in kidney transplant (KTx) recipients. In Europe, there are predominantly two BKPyV subtypes, BKPyV-I and IV. It has been shown that humoral immunity against one subtype does not protect against the infection caused by the other subtype. Consequently, the most vulnerable group of patients are mainly those KTx recipients paired with donors positive for different BKPyV subtypes. In such a case, the donor's kidney serves as a potential virus reservoir which is ready to replicate in an immunosuppressed recipient who lacks protective neutralizing antibodies.

Currently, there are no effective antivirals against BKPyV infection, and the only management of virus reactivation is the reduction of immunosuppression. On the other hand, this approach can lead to graft rejection. Therefore, the balance between those two states is very challenging, and screening donors and KTx recipients for BKPyV subtype-specific seropositivity could provide a reliable pretransplant predictive marker. However, BKPyV diagnosis is not routinely performed mainly because there is so far no easy serological test to determine between BKPyV subtypes which would be suitable for clinical practice.

In this thesis, we followed up on previous projects conducted in our laboratory, which focused on improving BKPyV subtype-specific diagnostics using ELISA. The biggest obstacle when using this assay to determine between BKPyV subtypes is the cross-reactivity of serum antibodies. One possibility how to eliminate this cross-reactivity is to perform an antigen competition assay (ACA). ACA is based on the saturation of serum samples with homologous (competing) antigens, and the remaining antibodies are later detected using ELISA. ACA was already shown to serve as a confirmation test when testing seropositivity of closely relative JC polyomavirus as it eliminates potential cross-reactivity with BKPyV. However, there are only two studies in which the authors used this method to differentiate between BKPyV subtypes, and both concluded that it needs further optimizations.

It is assumed that different antigenic potentials of BKPyV subtypes are given by the structure of the major structural protein (VP1). BKPyV subtypes have a distinct composition of amino acids exposed on the capsid surface. Specifically, these subtype differences cluster mainly in three surface-exposed loops of VP1: BC, DE and EF loop. Previously in our laboratory, Tomanová (2019) targeted DE and EF loops and created two antigens with the potential to saturate serum antibodies in ACA. This thesis aims to test these antigens with the panel of human serum samples from KTx recipients, some of which have known

origins of past BKPyV infection, and thus evaluate the role of DE and EF loop of VP1 in cross-reactivity against BKPyV subtypes I and IV. Identifying epitopes with binding either subtype-specific or cross-reactive antibodies could potentially contribute to the development of a more reliable diagnostic test.

Furthermore, it was shown that the accumulation of BKPyV VP1 mutations is not exceptional. For other polyomaviruses, it is well documented that some specific mutations in VP1 change the viral tropism, which results in increased pathological potentials. Therefore, we aimed to investigate the evolution pressure in VP1, focusing mainly on less explored VP1 loops, DE and EF. Also, different BPyV subtypes have been proposed to have a higher ability to cause nephropathy, which is further investigated in this work.

1. Literature review

1.1 Polyomaviruses

Polyomaviruses (PyVs) are widespread, primarily found in mammals and birds, causing severe illness and death on an epidemic scale. The first PyV was discovered in 1953, and this virus was named due to its ability to cause neoplasms in experimental animals. Polyoma is assembled from two words: poly-, meaning many or much, and -oma, meaning tumours. Since now, many members of the *Polyomaviridae* family have been shown to have oncogenic potential in animals. However, only one representative out of 14 human PyVs has been associated with human cancer.

In the human population, PyVs cause an asymptomatic infection usually acquired in childhood. However, severe illness can appear in immunocompromised individuals. The presently well-known human PyVs are BK (BKPyV, isolated from a patient with the initials BK) virus, JC polyomavirus (JCPyV, isolated from a patient with the initials JC) virus and Merkel cell polyomavirus (MCPyV). Immunodeficiency or immunosuppression allows these viruses to reactivate. In such a case, BKPyV causes an opportunistic infection of the kidneys, which may result in nephropathy. JCPyV can cause brain disease, known as progressive multifocal leukoencephalopathy, and MCPyV is associated with a rare skin cancer called Merkel cell carcinoma (Carter et al., 2009).

1.1.1 Genome structure

Polyomaviruses are small viruses with a double-stranded closed-circular DNA genome. DNA of approximately 5,200 bp is associated with host histones H2A, H2B, H3 and H4 (Fareed and Davoli, 1977) and forms a structure called minichromosome. The genome sequence may be divided into three functional regions: early, late, and regulatory. The early region is expressed before the DNA replication and encodes large, middle and small T antigens in the case of rodent viruses, e.g. mouse polyomavirus (MPyV). The "T" in T antigen comes from the ability of these proteins to induce tumours (Black et al., 1963) as T antigens participate in many processes during the virus cycle; however, they also interact with host cell factors. Large T antigen of many PyVs binds directly to tumour suppressor p53 (or the DNA-binding domain of p53), whereas large T antigen of all known PyVs binds tumour suppressors proteins from the retinoblastoma family (pRb, p107 and p130; reviewed in Knipe and Howley, 2013). Human PyVs (BKPyV, JCPyV and MCPyV) lack the middle T antigen and express only large and small T antigens. Both middle and small T antigen binds the cellular protein phosphatase 2A as well as many other proteins involved in signal transduction (Pallas et al., 1990). Furthermore, an additional T antigen was identified in the

nucleus of BKPyV-transformed or lytically infected cells (Abend et al., 2009). Because this antigen is expressed after alternative splicing of mRNA for large T antigen (TAg), it was called truncated TAg. The late region encodes structural viral proteins and, in the case of human and simian PyVs, agnoprotein, a protein with multiple functions in the virus life cycle (reviewed in Gerits and Moens, 2012). The regulatory region also called the non-coding control region (NCCR), controls DNA replication and RNA transcription. The regulatory sequence includes the origin of replication and promotors for early and late transcription. For the detailed genomic structure of BKPyV, see Figure 1.1.

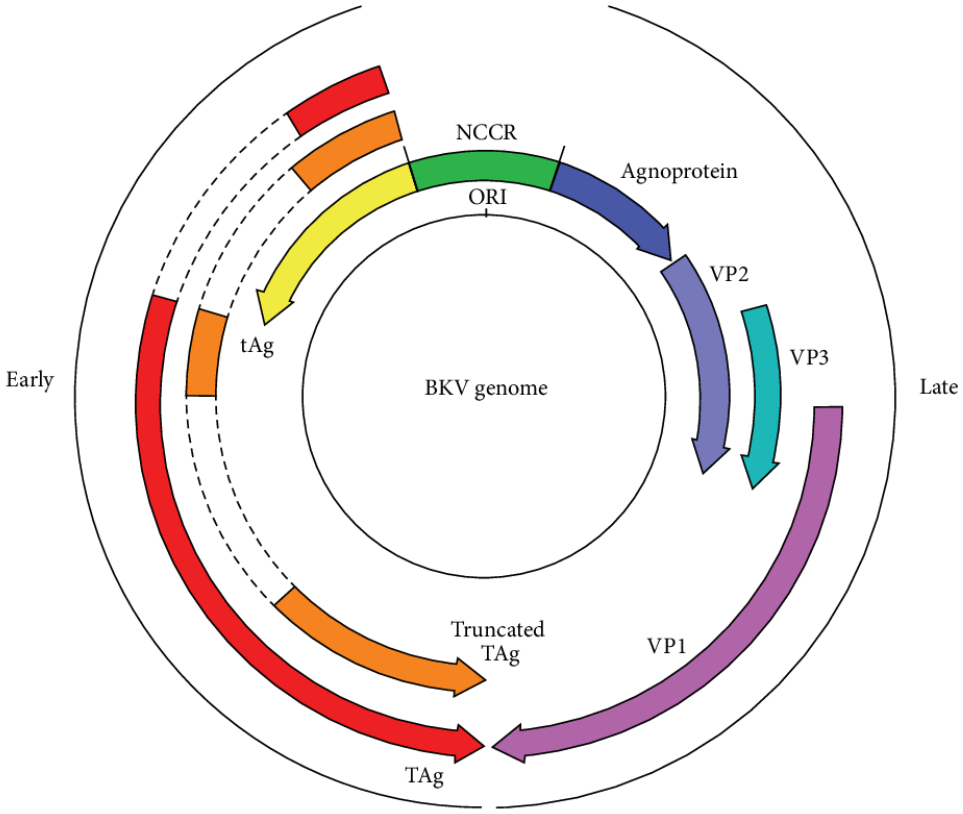

Figure 1.1: The schematic structure of the BKPyV DNA. The genome is divided into three regions: regulatory (non-coding control region - NCCR), early and late. NCCR contains the origin of replication (ORI) and promotors for both early and late transcripts (highlighted by arrows). Dashed lines represent alternative splicing events. The early region encodes large T antigen (TAg), small T antigen (tAg) and truncated T antigen (tAg), while the late region encodes the structural proteins (VP1, VP2 and VP3) and agnoprotein. This figure was adapted from De Gascun and Carr (2013).

1.1.2 Virion structure

Polyomaviruses are non-enveloped viruses. Their genome is covered by a capsid with icosahedral symmetry (40-50 nm in diameter), which is composed of viral protein 1 (VP1), VP2 and VP3 (see Figure 1.2). The major protein VP1 is arranged in 72 pentamers, each containing five molecules of VP1 and one molecule of minor protein VP2 or VP3. Only VP1 is exposed on the capsid surface; VP2 and VP3 are hidden inside. VP1 pentamers form

pentavalent and hexavalent contacts as 12 pentamers neighbour with five pentamers and 60 pentamers neighbour with 6 pentamers. (Knipe and Howley, 2013)

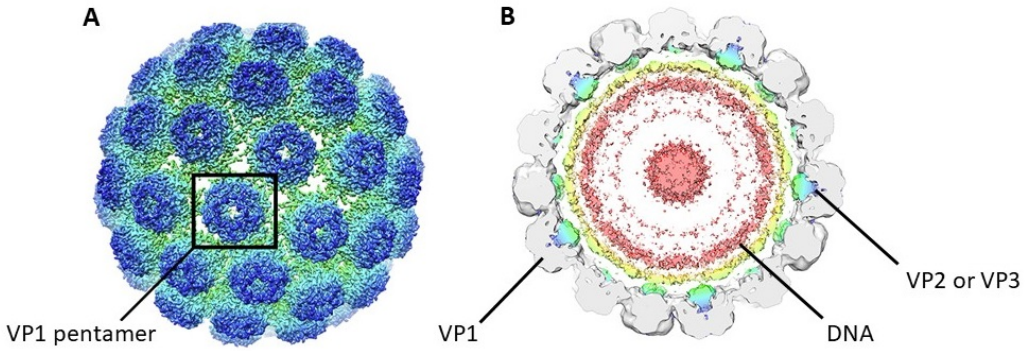

Figure 1.2: Representation of the cryo-electron microscopy structure of BK virus, showing A) a 2-fold external view (adapted from Hurdiss et al., 2018) and B) a cross-section through the virion showing minor proteins VP2 or VP3 and viral DNA (adapted from Hurdiss et al., 2016).

The capsid of PyVs consists of 360 molecules of VP1 and acts as the main antigen (stimulates antibody response). VP1 monomer of BKPyV, which is shown in Figure 1.3, is 362 amino acids long and contains four surface-exposed loops - BC, DE, EF a HI (Stehle et al., 1996).

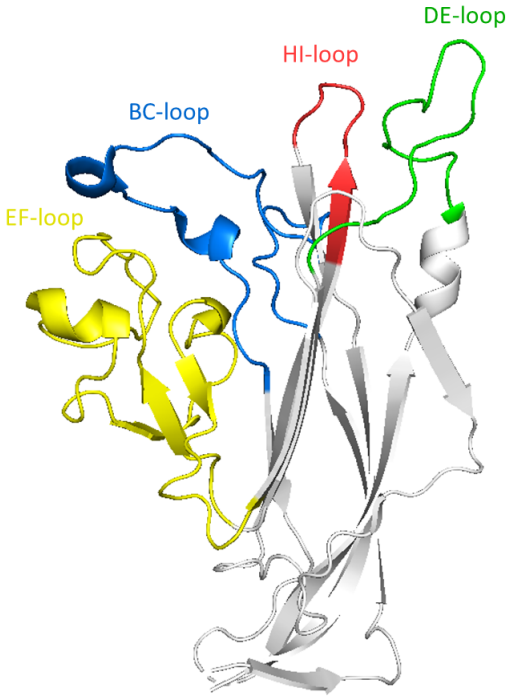

Figure 1.3: The surface-exposed loops of the VP1 protein monomer: BC loop (blue), DE loop (green), EF loop (yellow) and HI loop (red). The figure was based on the structure published by Neu et al. (2013) (RCSB protein data bank, entry code 4MJ1) and created using PyMOL software.

1.1.3 Replication cycle

The first step in the polyomavirus replication cycle is attachment to the host cell surface. PyVs engage various amino acid residues in VP1 to interact with distinct surface molecules, including sialic acid-containing receptors (glycoproteins or glycolipids) or glycosaminoglycans and integrins (reviewed in Mayberry and Maginnis, 2020). The nature of this interaction is important as it further determines host cell tropism (Neu et al., 2011; Gorelik et al., 2011; Neu et al., 2013; Ströh et al., 2015). Virus attachment to the cell induces signalling pathways leading to the next step of the virus replication cycle: cell entry. PyVs use a broad spectrum of entry pathways, including caveolin-, clathrin- and lipid raft-mediated endocytosis. However, PyVs were also shown to be hidden inside extracellular vesicles, which normally transport material and mediate communication between neighbouring cells (Morris-Love et al., 2019; Handala et al., 2020). After the internalization, all PyVs are targeted through early and late endosomes to the endoplasmic reticulum (ER), where the virus capsid begins to disassemble. Partial disassembly of the virus capsid leads to the exposure of minor proteins VP2 and VP3 with viroporin activity (Daniels et al., 2006b). This process is vital to overcome the ER membrane and escape into cytosol (Daniels et al., 2006a; Huérfano et al., 2017), which is followed by the translocation of the PyV genome through nucleopore into the cell nucleus (Soldatova et al., 2018; reviewed in Horníková et al., 2020). Once inside the nucleus, transcription of the early region, followed by viral DNA replication and late region transcription, is initiated. New virus progeny were shown to assemble in the nucleus (Erickson et al., 2012); however, the mode of their release from the cell is not very well understood.

1.2 BK polyomavirus

BKPyV, the member of the *Polymoviridae* family, was first isolated from a patient's urine after renal transplantation in 1971 (Gardner et al., 1971). BKPyV is a ubiquitous pathogen as more than 80% of humans are seropositive for this virus (Egli et al., 2009). Primary BKPyV infection usually occurs in the first decade of human life and is clinically insignificant or manifests as a mild respiratory infection (Stolt et al., 2003). After this primary phase, the virus predominantly establishes a life-long chronic infection of the urogenital tract, renal tubular and uroepithelial cells (Chesters et al., 1983; Boldorini et al., 2005), which is accompanied by episodic viral shedding in urine (viruria). BKPyV viruria is detected in 7 - 44 % of samples from immunocompetent individuals (Egli et al., 2009; Kling et al., 2012) and gradually increases with age (Zhong et al., 2007). Higher frequencies of BKPyV viruria are detected in immunosuppressed individuals and pregnant women (Bressollette-Bodin et al., 2005; Mcclure et al., 2012). The clinical course of BKPyV infection is shown in Figure 1.4.

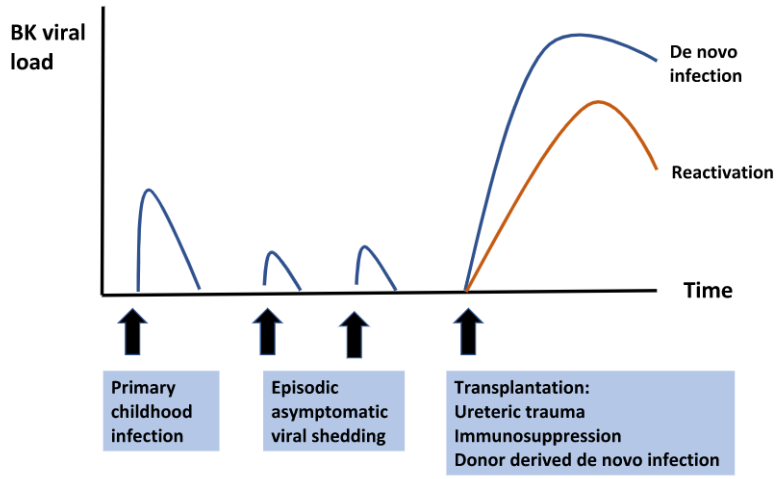

Figure 1.4: The schematic representation of the clinical course of BKPyV infection. Primary infection occurs in the first decade of human life, remaining clinically silent. From time to time, the virus's presence can be detected in the urine; however, the infection is still asymptomatic. BKPyV reactivation and consequent higher viral loads in blood appear only in patients with disrupted immunity, affecting mostly KTx and stem cell recipients. Some predictive markers for BKPyV pathology have been observed, e.g., donor-derived *de novo* infection. This figure was adapted from Chong et al. (2019).

1.2.1 Subtypes and serotypes

The study of Knowles et al. (1989) first proposed a typing scheme for BKPyV. This particular scheme was based on three characteristics of BKPyV isolates studied by the following methods: restriction digestion, haemagglutination and neutralization tests. Specifically, neutralization properties were tested with rabbit sera after experimental immunizations with respective isolates. Combining the results from all three methods enabled distinguishing BKPyV from JCPyV and further dividing BKPyV into four groups, today known as subtypes I, II, III and IV.

Later, Jin (1993) introduced another more detailed BKPyV subtyping scheme based on a sequence variation in the genomic region of VP1 between nucleotides 1744 and 1812. Since then, additional subgroups have been added within the four major subtypes. BKPyV-I was further divided into four subgroups: Ia, Ib1, Ib2 and Ic; and BKPyV-IV into six subgroups: IVa1, IVa2; IVb1, IVb2; IVc1 and IVc2 (Nishimoto et al., 2007). Amino acid differences between the four main subtypes are shown in Figure 1.5.

It is generally believed that different BKPyV subtypes induce the production of specific neutralizing antibodies and thus behave as distinct serotypes Pastrana et al. (2012). Pastrana et al. (2013) suggested a model in which individuals seropositive for BKPyV-I are humorally vulnerable to *de novo* infection caused by subtypes II, III and IV (Pastrana et al., 2013). Furthermore, they also showed that all subgroups of subtype IV behave as single serotypes, whereas subgroups of subtype I can be divided into two serotypes: Ib2, Ic versus Ia and Ib1.

Researchers studied the distribution of BKPyV subtypes and subgroups and found that their geographical pattern is unique (Takasaka et al., 2004; Ikegaya et al., 2006; Zheng et al., 2007; Nishimoto et al., 2007; Zhong et al., 2009). Specifically, subtype I is the most prevalent worldwide; subtype IV is most common in Asia and Europe, while subtypes II and III are rarely detected. In Europe, the most prevalent subgroup of subtype I is Ib2 (almost 80%), and the only subgroup of subtype-IV detected is IVc2.

1.2.2 Pathology associated with BKPyV

BKPyV is a non-enveloped virus; therefore, the release of a new progeny results in cell lysis and cytopathic effect (Purchio and Fareed, 1979). Reactivation of BKPyV is accompanied by the presence of the virus in the blood (viremia), which occurs almost exclusively in immunocompromised individuals. For instance, patients during renal transplantation are under heavy immunosuppressive treatment favouring virus replication. Also, the fact that BKPyV persists mainly in the kidneys predetermines these patients to be more susceptible to BKPyV reactivation. The first evidence that BKPyV replication endangers a kidney graft survival was found by Randhawa et al. in 1999. BKPyV infection of the kidney allograft is called BKPyV-associated nephropathy (BKPyVAN), manifests as acute or progressive allograft dysfunction and affects up to 10 % of recipients (reviewed in Kuypers, 2012). In approximately 50 % of the cases, extensive viral replication, mainly in tubular epithelial cells, leads to necrosis and graft loss (reviewed in Nickeleit et al., 2000). Currently, the only relevant tool to prevent BKPyVAN in clinics continues to be a screening of BKPyV-replication and reduction of immunosuppression, which has been effective in preserving allograft function (Schaub et al., 2010). However, this strategy does not fully eliminate the risk of BKPyVAN and increases the risk of acute rejection (Sawinski et al., 2015; Seifert et al., 2017).

Another patient group significantly influenced by BKPyV pathology are stem cell transplant recipients. In 1986, prolonged BKPyV viruria was found to be associated with an inflammatory condition in the urine bladder referred to as hemorrhagic cystitis (Arthur et al., 1986). This pathology occurs in 9 % - 31 % of stem cell transplant recipients and leads to increased morbidity (reviewed in Han et al., 2014). BK viral load in the blood (>10,000 copies/mL) was proposed to be a predictive marker for a more severe outcome of hemorrhagic cystitis (Haines et al., 2011).

1.2.3 Risk factors for BKPyV reactivation

The state of immunosuppression is the most severe factor in developing polyomavirus-associated pathology. However, even under immunosuppressive therapy, only a minority of patients suffer from BKPyV-associated pathology. High viral loads in urine and blood

```
Loops
BKPyV-I          1 MAPTKRKGEC PGAAPKKPKE PVQVPKLLIK GGVEVLEVKT GVDAITEVEC
BKPyV-II           MAPTKRKGEC PGAAPKKPKE PVQVPKLLIK GGVEVLEVKT GVDAITEVEC
BKPyV-III          MAPTKRKGEC PGAAPKKPKE PVQVPKLLIK GGVEVLEVKT GVDAITEVEC
BKPyV-IV           MAPTKRKGEC PGAAPKKPKE PVQVPKLLIK GGVEVLEVKT GVDAITEVEC

Loops                 <               BC                    >
BKPyV-I         51 FLNPEMGDPD ENLRGFSLKL SAENDFSSDS PERKMLPCYS TARIPLPNLN
BKPyV-II           FLNPEMGDPD DNLRGYSLKL TAENAFDSDS PDKKMLPCYS TARIPLPNLN
BKPyV-III          FLNPEMGDPD DNLRGYSQHL SAENAFESDS PDRKMLPCYS TARIPLPNLN
BKPyV-IV           FLNPEMGDPD NDLRGYSLRL TAETAFDSDS PDRKMLPCYS TARIPLPNLN

Loops                                        <          DE         >
BKPyV-I        101 EDLTCGNLLM WEAVTVQTEV IGITSMLNLH AGSQKVHEHG GGKPIQGSNF
BKPyV-II           EDLTCGNLLM WEAVTVKTEV IGITSMLNLH AGSQKVHENG GGKPVQGSNF
BKPyV-III          EDLTCGNLLM WEAVTVKTEV IGITSMLNLH AGSQKVHENG GGKPVQGSNF
BKPyV-IV           EDLTCGNLLM WEAVTVKTEV IGITSMLNLH AGSQKVHENG GGKPIQGSNF

Loops                  <                          EF
BKPyV-I        151 HFFAVGGEPL EMQGVLMNYR SKYPDGTITP KNPTAQSQVM NTDHKAYLDK
BKPyV-II           HFFAVGGDPL EMQGVLMNYR TKYPQGTITP KNPTAQSQVM NTDHKAYLDK
BKPyV-III          HFFAVGGDPL EMQGVLMNYR TKYPQGTITP KNPTAQSQVM NTDHKAYLDK
BKPyV-IV           HFFAVGGDPL EMQGVLMNYR TKYPEGTVTP KNPTAQSQVM NTDHKAYLDK

Loops                            >
BKPyV-I        201 NNAYPVECWV PDPSRNENAR YFGTFTGGEN VPPVLHVTNT ATTVLLDEQG
BKPyV-II           NNAYPVECWI PDPSRNENTR YFGTYTGGEN VPPVLHVTNT ATTVLLDEQG
BKPyV-III          NNAYPVECWI PDPSRNENTR YFGTYTGGEN VPPVLHVTNT ATTVLLDEQG
BKPyV-IV           NNAYPVECWI PDPSKNENTR YFGTYTGGEN VPPVLHVTNT ATTVLLDEQG

Loops                               <   HI   >
BKPyV-I        251 VGPLCKADSL YVSAADICGL FTNSSGTQQW RGLARYFKIR LRKRSVKNPY
BKPyV-II           VGPLCKADSL YVSAADICGL FTNSSGTQQW RGLARYFKIR LRKRSVKNPY
BKPyV-III          VGPLCKADSL YVSAADICGL FTNSSGTQQW RGLARYFKIR LRKRSVKNPY
BKPyV-IV           VGPLCKADSL YVSAADICGL FTNSSGTQQW RGLPRYFKIR LRKRSVKNPY

Loops
BKPyV-I        301 PISFLLSDLI NRRTQRVDGQ PMYGMESQVE EVRVFDGTER LPGDPDMIRY
BKPyV-II           PISFLLSDLI NRRTQKVDGQ PMYGMESQVE EVRVFDGTEQ LPGDPDMIRY
BKPyV-III          PISFLLSDLI NRRTQKVDGQ PMYGMESQVE EVRVFDGTEQ LPGDPDMIRY
BKPyV-IV           PISFLLSDLI NRRTQRVDGQ PMYGMESQVE EVRVFDGTEQ LPGDPDMIRY

Loops
BKPyV-I        351 IDKQGQLQTK ML
BKPyV-II           IDRQGQLQTK MV
BKPyV-III          IDRQGQLQTK MV
BKPyV-IV           IDRQGQLQTK MV
```

Figure 1.5: Alignment of 362 amino acids long VP1 sequences of four BKPyV subtypes. For each subtype, one sequence with the following accession number from GenBank was aligned: YP_717939 (BKPyV-I), CAA79596 (BKPyV-II), AAA46882 (BKPyV-III) and BAG84476 (BKPyV-IV). VP1 surface-exposed loops (BC, DE, EF and HI) are shown in the picture. Subtype differences are marked in bold letters.

during the post-transplantation period were shown to be a useful marker predicting severe clinical outcomes of both BKPyVAN and hemorrhagic cystitis. However, not all patients with increased viral loads develop virus-associated pathology. Consequently, other predictive markers based on either virus molecular mechanisms or host antibody response were proposed to participate in pathology.

1.2.3.1 Virus molecular determinants

The study of Bauer et al. (1995) revealed a molecular basis responsible for the highly virulent phenotype of the LID strain of MPyV. LID strain, which causes lethal infection of newborn mice, was derived from a less pathogenic tumour-inducible PTA strain. VP1 proteins of these strains differ only in two amino acids. By creating recombinant viruses, it was shown that only one amino acid change is responsible for the virulent phenotype: substitution of valine for alanine at position 296. Contra-intuitively, this specific mutation reduced avidity to cell receptors, leading to rapid virus spread and increased pathogenic potential of MPyV.

Likewise, the work of Stoner and Ryschkewitsch (1995) first proposed the association of pathology caused by JCPyV with specific mutations in VP1. A few years later, this suggestion was confirmed by two studies (Zheng et al., 2005a,b), which identified positions of frequently occurring mutations in three surface-exposed loops: BC (55, 60, 66), DE (126) and HI (265, 267, and 269). Later, it was shown that the same VP1 mutations (except amino acid 60) change virus receptor specificity leading to loss of the virus's ability to agglutinate red blood cells (Gorelik et al., 2011). The interaction of the virus with red blood cells depends on sialic acid as an entry receptor, which is present in most cell types. Consequently, these mutants were shown to favour entry by non-sialic receptors to the cells of the central nervous system and were, therefore, associated with the development of progressive multifocal leukoencephalopathy. The study of Geoghegan et al. (2017) showed that both wt and mutated JCPyV pseudotype particles carrying previously described mutations L55F and S267F first attach to glycosaminoglycans (GAG) on the cell surface. After this initial attachment, the entry of wt JCPyV strain depends on sialylated glycans; however, mutants engage non-sialylated non-GAG co-receptor glycans.

In the context of BKPyV, VP1 mutations have also been investigated as a potential factor in viral pathogenesis. However, the situation is more complex than it is for MPyV and JCPyV. Randhawa et al. (2002) first observed broad heterogeneity of VP1 sequences isolated from patients with BKPyVAN and identified hot spots of these mutations in codons for amino acids at positions 69 and 82 (BC loop of VP1). Furthermore, they collected biopsies samples from three patients over a longer period and showed that BKPyV sequences evolve within an individual with the disease progression. Opposed to this finding, in the work of

Tremolada et al. (2010b), authors sequenced VP1 coding region from KTx recipients who 1) developed and 2) did not develop nephropathy and observed an equal distribution of BKPyV variants in both patient groups. Therefore, they suggested the accumulation of mutations to be more likely a consequence of the frequent multiplication of the virus, not the disease progression. The study of Tremolada et al. (2010b) was the first mapping the regions of all VP1 surface-exposed loops and found that variations cluster primarily within BC and DE loops and less frequently in the EF loop. A more recent study found that in Ktx recipients, the number of BC loop mutations correlated with the duration of BKPyV viruria and the occurrence of mutations was not restricted to KTx with BKPyVAN (McIlroy et al., 2020). Pseudovirions based on BK variants frequently observed *in vivo* were used to analyze the functional impact of these mutations. For some specific mutants, more efficient replication *in vitro*, change in glycan receptor usage and neutralization escape to the patient's cognate serum were observed. In contrast, Krautkrämer et al. (2009) showed that BC loop mutations do not impact viral loads. In summary, *in vitro* experiments imply a significant role of VP1 mutations in viral pathogenesis; however, their impact has not yet been clearly established *in vivo*.

Not only changes in VP1, but also rearrangements in NCCR region were associated with higher replication rates of BKPyV. Two variants of NCCR have been described: archetype (ww) and rearranged (rr). Archetype strains are believed to be transmissible forms of the virus (Iida et al., 1993). In the study of Rubinstein et al. (1991), rearranged forms of BKPyV occurred after the first passage when propagating cells *in vitro*. Later, rrNCCR was primarily isolated from urine samples of patients with immunosuppressive therapy, which supports the hypothesis that these variants occur more likely without an effective host immune response. rrNCCR is usually characterized by mutations, duplications, deletions or rearrangements of the whole sequence blocks of NCCR compared to archetypal variants. Such rearrangements were observed predominantly in biopsies from BKPyV-nephropathy patients and were linked to higher rates of BKPyV replication and increased inflammatory presentation (Olsen et al., 2006; Gosert et al., 2008). Furthermore, *in vitro* studies showed that recombinant BKPyV with diverse rearrangements in different NCCR blocks positively impacts early gene expression and viral replication (Gosert et al., 2008; Olsen et al., 2009). However, the mechanism underlying these changes is poorly understood (reviewed in McIlroy et al., 2019). Taken together, mutations and rearrangements of the regulatory region (NCCR) of BKPyV appear more frequently in pathological individuals and are, therefore, one of the possible viral determinants for higher pathogenicity. In recent years, the number of studies on this topic has declined. However, with the increasing amounts of sequenced genomes, there is open space for further analysis.

In 2018, Peretti and colleagues proposed that accumulation of BKPyV mutations may be

caused by one viral restriction factor - apolipoprotein B messenger RNA-editing, enzyme-catalytic, polypeptide-like 3 (APOBEC3). Historically, two members of this protein family (APOBEC3A and APOBEC3B) were shown to inhibit infection of many different viruses: human immunodeficiency virus 1 (Doehle et al., 2005; Berger et al., 2011), parvovirus (Narvaiza et al., 2009), herpesvirus (Suspene et al., 2011), hepatitis B virus (Henry et al., 2009), and human papillomavirus (Vartanian et al., 2008). These enzymes have the function of cytosine deaminase, as they convert cytosine to uracil leading to fatal DNA damage of viral genomes. However, Peretti et al. (2018) suggested that APOBEC3B drives the intrapatient evolution of BK virus, which may result in a selective advantage for the virus. The authors of this study analysed mutations in surface loops of VP1 from two KTx recipients who developed BKPyVAN followed by renal carcinoma and showed that the nature of observed mutations was consistent with DNA damage caused by APOBEC3B (transition C -> U). Furthermore, tissue sections from kidney biopsy samples were stained with antibodies against T antigen and APOBEC3. This immunohistochemical analysis revealed frequent colocalisation of both T antigen and APOBEC3, suggesting the possible contribution of viral factors to the upregulation of APOBEC3. In summary, even though APOBEC3B is a host restriction factor, it may drive BKPyV mutagenesis resulting in replication advantages for the virus (Peretti et al., 2018).

To date, authors of several studies postulated the hypothesis that specific BK subtypes might be associated with a higher risk of BKPyV-associated pathology (reviewed in Blackard et al., 2020). These ideas are supported by the functional study of Nukuzuma et al. (2006), which evaluated for the first time replication rates of the two most common BKPyV subtypes I and IV and showed that subtype BKPyV-I has a higher replication rate than BKPyV-IV in human kidney cells (renal proximal tubule epithelial cells and renal epithelial cells derived from whole kidneys of two donors). The authors also pointed out that the increased replication potential of BKPyV-I could explain its highest seroprevalence in the human population. On the contrary, the replication rates of the BKPyV subtypes I, II and IV were shown to be equal in the study of Tremolada et al. (2010c) when propagated in Vero cell line (kidney epithelial cells from an African green monkey *Chlorocebus*), whereas subtype III was shown to have a significantly lower replication rate. Yet cells infected with subtype IV showed a worse cytopathic effect, and the authors hypothesised that this subtype could be, therefore, potentially linked to more severe outcomes of BKPyV infection. A retrospective study of Korth et al. (2019) showed that less frequent subtypes II and IV were more likely to be associated with BKPyVAN and consequent graft loss. They explained this finding by the fact that the general population protected against the most common subtype I is lacking neutralizing antibodies (NAbs) against rare subtypes (II and IV) and is, therefore, more susceptible to infection caused by subtype II or IV. This study did not identify any patient with subtype

III and thus could not determine its pathological potential. BKPyV subtype III was detected only once in KTx recipient suffering from nephropathy (Kapusinszky et al., 2013).

1.2.3.2 The role of immune response against BKPyV

In BKPyV infection, innate and adaptive immunity both play a significant role. T lymphocytes are mainly responsible for long-term immune surveillance against persistent viruses. However, if this immune surveillance is disrupted, it can lead to the virus's reactivation. Therefore, during immunosuppression, it is necessary to rely on another part of adaptive immunity - antibody response. Antibodies are already present in patient serum and can inhibit BKPyV replication despite the immunosuppression.

As mentioned previously, around 20 % of the human population does not have humoral immune protection against BKPyV. In KTx patients, it was shown that BKPyV reactivation occurs most frequently when a kidney from a BKPyV-seropositive donor is transplanted into a BKPyV-seronegative recipient (Andrews et al., 1983; Shah, 2000) indicating that antibody status of both donor and recipient is an important risk factor for BKPyV nephropathy.

More recent studies investigated the possibility of increased risk when matching KTx donors and recipients seropositive for different BKPyV subtypes. Pastrana et al. (2012) monitored the neutralization status of KTx recipients and observed changes in serum-specificity after the transplantation. Specifically, a particular group of KTx with undetectable neutralizing titres against BKPyV-IV established seroconversion against this subtype within one year after transplantation. This result implies the importance of *de novo* BKPyV infection originating from the graft. The authors of this study even suggested a vaccination with BKPyV VLPs as a possible protection against BKPyV replication for those with low antibody titres. Furthermore, the study of Schmitt et al. (2014) proved BKPyV donor origin in KTx recipients for the first time. They showed that BKPyV genome sequences from donors were identical to sequences predominantly observed in their paired KTx recipients following the transplantation.

A retrospective study of Wunderink et al. (2017) showed that the risk of viremia and BKPyVAN was 10-fold higher for recipients paired with donors with elevated IgG levels. Accordingly, the work of Solis et al. (2018) revealed that KTx recipients with low NAb titer against the donor's BKPyV strain had a higher risk of developing BKPyV viremia. KTx patients in a high-risk group had NAb titre below the cut-off value (4 $\log_{10}$ IC_{50}), and the authors proposed this cut-off value as a predictive marker at the time of transplantation, enabling further monitoring recipients within the higher BKPyV disease risk group. Overall, KTx donor and recipient matched according to their subtype-specific neutralizing antibody response had a lower chance of graft failure.

Taken together, during BKPyV reactivation, more factors were shown to play a signif-

icant role. Particularly antibody status of the donor and recipient provides valuable information about a possible risk of developing BKPyVAN. Pre-transplantation screening of the donor and recipient BKPyV subtype-specific serostatus could identify high-risk patients and help to avoid complications after the surgery. Reliable diagnostics of specific BKPyV subtypes is therefore necessary for better predicting and managing post-transplant complications.

1.2.4 Serology methods used for BKPyV serotyping

To determine the specific subtype of BKPyV circulating in KTx recipients, one can use either PCR-based approaches or serology methods. PCR-based approaches are a standard clinical tool for monitoring BKPyV DNA from plasma and urine (Korth et al., 2019). However, BKPyV DNA is present only during virus re-activation, which is triggered by immunosuppression. In nonviremic and nonviruric individuals, information about BKPyV subtype specificity can be obtained only by serology methods, thus providing the same valuable information about possible risks of developing BKPyV before transplantation.

In laboratories, the major structural protein of polyomaviruses (VP1) is frequently used as an antigen for various diagnostic methods. Polyomavirus VP1 is easy to produce using different expression systems. The main advantage of this protein is that it spontaneously assembles and forms viral particles that morphologically resemble native virions even without the presence of minor proteins VP2 and VP3 (Salunke et al., 1989). The whole particles have on their surface conformational epitopes that were shown to be the main target for antibodies (Randhawa et al., 2009); therefore, these particles seem to function as a better antigen than VP1 monomers alone. There are two types of particles consisting of VP1: virus-like particles (VLPs) or pseudovirions (PsVs). VLPs are most commonly produced in insect cell lines using a baculovirus expression system, specifically baculovirus genetically engineered to express VP1 but, in some cases, also VP2 and VP3. PsVs are produced in a mammalian expression system and usually contain VP1, VP2, VP3 and a reporter gene. Despite this difference, in this thesis, the term "VLPs" is used for viral particles composed of VP1 produced in the baculovirus expression system, and the term "PsVs" is used for viral particles also composed of VP1 only (and with no reporter gene), which were produced in the mammalian expression system. We believe that this terminology helps to better understand figures throughout section 4.

Subtype-specific antibody response can be analyzed by different methods using both VLPs and PsVs. Neutralization assay is a method used to quantify antibody titres that neutralize different BKPyV genotypes (Pastrana et al., 2012). PsVs consisting of VP1 of different genotypes, VP2 and VP3, carry plasmid with a reporter gene (e.g. green fluorescent protein, luciferase), which is later detected in transduced cells. By adding serum with a suf-

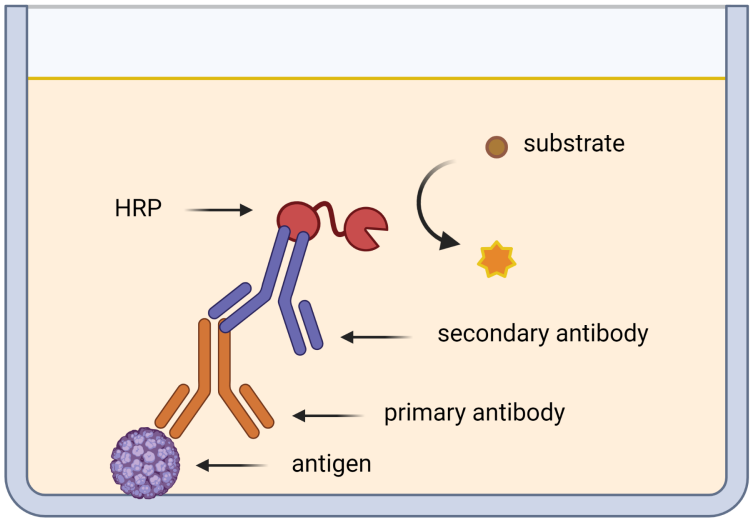

Figure 1.6: Schematic representation of ELISA. First, coating antigen (VLPs or PsVs) is immobilized on the bottom of a 96-well microtiter plate, followed by a washing step which removes any compounds (protein or antibodies) that are non-specifically bound. Second, primary antibody (serum antibodies in our case) is added, and the plate is washed again. Third, a secondary antibody conjugated with horseradish peroxidase (HRP) is added to each well, followed by the last washing step. Finally, a compound containing substrate reacts with HRP creating a detectable signal. This figure was created with biorender.com.

ficient titre of neutralizing antibodies, the transduction potential is inhibited. This method is reliable in determining a distinct neutralization serotype of BKPyV (Wunderink et al., 2019); however, it is not very suitable for routine use in clinics as it is demanding and time-consuming.

ELISA (enzyme-linked immunosorbent assay) is easy to perform and routinely used as a detection method for many viruses. This assay is based on detecting molecular interactions of an immobilized antigen with serum antibodies. The schematic representation of this method is shown in Figure 1.6. One of the limitations of ELISA is that it only provides information about the titre of the antibodies present in the serum sample, not about neutralizing ability of these antibodies.

The type of coating antigen used in the ELISA test can dramatically affect the specificity of this method. In the studies investigating BKPyV seroepidemiology, VLPs assembled from VP1 of BKPyV subtype I were most commonly used as a coating antigen (Viscidi and Clayman, 2006; Šroller et al., 2014). Recently, Hejtmánková et al. (2019) observed higher seroprevalence for BKPyV when coating a mix of VLPs derived from two BKPyV subtypes, I and IV. Furthermore, they showed that 27% and 12% (out of 88% positive samples) reacted specifically with one of the coated antigens (BKPyV-I or BKPyV-IV, respectively), while the remaining 49% cross-reacted with both antigens. The correlation between anti-BKPyV-I and anti-BKPyV-IV antibody titres, which measure the level of cross-reactivity, was not significant. This finding was in contrast to the previously published study of Pastrana et al.

(2012) in which authors observed a strong correlation between subtype antibodies and, thus higher level of cross-reactivity. This discrepancy may be caused by the fact that Pastrana et al. (2012) used a different coating antigen, namely PsVs composed of VP1, VP2 and VP3. Despite the amino acid sequence differences in minor proteins between these two subtypes, Pastrana et al. (2012) produced VP2 and VP3 identical to subtype IV for both BKPyV-I and BKPyV-IV-based PsVs. As minor proteins VP2 and VP3 are not exposed on the capsid surface, the authors of this study supposed that they do not participate in antibody binding. However, research on other polyomaviruses (SV40, JCPyV, WUPyV and KIPyV) showed that not only antibodies against VP1 but also against VP2 and VP3 circulate in the human population (Corallini et al., 2012; Lagatie et al., 2014; Kantola et al., 2010). Taken together, it seems that viral particles assembled only from VP1 exposed on the surface subtype-specific conformational epitopes are, therefore, more suitable for use in ELISA than PsVs containing minor proteins.

Cross-reactivity is one of the biggest obstacles when differentiating between BKPyV subtypes. However, cross-reactivity can also occur between more distant members of the *Polyomaviridae* family. The main focus was on the cross-reactivity of BKPyV and JCPyV, as these two viruses share the highest level of amino acid similarities in VP1 across all human polyomaviruses (78%; National Center for Biotechnology Information (NCBI) Blast algorithm). ELISAs testing the reactivity of human serum samples with VLPs based on BKPyV and JCPyV revealed none or only a very mild level of cross-reactivity (Viscidi et al., 2003; Egli et al., 2009; Šroller et al., 2014; Hejtmánková et al., 2019). Alternatively, another method called Luminex IgG immunoassay was used to study both seroprevalence and cross-reactivity between BKPyV and JCPyV. The main difference from standard ELISA is the use of different antigens and detection processes. Specifically, VP1 monomer fused with glutathione S-transferase (GST) is expressed in a bacterial system and coated on the surface of fluorescent beads via glutathione-casein cross-links. It is important to highlight that fused VP1-GST does not assemble into pentamers or VLPs; therefore, this antigen presents more likely linear instead of conformational epitopes. In Luminex, the interaction of bound VP1 is later detected with a biotinylated antibody, followed by incubation with streptavidin-R-phycoerythrin, which produces a fluorescence signal. The study of Kamminga et al. (2018) used Luminex technology to determine the level of cross-reactivity between human polyomaviruses and observed only very low values for correlation of BKPyV and JCPyV seroreactivity supporting the data from the previous studies. Additionally, they compared newly developed Luminex with standard ELISA, and despite the fact that Luminex uses VP1 monomer and ELISA uses VLPs as antigen, they observed similar results.

There is one approach which can resolve the question of cross-reactivity on the level of individual serum samples: antigen competition assay (ACA; so-called preadsorption assay,

serum competition analysis, or competitive binding assay). This approach relies on the saturation of a serum sample with homologous antigen. For instance, saturation with JCPyV VLPs can inhibit false seroreactivity of BKPyV-specific serum samples with JCPyV but not with BKPyV. Generally, before testing the reactivity of a serum sample, this sample is first pre-incubated with homologous and heterologous antigens. Only homologous antigen is able to saturate all antibodies from the sample, which is consequently shown as a lack of the signal on ELISA or Luminex. This approach is already used in FDA-approved JCPyV ELISA as a confirmation of JCPyV specificity/exclusion of BKPyV cross-reactivity (STRATIFY JCPyV™ Antibody ELISA).

Four BKPyV subtypes share 93% (NCBI Blast algorithm) amino acid similarities in VP1. Therefore, cross-reactivity in ELISA settings is abundant and problematic when distinguishing between specific BKPyV subtypes. ACA was performed to differentiate between BKPyV subtypes in two studies (Wunderink et al., 2019; Hejtmánková et al., 2019). These studies determined the serum specificity based on the saturation scheme shown in Figure 1.7. For simplicity, this scheme distinguishes only between the two most common BKPyV subtypes, I and IV. If we assume the existence of these two subtypes only, serum positive for BKPyV can be: positive for BKPyV-I, positive for BKPyV-IV or positive for both subtypes. First, if a serum sample is BKPyV-I-positive (Fig. 1.7.A), the reactivity of this sample with coating antigens BKPyV-I and BKPyV-IV is inhibited by saturation with BKPyV-I only. Second, if a serum sample is BKPyV-IV-positive (Fig. 1.7.B), the reactivity of this sample is completely inhibited by saturation with BKPyV-IV. And third, if a serum sample is double-reactive (Fig. 1.7.C), the reactivity of this sample cannot be inhibited.

Wunderink et al. (2019) used Luminex technology to develop a serotyping assay for all known BKPyV serotypes (Ib1, Ib2, Ic, II, III and IV) and ACA to analyze the cross-reactivity of these serotypes further. Specifically, they performed ACA with six serum samples and showed that BKPyV-I and BKPyV-IV have relatively little chance of cross-reactivity in comparison to BKPyV-II and III as the reactivity of subtype II and III was completely inhibited by saturation with soluble GST-VP1 derived from all subtypes (Ib1, Ib2, Ic, II, III and IV). However, it seems that the BKPyV antibody response is directed preferably against conformational, not sequence epitopes. Therefore, diagnostic tests should favour the use of whole viral capsids as antigens. ELISA analysis comparing antibody responses against GST-VP1 and VLPs carried out by Bodaghi et al. (2009) found that VLPs-based ELISA proved more sensitive than GST-VP1-based ELISA. To confirm the importance of three-dimensional epitopes, they denaturated VLPs and observed a drop in reactivity to levels comparable with GST-VP1.

In accordance with the findings of Wunderink et al. (2019), data from the study of Hejtmánková et al. (2019) showed that cross-reactivity of subtype-specific serum samples could

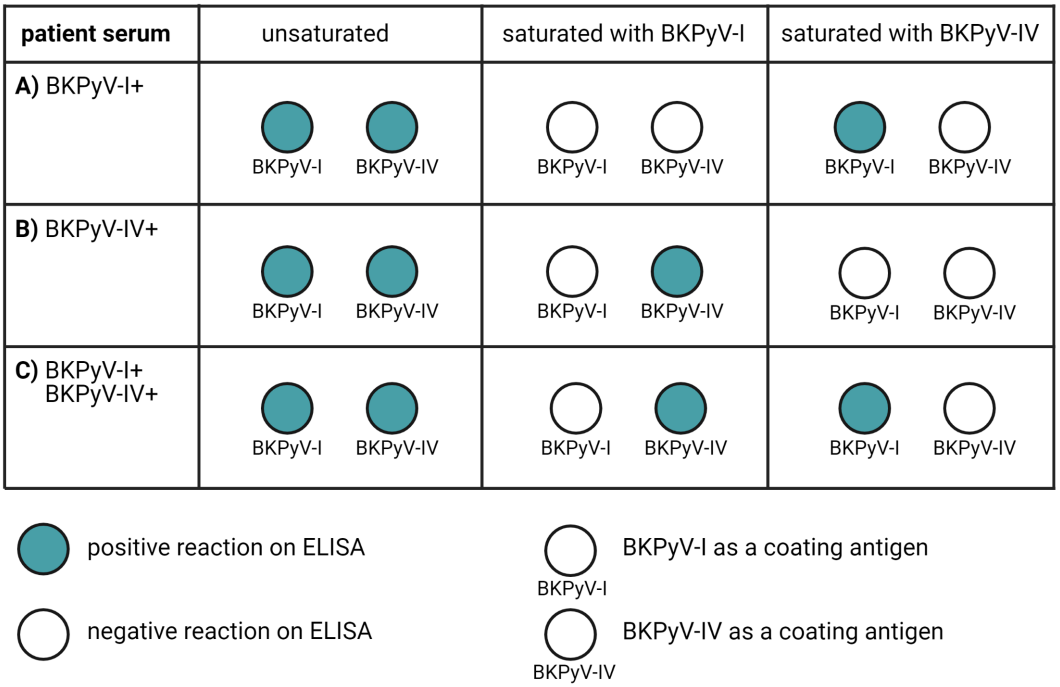

Figure 1.7: The cross-saturation scheme showing the reaction of BKPyV positive sera with homologous and heterologous antigens. The reactivity of A) BKPyV-I-positive serum, B) BKPyV-IV-positive serum, and C) BKPyV-I- and BKPyV-IV-positive sera after saturation with homologous and heterologous antigens. This is an ideal model showing how to distinguish between cross-reactivity and co-infection, which was achieved only in some of the sera tested by Hejtmánková et al. (2019).

be depleted after incubation with respective subtype. However, the reactivity of one (out of three) serum samples was not diminished completely. Whether this was caused by a high titre of antibodies (low concentration of competing antigen) or this sample is really double-reactive is not known.

Overall, ACA has the potential to answer the question of how to distinguish between cross-reactivity and co-infection caused by different BKPyV subtypes and thus contribute to the prediction and better management of post-transplant complications. However, data interpretation seems problematic in the case of serum samples with high titres of antibodies, and this method needs further optimization.

1.2.5 Epitopes on BKPyV VP1 responsible for cross-reactivity

Differences between BKPyV subtypes cluster within the BC loop of VP1 (Fig. 1.8) and this loop is therefore called a hyper-variable region. The nucleotide sequence coding for amino acids (aa) at positions 61 - 83 (typing region) within the BC loop is used to differentiate between BKPyV subtypes (Jin, 1993). Furthermore, the BC loop interacts with cell receptors, namely sialic acid of N-linked glycoproteins (Dugan et al., 2005), and it also contains a binding region for neutralizing antibodies (Murata et al., 2008; Lindner et al., 2019). Cryo-EM structure of the interaction between cross-neutralizing antibody IgG and capsid

of different polyomaviruses showed that this antibody binds a conserved quaternary viral epitope, which is present on all BKPyV subtypes, JCPyV and MCPyV (Lindner et al., 2019). The complex binding side of this cross-neutralizing antibody was identified in three regions: BC loop, EF loop and the C-end of VP1 (Lindner et al., 2019).

To design a new antigen with the potential to distinguish between BKPyV subtypes and detect subtype-specific antibodies, Sekavová (2017) substituted BC loop of MPyV with A) BC loop of BKPyV-I subtype and B) BC loop of BKPyV-IV subtype. VP1 protein of both constructs was successfully produced in baculovirus-infected cells; however, compact viral particles were observed only rarely. Subsequent testing of the disassembled material on ELISA showed poor reactivity. This finding was unexpected, as Kojzarová (2011) had previously introduced changes to the DE loop and observed a large number of intact particles.

Later, Sekavová (2017) changed the approach and used ACA to determine between BKPyV subtypes. This approach was successful only in some of the tested sera and needed further optimization (Sekavová, 2017; Hejtmánková et al., 2019). Therefore, the aim of the study of Tomanová (2019) was to design two antigens with the potential to saturate serum antibodies in ACA and thus determine BKPyV subtype specificity. As the DE loop differs only in 1 amino acid between BKPyV-subtype I and IV and EF loop differs in 2 amino acids exposed on the capsid surface, these two loops were mutated on the backbone of BKPyV-IV in favour of BKPyV-I. Preliminary results showed that antigen mutated in DE loop (PsVs) reacted on ELISA with BKPyV-I-positive and BKPyV-IV-positive serum samples more than original BKPyV-IV antigen (Tomanová, 2019). These results imply that the antigen mutated in the DE loop had an increased potential to capture subtype-specific antibodies and could thus serve as a good competing antigen in ACA. The last surface-exposed loop (HI loop) was not chosen as a target for mutation as it does not differ across BKPyV subtypes.

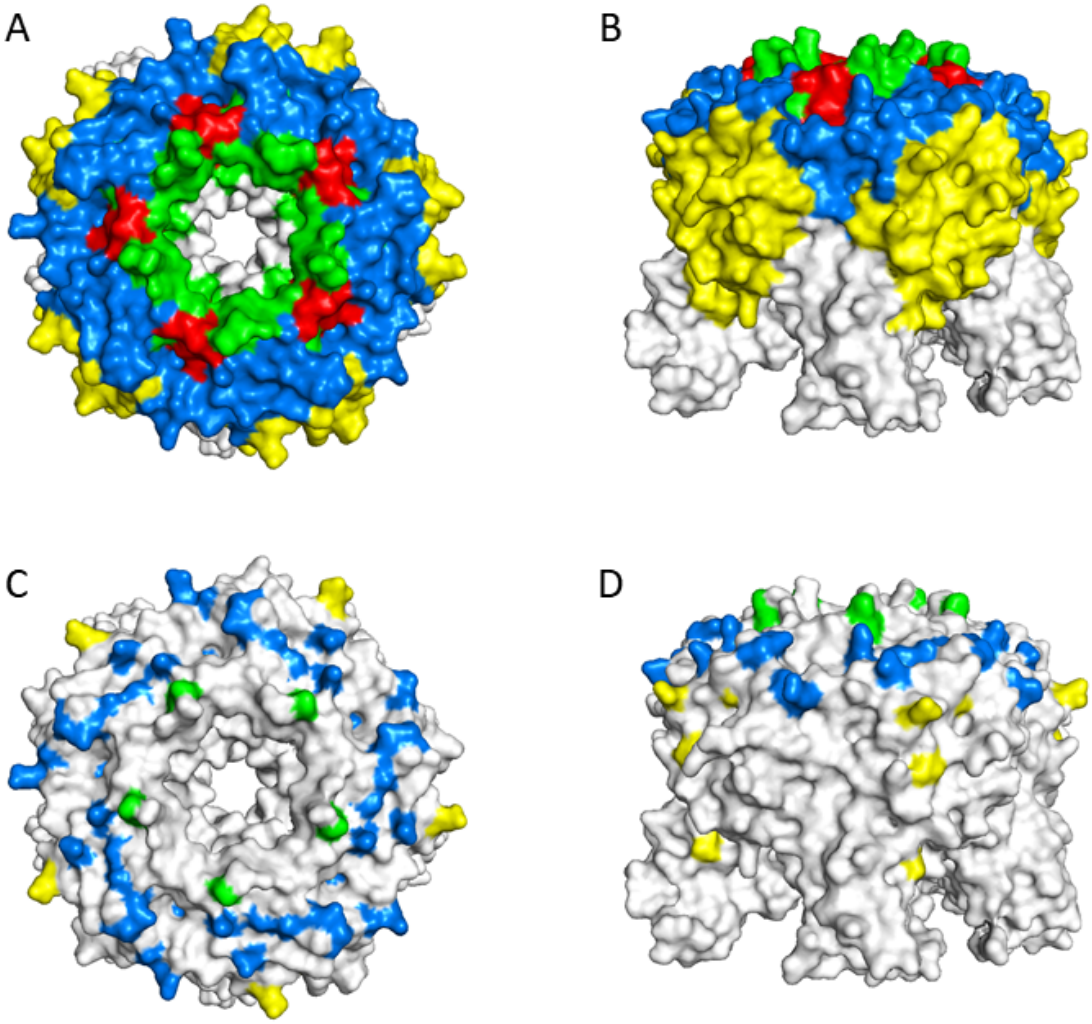

Figure 1.8: The structure model of the BKPyV VP1 pentamer showing A, C) view from above and B, D) side view. A and B show the distribution of four loops on the pentamer surface. C and D show amino acid differences between the most common BKPyV subtypes (I and IV), which are located mostly in BC loop (blue), less frequently in EF loop (yellow), and only one amino acid difference is in DE loop (green), and none can be found in HI loop (red). These models were generated using PyMOL based on the structure created by (Neu et al., 2013), which is deposited in Research Collaboratory for Structural Bioinformatics (RCSB) protein data bank with entry code 4MJ1.

2. Aims

Cross-reactivity of serum antibodies is the biggest obstacle when differentiating between the two most common BKPyV subtypes, BKPyV-I and BKPyV-IV. Therefore, this project's primary aim is to identify epitopes responsible for the binding of cross-reactive and subtype-specific antibodies.

Aim 1: To identify the role of DE and EF loop of BKPyV VP1 in serological cross-reactivity between subtypes I and IV.

- To prepare control and mutant antigens (PsVs) and verify their suitable use as antigens for serological methods - ELISA and antigen competition assay.
- To determine the role of viral epitopes, namely DE and EF loop of BKPyV VP1, in serological cross-reactivity between BKPyV subtypes I and IV while testing the reactivity of prepared mutant antigens (PsVs) with hyperimmune rabbit sera and human sera from KTx.

The course of BKPyV pathogenicity is poorly understood, and many risk factors have been proposed to be associated with increased viral load. For example, one potential risk factor is the accumulation of mutations in the VP1 protein, which can result in changed viral tropism and virus neutralization escape. Furthermore, it is commonly indicated that different BKPyV subtypes may have different pathogenic potentials. This project's secondary and tertiary aim is to associate some of the proposed risk factors with the worsened course of BKPyV infection.

Aim 2: To characterize the effect of mutations introduced in DE and EF loop of BKPyV VP1 on the virus biology.

- To prepare control and mutant antigens (PsVs) containing minor capsid proteins and a reporter gene and determine their transduction potential.
- To determine the potential of mutant PsVs to escape from neutralizing antibodies present in human sera from KTx.

Aim 3: To investigate the impact of VP1 mutations on pathology associated with BKPyV through the use of bioinformatics tools.

- To determine the influence of specific BKPyV subtypes/mutations in VP1 on a higher risk of BKPyV-associated pathology using data from online databases connected to a patient's clinical status.

3. Material and methods

3.1 Material

3.1.1 Laboratory equipment

Centrifuge 3K30 (Merck)

Centrifuge GS-15R (Beckman)

Centrifuge Megafuge 1.0R (Heraus Sepatech)

Centrifuge Microfuge 16 (Beckman)

CO_2 thermostat (Forma Scientific)

DeepFreeze MDF-U53V (Sanyo)

Electroporator Gene Pulser Apparatus (Bio-Rad)

ELISA reader (Epoch BioTek)

Fraction recovery system (Beckman)

Horizontal agarose electrophoresis apparatus multiSub Mini (Cleaver)

Laminar hood (FormaScientific)

Magnetic stirrer IKA® Big Squid

Microwave (Vestel)

Microscope Leica DMi1 (Leica)

Mini Centrifuge C1200 (Labnet)

NanoDrop Spectrophotometer ND-1000 (NanoDrop Technologies)

Nitrocellulose membrane Whatman™ Protran™ (GE Healthcare Life Sciences)

Orbi-Safe TS - cultivation shaker (Gallenkamp)

Orbital Shaker (Forma Scientific)

Parafilm® (Merck)

PCR cycler Mastercycler EP gradient S (Eppendorf)

pH metr S20 SevenEasy (Mettler Toledo)

Power supply Power Pactext trademark Basic (BioRad)

Protein electrophoresis apparatus (Bio-Rad)

Qubit® fluorometer (Invitrogen)

Refractometer ABBE (Carl Zeiss Jena)

Shaker Duomax 1030 (Heidolph)

Sidelight magnifier SD30 (Olympus)

Slide-A-Lyzer™ MINI Dialysis Device, 0.5 mL (ThermoFisher Scientific)

Sonicator QSonica (Q500)

Thermoblock CH-100 (Biosan)

Termostat TCH100C (Biosan)

Transmission electron microscope JOEL JEM 1200EX

Ultracentrifuge Optima TML-90K (Beckman)

Vilber Fusion Fx (BioConsult Laboratories)

Vortex-Genie 2 (Scientific Industries)

Waterbath (Grant Instruments)

Weighing scale 440-33 (Kern)

Weighing scale, analytical (Ohaus)

Western blot apparatus (Bio-Rad)

3.1.2 Solutions and chemicals

AA (acrylamide)

- 29% acrylamide (Serva)
- 1% bis-acrylamide (Serva) in demiH_2O

ABTS ((2,2'-Azino-bis(3-ethylenbenzythiazoline-6-sulfonicacid)) ammonium salt)

- 4 mg/mL in citrate buffer (Merck)

ABTS substrate

- 5.5 ml 10% citrate buffer, pH 4
- 0.5 ml ABTS
- 5 µl 30% H_2O_2

Agarose (Amresco)

Antibiotic-Antimycotic solution for tissue cultures (Merck)

AP (ammonium persulfate, Merck)

Blotting buffer, pH 8.3

- 25 mM Tris
- 195 mM glycine
- 20% methanol

Bradford reagent

- 100 mg Coomassie Brilliant Blue G250 (Serva)
- 50 mL 96% ethanol
- 100 mL 85% H_3PO_4
- 750 mL ddH_2O

BSA (bovine serum albumin, Merck)

Buffer B

- 10 mM Tris HCl (pH = 7.4)

- 150 mM NaCl
- 0.01 mM $CaCl_2$

Citrate buffer

- 0.1 M Citric acid monohydrate
- pH adjusted with 1M NaOH to 4.0

Coumaric acid (Merck)

- 90mM in DMSO
- 80µl aliquots stored at -70°C

Chemiluminescence solution 1

- 2 mL 1M Tris-HCl, pH 8.5
- 80 µl 90mM p-coumaric acid in DMSO (Merck)
- 200 µl 250mM Luminol in DMSO (Merck)
- 18 mL ddH_2O

Chemiluminescence solution 2

- 2 mL 1M Tris-HCl, pH 8.5
- 12 µl 30% H_2O_2
- 18 mL ddH_2O

CsCl (Serva)

Disassembly buffer

- 20 mM Tris-HCl, pH 8.8
- 5 mM or 2 mM EDTA
- 50 mM NaCl
- 2 mM DTT

Dulbecco's Modified Eagle's Medium (DMEM, high glucose, Merck), supplemented with serum

- 10% fetal bovine serum (ThermoFisher Scientific)
- 1% non-essential amino acids (ThermoFisher Scientific)
- 400 µg/mL Hygromycin B Gold

Dulbecco's Modified Eagle's Medium (DMEM, high glucose, Merck), serum-free

DPBS (Dulbecco's phosphate buffered saline, Lonza)

EDTA (ethylenediaminetetraacetic acid)

- 0.5 M $Na_2EDTA.2H_2O$ (Serva) in dH_2O
- pH adjusted with NaOH to 8.0

Fetal bovine serum (ThermoFisher Scientific)

H_2O_2, 30% (Roth)

HCl (Lachner)

Hygromycin B Gold (InvivoGen)

Imperial Protein Stain (ThermoFisher Scientific)

Laemmli buffer, 5x

- 5% SDS (sodium dodecyl sulphate)
- 50 mM Tris-HCl, pH 6.8
- 50% glycerol (v/v)
- 25% β-mercaptoethanol
- 0.005% bromophenol blue (w/v)

LB (Luria-Bertani) agar

- 1% pepton (w/v, Imuna)
- 0.5% yeast extract (w/v, Imuna)
- 1% NaCl (w/v)
- 1.5% agar (w/v, Imuna)

LB (Luria-Bertani) medium

- low salt (Merck)
- high salt (Fluka)

Loading Dye (ThermoFisher Scientific)

Luminol (3-aminophthalygrazide, Merck)

- 250mM in DMSO
- 200µl aliquots stored at -70°C

MIDORI Green Stain Gel (Nippon Genetics)

Milk

- 5% powdered milk in PBS (w/v)

NaOH (Merck)

Non-essential amino acids (ThermoFisher Scientific)

Optiprep (Axis Shield)

- 60% iodixanol, w/v

Paraffin oil (Bayol F)

PBS (Phosphate buffered saline)

- 137mM NaCl
- 2.7mM KCl
- 10mM Na_2HPO_4
- 1.8mM KH_2PO_4

- pH adjusted with HCl to 7.4

PTA (phosphotungstic acid), 2%, pH 7.3

RIPA buffer

- 5mM EDTA
- 1% Sodium deoxycholate (w/v, Fluka)
- 150mM NaCl (Lachner)
- 0.05% Nonidet P-40 (Merck)
- 0.1% SDS (w/v, Merck)
- 50mM Tris-HCl, pH = 7,4 (Serva)
- 1% Triton X-100 (Serva)

Running buffer, pH 8.3

- 25mM Tris
- 192mM glycine
- 0.1% SDS (w/v)

SDS (Sodium dodecyl sulfate)

SOC medium (Clontech)

Solution I (Sol I)

- 2mM Tris-HCl, pH = 8 (Serva)
- 10mM EDTA-NaOH, pH = 8

Solution II (Sol II)

- 1%SDS (w/v), freshly prepared (Merck)
- 0.2M NaOH

Solution III (Sol III)

- 3M potassium acetate
- glacial acetic acid

TAE (Tris-acetate-EDTA)

- 40 mM Tris
- 45 mM boric acid
- 1 mM EDTA

TBE (Tris-borate-EDTA)

- 45 mM Tris
- 20 mM acetic acid
- 1 mM EDTA

TE buffer

- 10 mM Tris, pH adjusted with HCl to 8.0

- 1 mM EDTA, pH adjusted with NaOH to 8.0

TEMED (tetramethylenediamin, Merck)

TNM-FH insect medium supplemented with serum (Merck)

- 10% fetal bovine serum
- 1/100 volume of Antibiotic-Antimycotic solution for tissue cultures

TNM-FH insect medium serum-free (Merck)

Tris-HCl (1M)

- Tris-(hydroxymethyl)-aminomethane (Serva) in dH_2O
- pH adjusted with HCl (Lachner)

Triton X-100 (Serva)

TurboFect Transfection Reagent (ThermoFisher Scientific)

Tween-20 (Serva)

Zeocin™ (InvivoGen, working concentration 50 µg/mL)

3.1.3 Enzymes

Benzonase (Merck)

Neuraminidase (Merck)

PlasmidSafe (ThermoFisher Scientific)

RNase A (Merck)

Restriction endonucleases (Fermentas)

- BamHI (10,000 U/mL)
- EcoRI (10,000 U/mL)
- EcoRV (10,000 U/mL)

Thermostable polymerases

- High Fidelity PCR Enzyme Mix (ThermoFisher Scientific; 5,000 U/mL)
- Vent DNA polymerase (NEB; 2,000 U/mL)

Trypsin (Merck)

- 0.4% (w/v) in PBS

3.1.4 Commercial kits

Qubit® Protein Assay Kit (Invitrogen)

In-Fusion® HD Cloning (Clontech)

NucleoBond® Xtra Midi (Macherey-Nagel)

QIAquick Gel Extraction Kit (QIAGEN)

3.1.5 Vectors

Table 3.1 shows all vectors used in this thesis. pBKPyV-I (pIaw, a kind gift from C. Buck), pBKPyV-IV (pwB), pwB2B, pwB3b, ph2b and ph3b were obtained from Addgene, pGL3-Control was obtained from Promega. Vector pBKPyV-IV was constructed from pwB2b (kindly donated by C. Buck) in the work of Mrkáček (2018). Specifically, the BKPyV-IV sequence of pwB2b was cloned into phGf (Addgene, plasmid #22516) to generate a vector expressing BKPyV VP1 and enhanced green fluorescent protein (EGFP) from separate promoters. In addition, the start codon from EGFP was mutated to obtain a construct that express VP1 only. pBKPyV-IV-DEmut and pBKPyV-IV-EFmut were created by Tereza Tomanová using site-directed mutagenesis of the original pBKPyV-IV.

Table 3.1: Vectors with the genes they carry.

Vector	**Coding region (GenBank accession No.)**	**Addgene No.**
pBKPyV-I	BKPyV-I VP1 (6GG0_1)	—
pBKPyV-IV	BKPyV-IV VP1 (BAG84476)	—
pBKPyV-IV-DEmut	BKPyV-IV VP1 with one point mutation H139N	—
pBKPyV-IV-EFmut	BKPyV-IV VP1 with two point mutations D175E and I178V	—
pwB2b	BKPyV-IV VP1 (BAG84476), VP2 (BAG84474)	#32094
ph2b	VP2	#32109
pwB3b	BKPyV-IV VP1 (BAG84476), VP3 (BAG84475)	#32106
ph3b	VP3	#32110
pGL3-Control	luciferase	—

3.1.6 Primers

Primers used in this work (Table 3.2) were obtained from Integrated DNA Technologies. Both sets of primers were used for In-Fusion cloning.

Table 3.2: Primers used in this work.

Primer	**Sequence**
BKPyV-VP2-Fw	5′- GCT TCC GGA GCC ACC ATG GGC GCA GCT CTG GCA - 3′
BKPyV-VP2-Rv	5′- AGC TGG GTA CTA GTC TCA CTG CAT TCT AGT TGT GGT TTG T - 3′
pwB3b-Fw	5′- GAC TAG TAC CCA GCT TTC TTG TAC - 3′
pwB3b-Rv	5′- GGT GGC TCC GGA AGC CTG - 3′

3.1.7 Cell lines and bacterial strains

3.1.7.1 Eukaryotic cell lines

Sf9 cells - established from ovarian tissue of *Spodoptera frugiperda* (ATCC No. CRL-1711)
293TT - human embryonic kidney-derived cells immortalized by adenovirus 5; with integrated SV40 early region of genomic DNA overexpressing SV40 Large T Antigen cassette under a hygromycin resistance (gift from C. Buck)

3.1.7.2 Bacterial cell lines

Stellar Competent Cells (Clontech) - *E. coli* HST08 strain with the following genotype: *F-, endA1, supE44, thi-1, recA1, relA1, gyrA96, phoA, ϕ80d lacZ ΔM15, δ(Lacha-argF) U169, δ(mrr-hsdRMS-mcrBC), δmcrA, λ-*

3.1.8 Viruses, virus-like particles and pseudovirions

Viruses

- recombinant baculovirus expressing VP1 (subtype BKPyV-Ia, GenBank accession No.: NC001538) used for VLPs production prepared by Veronika Hrušková and Mariana Stančíková
- recombinant baculovirus expressing VP1 (subtype BKPyV-IVc2, GenBank accession No.: BAG84476) used for VLPs production prepared by Alžběta Hejtmánková

Virus-like particles

- BKPyV-I VLPs - assembled from VP1 (subtype BKPyV-Ia) used on ELISA prepared by Tereza Tomanová
- BKPyV-IV VLPs - assembled from VP1 (subtype BKPyV-IVc2) used on ELISA prepared by Alžběta Hejtmánková

3.1.9 Antibodies and sera

Primary antibodies

- Rabbit antibody against VP1 BKPyV-I (polyclonal, dilution 1:1,000) prepared by M. Stančíková
- Rabbit antibody against VP1 BKPyV-IVc2 (polyclonal, 1:1,000) provided by Hena s.r.o. (antigen, VLPs of BKPyV-IVc2 subtype, was prepared by Alžběta Hejtmánková)
- Rabbit antibody against VP1 SV40 (RbαSV40, polyclonal, Abcam ab53977, dilution 1:1,000)
- Rabbit antibody against BKPyV VP2/3 (polyclonal, dilution 1:1,000) was provided by Clonestar Peptide Services s. r. o. (antigen was prepared by Vinšová, 2017)
- Human cytomegalovirus IgG (Cytotect CP - Biotest, 100 U/mL, dilution 1:400)

Rabbit sera

- RbαBKPyV-I prepared by Mariana Stančíková, rabbit was immunized with VLPs of BKPyV-Ia subtype
- RbαBKPyV-IV kindly provided by Hena s.r.o. (antigen, VLPs of BKPyV-IVc2 subtype, was prepared by Alžběta Hejtmánková)

Human sera

- All human sera were provided by VIDIA s.r.o. Serum samples were pre-characterized by Hejtmánková et al. (2019), however, only some of the tested sera are published in the research paper.

Secondary antibodies

- Goat antibody against rabbit IgG, conjugated with horseradish peroxidase, Fc fragment specific (GαRb-Px, Biorad, dilution 1:1,000)
- Goat antibody against human IgG, conjugated with horseradish peroxidase, Fc fragment specific (0.8 mg/mL, Jackson ImmunoResearch Europe Ltd, diluted 1:4000)

3.1.10 Molecular weight markers

Marker used for DNA electrophoresis: GeneRuler™ 1 kb (ThermoFisher Scientific, Fig. 3.1.A)
Marker used for SDS-PAGE (Sodium dodecyl sulphate–polyacrylamide gel electrophoresis): Spectra Multicolor Broad Range Protein Ladder (ThermoFisher Scientific, Fig. 3.1.B), The Color Prestained Protein Standard Broad Range (NEB, Fig. 3.1.C)

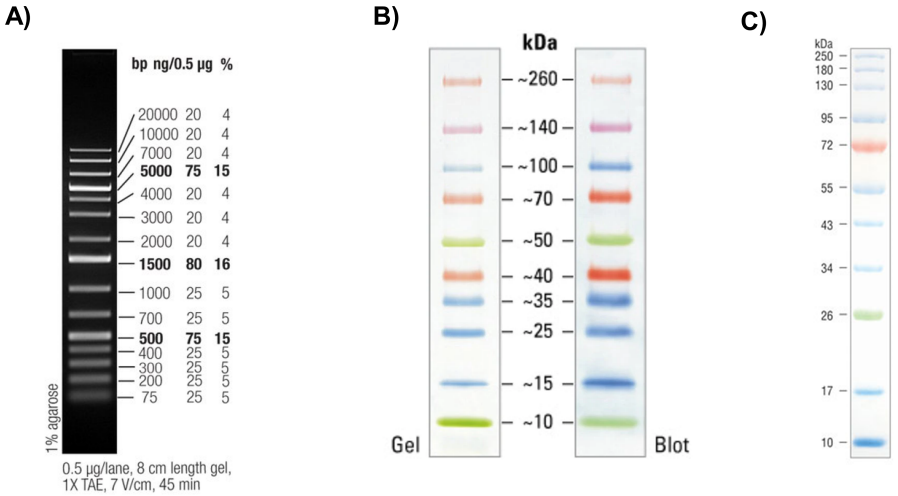

Figure 3.1: A) DNA marker used on 1% agarose gel, B) protein marker used for SDS-PAGE (Spectra Multicolor Broad Range Protein Ladder), C) protein marker used for SDS-PAGE (The Color Prestained Protein Standard Broad Range).

3.1.11 Software

AliView v.1.28
BKTyper tool v1.0
Datamonkey (https://www.datamonkey.org/)
GraphPad Prism 9.3.1
iTol v6 (Interactive Tree of Life)
NanoDrop
Seaview v.4.7.
SnapGene (GSL Biotech)
PyMOL Molecular Graphics System v 2.5.1 (Schrödinger, LCC.)

3.2 Methods

3.2.1 Sterilization

Most used solutions, micro test tubes, micropipette tips, stripettes and toothpicks were autoclaved at 120°C, 120 kPa for 30 minutes. Laboratory glass was covered with aluminium foil and sterilised by dry heat in a hot air oven for 3 hrs at 180°C. Metal and glass tools such as tweezers, inoculating wires and hockey-stick cell spreaders were sterilised in ethanol and passed through the flame. Laminar hoods were sterilised by UV light.

3.2.2 Bacterial cultures

3.2.2.1 Bacterial cultivation

Bacteria were cultivated on agar plates in a thermostat at 37°C for 16 hours or in a liquid medium in an orbital shaking incubator at 37°C, 250 rpm for 16 hours. Agar plates and media contained recommended concentrations of antibiotics which were necessary for clone selection.

3.2.3 Cell lines

3.2.3.1 Mammalian cell line 293TT

Passaging 293TT cells

293TT cells were grown at 37°C in a 5% CO_2 humidified incubator and passaged when they reached approximately 95% confluency. Cells were grown on Petri dishes (10 mm in diameter) in high glucose DMEM supplemented with serum. In a laminar hood, the medium was removed from cells, and 0.02% EDTA in PBS (2 mL) was pipetted on the top surface of the culture to run toward the bottom of the plate, then immediately removed. Afterwards, 1

mL of trypsin was added to the cells dropwise and incubated for 5 minutes at 37°C. Trypsin was inactivated by adding fresh DMEM with serum, and the detached cells were split 1:8 in a new plate.

Transfection of 293TT cells

One day before transfection, 1×10^6 cells in 5 mL DMEM with serum were seeded on a Petri dish (6 cm in diameter). Cells were transfected after 24 hours when they reached approximately 70% confluency. Plasmid DNA (6 µg) was diluted in 600 µL of serum-free medium mixed with 12 µL of TurboFect Transfection Reagent, followed by incubation for 20 minutes at room temperature. Then, the mixture was added to the cells dropwise, and the cells were placed in an incubator for 48 hours. Afterwards, a cell scraper was used to detach cells, and cells were collected into tubes and pelleted at 600 RCF (relative centrifugal force) for 6 minutes. Cells were resuspended in DPBS with 9.5 mM $MgCl_2$ and peletted again at 600 RCF for 6 minutes. The supernatant was removed, and a pellet volume was measured and recorded. The pellet was stored at -20°C and further used for PsVs isolation.

Preparation of transfected 293TT lysates for protein production evaluation

In one well of 24-well plate, 2.5×10^5 cells were seeded. Next day, the cells were transfected. 1 µg of DNA was pre-mixed with 100 µL of serum-free DMEM and 2 µL of TurboFect Transfection Reagent and this mixture was incubated 20 minutes at room temperature, then added to the cells dropwise. After 48 hours incubation, cells were carefully washed with PBS and placed on ice. RIPA buffer (100 µL) was added to each well and cells were incubated for 20 minutes on ice. Then, the supernatant (cell lysate) was transferred to microtubes, stored at -20°C and further used for western blot analysis to evaluate protein expression.

3.2.3.2 Insect cell line Sf9

Passaging Sf9 cells

Sf9 cells were grown on Petri dish (6 cm in diameter) in TNM-FH media with 10% FBS at 27°C. Confluent cells were harvested in culture media using a cell scraper, and media with cells were homogenized and split 1:4 in a new plate. Cell suspension in new plates was supplemented with TNM-FH media with 10% FBS and incubated at 27°C.

Infection of Sf9 cells

Confluent Sf9 cells were harvested in culture medium and further passaged 1:3 on a new Petri dish (15 cm in diameter). Cell suspension in new plates were supplemented with TNM-FH media and incubated at 27°C until they were attached to the plate surface (30 - 40

minutes). The medium was removed and viral inoculum was added (1 mL for 15 cm dish). The cells were incubated for 1 hour on a rocker at room temperature. Afterwards, TNM-FH medium supplemented with serum was added and cells were incubated for 72 hours at 27°C. Then, the infected cells were scrapped into medium and pelleted at 2,000 RCF for 5 minutes. Pellet was washed with 5 mL of PBS, cellular suspension was centrifuged (2,000 RCF for 5 minutes) and stored at -20°C.

3.2.4 Working with DNA

3.2.4.1 Plasmid DNA isolation

Bacteria carrying a plasmid of our interest were plated on LB agar with zeocin (final concentration 50 µg/mL) and grown for 16 hours at 37°C. Bacterial monocolonies were picked, and inoculated into 5 mL or 100 mL of LB medium with zeocin (50 µg/mL) for minipreparation and maxipreparation, respectively. Bacteria were grown for 16 hours at 37°C in a shaking incubator, at 200 rpm. The cell suspension was centrifuged at 4,000 RCF for 20 minutes at 4°C; and the pelleted cells were further used for DNA isolation. For minipreparation, alkaline lysis was used. For maxipreparation, NucleoBond® Xtra Midi (Macherey-Nagel) kit was used according to manufacturer's recommendations.

3.2.4.2 Plasmid DNA isolation by alkaline lysis

Bacterial monocolonies were picked with a sterile toothpick and transferred to a fresh plate. Bacteria that remained on the toothpick were inoculated into a sterile Eppendorf tube with 700 µL of LB containing antibiotics. Cells were grown overnight at 37°C. The cells on agar plates were then stored in refrigerator for future use, whereas the cells grown in liquid media were used for plasmid DNA isolation. Bacteria were pelleted (8,000 RFC, 10 minutes) and resuspended in 250 µL of TE buffer. 250 ul of Sol II was added to the mixture. The tube was inverted four times. Sol III was added immediately and the tube was gently inverted a few times. The sample was centrifuged at 10,000 RCF for 5 minutes, the supernatant was transferred to a new tube and mixed with 0.5 mL of 100% isopropanol. The tube was again inverted several times. The sample was centrifuged at 10,000 RCF for 10 minutes, the supernatant was removed and discarded. The pellet was washed with 200 µL of 80% ethanol, airdried and the precipitated DNA was redissolved in 30 µL of sterile ddH_2O.

3.2.4.3 Measuring DNA concentration

Measurement was performed using a NanoDrop® 2000 Spectrophotometer. The sample (2 µL) was placed on NanoDrop pedestal. This instrument read absorbance values of UV light with different wavelengths and calculated DNA concentration accordingly.

3.2.4.4 Horizontal agarose gel electrophoresis

Horizontal agarose gel electrophoresis was used to visualize DNA after isolation, restriction endonuclease digestion and PCR. Agarose was diluted in TAE or TBE buffer to a final concentration 1% (w/v) and heated until it completely dissolved. Then, the gel solution was cooled (approximately 50°C), MIDORI Green Stain Gel dye was added, and the solution was poured into a gel case with a comb insert. Once the gel solidified, it was placed in DNA electrophoresis tank and submerged in TAE or TBE. DNA ladder (GeneRuler™ 1 kb, Fermentas) was loaded into the first well, followed by DNA samples premixed with loading dye. The gel ran for approximately 45 minutes (5 V/cm) and then, the separated DNA was visualized by UV light using Vilber Fusion Fx (BioConsult Laboratories).

3.2.4.5 Restriction enzyme digestion

Restriction endonucleases (ThermoFisher Scientific) were used for DNA digestion. The reaction was set up depending on the chosen enzyme and according to a recommended protocol (see Table 3.3). Incubation usually lasted for 2-4 hours. Digested DNA fragments were visualized by agarose gel electrophoresis.

Table 3.3: Restriction enzyme digestion

Component	Volume
10x Buffer	1 µL
Sample DNA	0.5 µg
Restriction enzyme	5 U
ddH_2O	to 10 µL

3.2.4.6 Polymerase chain reaction

Polymerase chain reaction (PCR) was used to amplify DNA products for molecular cloning. Vent DNA polymerase (NEB) and High Fidelity PCR Enzyme Mix (ThermoFisher Scientific) were used for insert and vector amplification, respectively. Reactions were mixed on ice (see Table 3.4) in sterile 0.2ml thin-walled micro test tubes. PCR was run using different cycling conditions (see Table 3.5 and Table 3.6) in PCR cycler Mastercycler EP gradient S (Eppendorf).

3.2.4.7 Purification of PCR products

DNA bands were excised from the gel and purified using QIAquick Gel Extraction Kit (QIAGEN) according to the manufacturer's recommendations.

Table 3.4: PCR reaction mixture

Component	Volume (PCR + Vent)	Volume (PCR + HiFi)
Sterile H_2O	to 50 µL	to 50 µL
Buffer (10x)	5 µL	5 µL
$MgCl_2$ (25 mM)	NA	4 µL
dNTPs (10 mM)	1 µL	1 µL
Forward primer (10 µM)	2.5 µL	5 µL
Reverse primer (10 µM)	2.5 µL	5 µL
Polymerase	1 U	1 U
Template	20 ng	40 ng

Table 3.5: Cycling conditions for PCR reaction - Vent polymerase

Step	Temperature	Time	Number of cycles
Initial denaturation	95°C	5 min	1
Denaturation	95°C	30 s	
Annealing	64°C	30 s	30
Extension	72°C	1 min 10 s	
Final extension	72°C	5 min	1

Table 3.6: Cycling conditions for PCR reaction - HiFi polymerase

Step	Temperature	Time	Number of cycles
Initial denaturation	95°C	5 min	1
Denaturation	95°C	20 s	
Annealing	64°C	20 s	30
Extension	68°C	6 min	
Final extension	68°C	10 min	1

3.2.4.8 In-Fusion cloning

In-Fusion® HD Cloning kit (Clontech) enables to clone insert into vector using sequences with 15 bp long homologous ends was used. For that purpose, insert-specific primers with 15 nt extensions homologous to the vector were designed using In-Fusion Cloning Primer Design Tool. Purified PCR products were used in the reaction for In-Fusion cloning directly (Table 3.7). Alternatively, 5 µL of unpurified PCR products were incubated with 2 µL of Cloning Enhancer at 37°C for 15 minutes and then at 80°C for 15 minutes. In such a case, 1-2 µL of Cloning Enhancer-treated fragments were used in In-Fusion reaction.

Table 3.7: In-Fusion reaction mixture

Component	**Volume**
5x In-Fusion Premix	2 µL
Vector	50 ng
Insert	100 ng
ddH_2O	to 10 µL

In-Fusion reaction was incubated at 50°C for 15 minutes and then transferred on ice. The mixture was either used immediately for bacteria transformation by heat shock or stored at -20°C.

3.2.4.9 Bacteria transformation by heat shock

Stellar Competent Cells (Clontech) were placed on ice to thaw. 50 µL of cells were moved into a 15-mL Falcon tube and 2.5 µL of In-Fusion reaction was added. Cells were incubated on ice for 30 minutes, heat shocked at 42°C for 45 sec and placed on ice for 1.5 min. SOC medium was warmed to 37°C and added to the cells to bring the final volume to 500 µL. Transformed cells were incubated in an orbital shaker at 200 rpm for 1 hour, at 37°C. After incubation, 50 µL and 150 µL of the cell suspension were placed on plates with appropriate antibiotics while the remaining cells were centrifuged at 6,000 rpm for 5 minutes. The pelleted cells were placed on the third plate and all plates were incubated overnight at 37°C.

3.2.4.10 Colony PCR

Colony PCR was used to screen for colonies carrying the desired plasmid. Several bacterial monocolonies were picked using a sterile toothpick and transferred into 50 µL sterile ddH_2O. For cell lysis, the samples were briefly boiled (96°C, 5 min). The supernatant was further used as a template for PCR reaction (see Table 3.8). For the cycling conditions used, see Table 3.5 mentioned above. Primers used in this reaction were: BKPyV-VP2-Fw and BKPyV-VP2-Rv.

Table 3.8: Colony PCR mixture

Component	Volume
PCR H_2O	to 20 µL
Buffer (10x)	2 µL
Triton-X 1%	2 µL
Forward primer (10 µM)	0.6 µL
Reverse primer (10 µM)	0.6 µL
dNTPs (10 mM)	0.4 µL
Vent polymerase	0.5 U
DNA template	2.5 µL

3.2.5 Working with proteins

3.2.5.1 VLPs purification using ultracentrifugation in CsCl gradient

Pelleted Sf9 cells were resuspended in 5 ml of Buffer B, and cell lysis was performed on ice using sonication (Sonicator QSonica Q500), 4x 30-sec pulses of 40% amplitude. Cellular debris was pelleted at 2,800 RCF for 30 min at 4°C. The supernatant was transferred into an ultracentrifugation tube, and Buffer B was added to the final sample weight of 8 g and mixed with 3.65 g of CsCl. The content of the tube was mixed, and the refractive index was measured; the desired value was 1.363 - 1.364. If the refractive index was higher or lower, the B buffer or CsCl was added. The sample was then overlayered with paraffin oil. The ultracentrifugation tube was placed into the ultracentrifugation cuvette, and VLPs were purified by ultracentrifugation at 35,000 rpm for 20 hours at 18°C (Beckman, rotor SW41-Ti). CsCl gradient with separated proteins was divided into fractions, 500 µL each, using a fraction separator. Then the refractive index of each fraction was measured, and the presence of protein VP1 in each fraction was assessed by dot blot (section 3.2.5.5). According to both refractive index values and the signal detected in dot blot analysis, fractions were combined and transferred into a dialysis tubing closed by clamping closures. Dialysis was performed against 1 L of Buffer B at 4°C. Buffer B was changed after 1 hour, and dialysis was carried out overnight.

3.2.5.2 PsVs purification using ultracentrifugation in Optiprep gradient

Peletted 293TT cells collected after transfection (section 3.2.3.1) were resuspended in 1 volume of DPBS with 9.5 mM $MgCl_2$. Neuraminidase was added to the final concentration of 2 U/mL and the mixture was incubated for 15 minutes at 37°C. Then 1M Tris (pH 8) was added to the final concentration 5 mM as well as $1/20^{th}$ of a volume of 10% Triton X-100. After that, benzonase and PlasmidSafe were added to the final concentration of 0.1%. To increase the pH of the mixture, $1/40^{th}$ of a mixture volume of 1M ammonium sulfate (pH 9) was added. Finally, to prevent contamination, $1/100^{th}$ of a mixture volume of Antibiotic-

Antimycotic solution was added and the lysate was incubated for 2 hours at 37°C while mixed a few times. The lysate was chilled on ice for 5 minutes. By adding 0.17 volume of 5M NaCl, salt concentration was increased to the final concentration of 850 mM and the mixture was incubated on ice for 10 minutes, followed by centrifugation at 10,000 RCF for 15 minutes at 4°C. The supernatant was transferred into a new siliconized tube and the pellet was resuspended in 2 volumes of DPBS with 0.8 M NaCl, centrifuged again at 10,000 RCF for 15 minutes at 4°C and supernatant was added to the first supernatant. Combined supernatants were centrifuged at 10,000 RCF at 4°C for 10 minutes and then the supernatant was layered onto Optiprep gradient prepared in the meantime as follows. Optiprep (60% iodixanol, w/v) was diluted with DPBS/0.8M NaCl to 27%, 33% and 39% (w/v). 1.4 mL of each iodixanol solution was under-layered in a thin wall polyallomer 5 mL tube (Beckman) using a syringe with a needle in the following order: 27%, 33% and 39%. PsVs prepared using Optiprep protocol were purified by ultracentrifugation at 35 000 rpm for 3 hours at 16°C (Beckman, rotor SW55-Ti), on a slow acceleration and deceleration mode. Afterwards, fractions of 500 µL were separated and the presence of VP1 in fractions was checked by dot blot analysis (section 3.2.5.5), SDS-PAGE (section 3.2.5.7) and electron microscopy (section 3.2.5.6).

3.2.5.3 Protein concentration measurement using Qubit Fluorometer

Protein concentration was measured using Qubit Fluorometer (Invitrogen) and Qubit® Protein Assay Kit (Invitrogen) according to the manufacturer's protocol.

3.2.5.4 Protein concentration measurement using Bradford assay

Firstly, BSA was diluted in the buffer used for sample dilution (buffer B or iodixanol) to the following final concentrations: 0; 250; 500; 750 and 1,000 ng/mL; these samples were further used as protein standards. The assay was performed in a 96-well plate. In each well, 2 µL of a sample was mixed with 50 µL of Bradford reagent. Samples were run in duplicates, absorbance was measured at 595 nm using a microplate reader (Epoch BioTek), and a standard curve was created to assess the sample concentration.

3.2.5.5 Dot blot

All VLPs and PsVs fraction samples were applied on a nitrocellulose membrane Whatman™ Protran™ (GE Healthcare Life Sciences) in a single spot (2 µL). Afterwards, the membrane was airdried, then incubated in 5% milk in PBS for 30 minutes and immunostained according to section 3.2.5.9.

3.2.5.6 Electron microscopy

VLPs or PsVs samples (7 µL) were placed on Parafilm® (Merck) and adsorbed on formvar carbon or copper grids for 10 minutes. Then the grids were incubated for 1 min on the top of 100 µl water drop (two times) and 30 seconds on the top of 50 µl PTA drop (two times). After the incubation, grids were carefully dried with filter papers. The samples were visualized using a transmission electron microscope (JOEL JEM 1200EX).

3.2.5.7 SDS-PAGE

Sodium dodecyl sulphate–polyacrylamide gel electrophoresis (SDS-PAGE) was used to separate proteins according to their molecular weight. 5 µl of samples were mixed with 5 µl of buffer B and 3 µl of 5x Laemli buffer. The resulting mixture was boiled for 5 minutes, cooled to room temperature and then stored at -20°C or separated on SDS-PAGE directly. An apparatus (BioRad) was washed and assorted. First, the 10% separation gel was prepared as described in Table 3.9, poured into the apparatus and the top of the gel was layered with ddH_2O. In 30 minutes, the gel completely polymerized. Afterwards, the 5% stacking gel was mixed, applied on top of the separation gel and covered by combs to make wells. Glasses with polymerized gel were clamped into the apparatus, and both buffer chambers were filled with 1% running buffer. Molecular mass protein marker and samples were loaded into the wells. The gel ran at 80 V for 30 minutes and then at 140 V for 1-2 hours. The gel was taken from the apparatus, washed in ddH_2O and stained immediately in 20 ml of Imperial Protein Stain for 1.5 hour. Afterwards, the gel was washed with dH_2O and stained proteins were documented using Vilber Fusion Fx (BioConsult Laboratories).

Table 3.9: Gel mixture for SDS-PAGE

% Acrylamide (AA)	**Component**	**Volume**
5% stacking gel (5 mL)	AA	850 µL
	1M Tris, pH 6.8	650 µL
	10% SDS	50 µL
	ddH_2O	3.4 mL
	10% AP	20 µL
	TEMED	5 µL
10% separation gel (12 mL)	AA	4 mL
	1M Tris, pH 8.8	4.5 mL
	10% SDS	120 µL
	ddH_2O	3.25 mL
	10% AP	90 µL
	TEMED	8.5 µL

3.2.5.8 Western blot

SDS-PAGE gel containing separated proteins was washed in the blotting buffer for 10 minutes. Sponges, papers and Whatman™ Protran™ Nitrocellulose membrane (GE Healthcare Life Sciences) were submerged in the blotting buffer. The blot sandwich was assembled as follows: blotting sponge, four filter papers, one Whatman paper, polyacrylamide gel nitrocellulose membrane, one Whatman paper, four filter papers and blotting sponge. During each assembly step, bubbles were removed. The blot sandwich was put into the apparatus, the gel was oriented closer to the cathode. Proteins were transferred for 1.5-3 hours at 250 mA. The blot sandwich was disassembled, the membrane was washed twice with ddH_2O water for 5 minutes and proteins on the membrane were detected by specific antibodies.

3.2.5.9 Immunodetection after dot blot and Western blot

Nitrocellulose membrane was blocked in 5% milk in PBS for 1 hour. Afterwards, the membrane was incubated with primary antibody diluted in 5% milk in PBS for 1 hour and washed with PBS for 10 minutes, four times. The membrane was incubated with a secondary antibody conjugated with horseradish peroxidase diluted in 5% milk in PBS for 30 minutes. Then, the washing step was repeated and chemiluminescence solutions were prepared. The mix of solutions 1 and 2 (1:1) was poured onto the membrane and incubated for 30 sec. The excess of the solution was removed from the membrane and the chemiluminescent signal was visualized using Vilber Fusion Fx (BioConsult Laboratories).

3.2.5.10 ELISA assay

Antigens, VLPs or pseudovirions in PBS were coated to a surface of half area 96-well microtiter plate 50 ng/well, and adsorbed overnight at 4°C. After that, the wells were washed 4 times with PBS/0,1% Tween-20 (v/v) and blocked by 100 µl of the 5% milk (w/v) in PBS for 2 hours at room temperature. The blocking step was followed by incubation with sera serially diluted in 5% milk in PBS for 1 hour at room temperature. Wells were washed with PBS/0,1% Tween-20. A secondary antibody diluted in 5% milk in PBS was added (50 µL/well) and incubated for 30 minutes at room temperature. Then wells were washed with PBS/0,1% Tween-20 and ABTS substrate was added (50 µl/well). After 30 minutes, absorbance at 415 nm was measured using ELISA reader (Epoch BioTek). ELISA samples and negative controls were run in duplicates, triplicates or quadruplicates.

3.2.5.11 Antigen competition assay

Diluted human sera (1:100) were pre-incubated with PsVs in concentration 5 µg/mL on a rolling shaker overnight at 4°C. Samples were further serially diluted: rabbit sera 1:2,000;

1:4,000; 1:8,000 and 1:16,000; human sera: 1:200, 1:400, 1:800 and 1:1,600; and tested on ELISA as described in the section above. In the Results section, we showed measured OD values of rabbit and human sera in one dilution (1:2,000 and 1:200, respectively). In both cases, the serum reactivity in the lowest sera dilution enabled better comparisons after saturation with competing antigens.

3.2.5.12 Rabbit immunization

BKPyV-IV-EFmut PsVs were used for rabbit immunization performed by HENAntibody, s. r. o.

3.2.5.13 PsVs disassembly

PsVs fractions were placed into mini dialysis devices (Slide-A-Lyzer™ MINI Dialysis Device, 0.5 mL) and dialysed by two dialysis cycles, each 1.5 hours. The first cycle was against 20 mM Tris-HCl (pH 8.8), 50 mM NaCl, 2 mM DTT, and 5 mM EDTA at 4°C and the second cycle was against 20 mM Tris-HCl (pH 8.8), 50 mM NaCl, 2 mM DTT, 2 mM EDTA at 4°C. Disassembled particles were visualized using electron microscopy, measured for protein concentration and evaluated on ELISA.

3.2.6 Data analysis

3.2.6.1 Statistics

Key experiments performed using antigen competition assay ran in quadruplicates. To determine if the data are normally distributed, we performed the Shapiro-Wilk test. According to the outcome of this test, we used either one-way ANOVA with Welch and Brown-Forsythe test with Tamhane's T2 multiple comparisons test or Kruskal-Wallis with Dunn's post hoc test. This analysis was kindly performed by Hana Španielová using GraphPad Prism v. 8.0.1.

3.2.6.2 Phylogenetic tree construction

DNA sequences were aligned using the MUSCLE algorithm integrated into the AliView program. Using the Seaview program, aligned sequences were further used to construct a phylogenetic tree. A phylogenetic tree was constructed using the PhyML tool. Specifically, we used the maximum likelihood method (K80 substitution model). A gamma distribution (4 categories) modelled the sequence variability between positions. BKTyper tool (v1.0) was used to divide BKPyV sequences into four major genotypes (Martí-Carreras et al., 2020).

3.2.6.3 Selection analysis

The selection analysis was performed using the HyPhy tool integrated into the Datamonkey web interface (https://www.datamonkey.org/). Specifically, the FEL (Fixed Effects Likelihood) approach was used (Kosakovsky Pond and Frost, 2005). This approach test a ratio of synonyms (α) and of non-synonymous (β) substitutions at specific amino acid positions and identifies sites which may have experienced positive, negative or neutral selection.

4. Results

So far, it is impossible to serologically distinguish between the BKPyV subtypes due to the cross-reaction of BKPyV serum antibodies without the need to implement a neutralization assay. The main aim of this project is to identify epitopes involved in the cross-reactivity against BKPyV subtypes I and IV. This project follows up on previous research of Tomanová (2019) conducted in our laboratory, which aimed to develop antigens with the potential to bind subtype-specific antibodies. This potential was further investigated in this work while using new antigens designed by Tomanová (2019) as competing antigens in antigen competition assay performed on the panel of human serum samples from KTx recipients.

In our laboratory, we use both PsVs and VLPs as antigens for serum testing. We are aware that the term pseudovirion correctly refers to a viral particle that carries a reporter plasmid. However, in this thesis, we refer to all viral particles produced in mammalian cells as PsVs, and to viral particles produced using baculoviruses in insect cells as VLPs. In the case of PsVs, we transfect cells with plasmids encoding the major structural protein of BKPyV (VP1). Generally, VP1 monomers of all polyomaviruses have the ability to self-assemble into viral capsids and form viral particles, pseudovirions in our case. PsVs created previously by Tomanová (2019) to capture subtype-specific antibodies were based on the VP1 sequence of BKPyV-IV; however, they had specific mutations characteristic for BKPyV-I. These mutations were located in the surface loops of the VP1 protein.

VP1 monomer within the pentamer has four loops on the surface: BC, DE, EF and HI loop. BC loop is called a hyper-variable region as it usually accumulates many mutations, and the differences between BKPyV subtypes I and IV cluster in this loop. Furthermore, the BC loop is crucial for BKPyV biology as it binds cell receptors and neutralizing antibodies. However, neutralizing antibodies were shown to target not only the BC loop but the neighbouring EF and DE loops as well Lindner et al. (2019).

When designing antigens with the potential to identify molecular determinants for binding subtype-specific antibodies in serum, Tomanová (2019) focused on the less explored DE and EF loops, which differ only in a few amino acids between the two BKPyV subtypes. Tomanová (2019) introduced one and two point-mutations specific for subtype I to the plasmid encoding the VP1 protein of the BKPyV-IV subtype. The first point mutation was in the DE loop at position 139, histidine was substituted for asparagine (H139N). In the EF loop, two point mutations were introduced (D175E and I178V). Figure 4.1 shows the exact position of these mutations in the VP1 monomer. Such mutated plasmids were used for the transfection of a mammalian cell line (293TT), VP1 protein was expressed and formed mutant pseudovirions named BKPyV-IV-DEmut and BKPyV-IV-EFmut.

Tomanová (2019) tested the reactivity of mutant PsVs with hyperimmune rabbit and hu-

man sera on ELISA. Preliminary data showed that BKPyV-IV-DEmut reacted more than its parent antigen BKPyV-IV when tested with serum samples cross-reacting with both antigens. This indicates that the DE loop might be a critical epitope for cross-reactivity. Nevertheless, BKPyV-IV-EFmut in the same study did not react with any of the sera tested. We did not expect a complete loss of reactivity, as BKPyV-IV-EFmut differs from its parent BKPyV-IV in only two amino acids. This thesis project builds on the preliminary results from the work of Tomanová (2019) and further verifies the role of DE and EF loop in serological cross-reactivity against BKPyV subtypes I and IV using previously designed antigens BKPyV-IV-DEmut and BKPyV-IV-EFmut.

Figure 4.2 shows a scheme of the main experimental work done in this thesis. First, we isolated plasmids, which were further needed for transfection and production of PsVs. We purified four types of PsVs: two control (BKPyV-I and BKPyV-IV) and two mutant (BKPyV-IV-DEmut and BKPyV-IV-EFmut). The presence of PsVs was verified in a three-step analysis using immunodetection (dot blot), SDS-PAGE and TEM. Then, we measured the protein concentration of chosen PsVs fractions and used these PsVs 1) to analyse serological cross-reactivity and 2) to analyse the influence of mutations introduced in exposed loops of VP1 monomer.

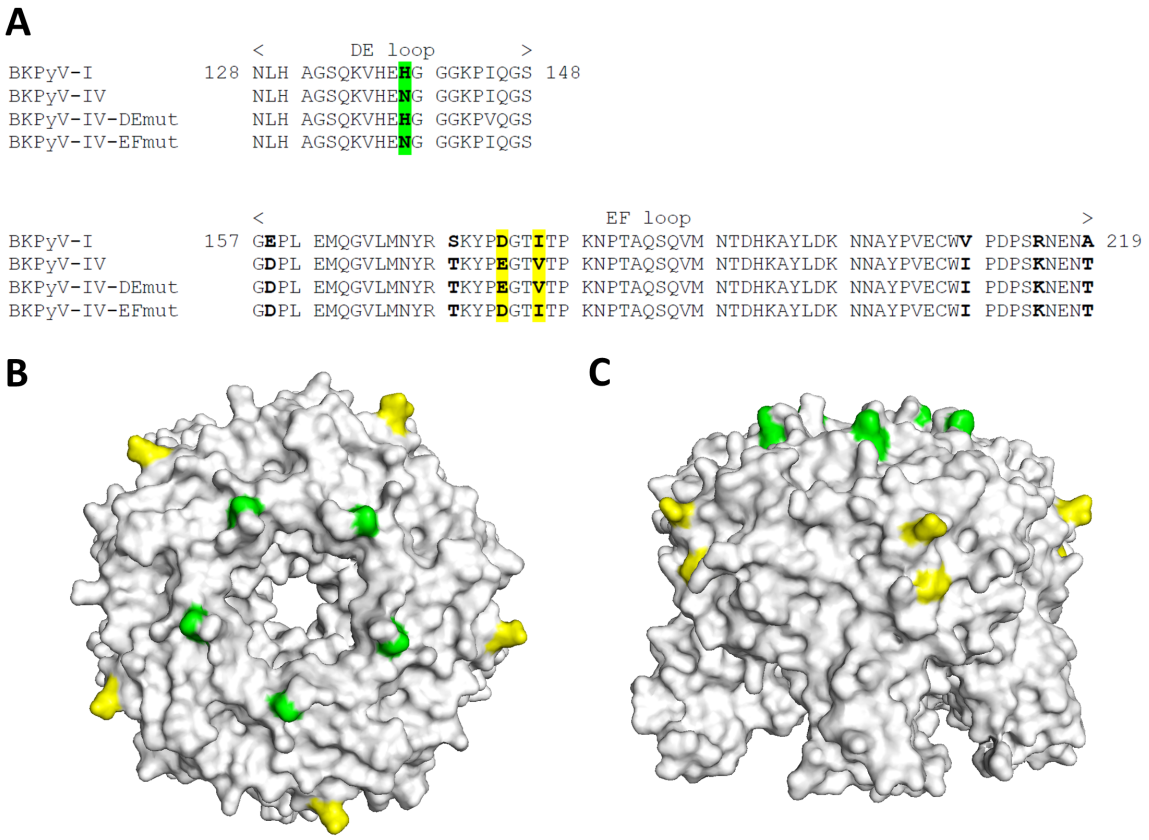

Figure 4.1: Alignment of A) DE loop and EF loop of VP1 protein. Two mutant PsVs, BKPyV-IV-DEmut and BKPyV-IV-EFmut, are based on BKPyV-IV and contain mutations characteristic for BKPyV-I: one point-mutation (N139H) in the DE loop (green), and two point-mutations in EF loop (E175D and V178I, yellow). Amino acid differences between subtypes I and IV are marked in bold letters. The structure model of the BKPyV VP1 pentamer B) view from above and C) side view with introduced mutations. The structure was generated using PyMOL based on the model (RCSB data bank, entry code 4MJ1) published by Neu et al. (2013).

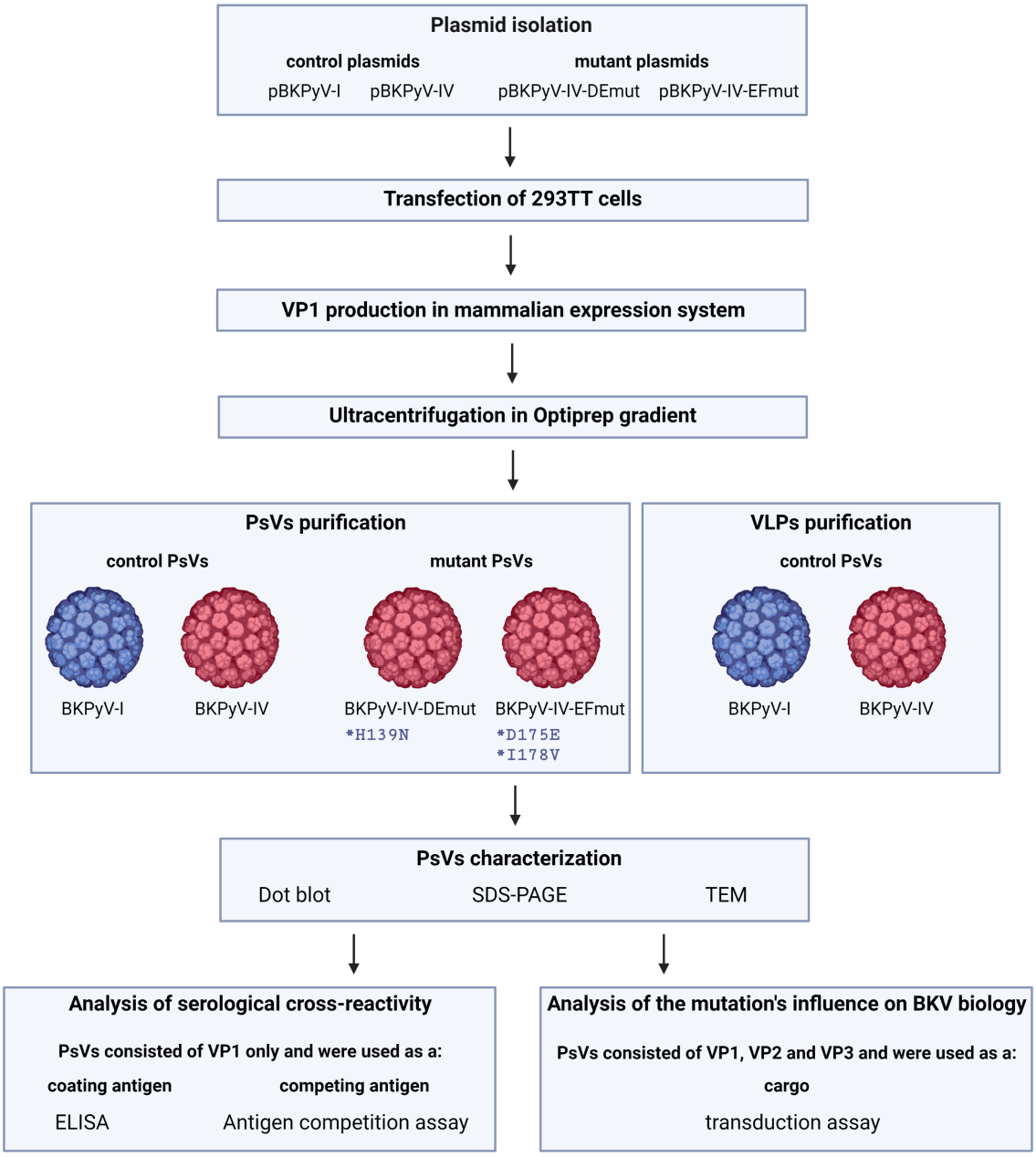

Figure 4.2: Simplified project scheme. We isolated plasmids and used them for the transfection of 293TT cells. Two days post-transfection, we harvested cells and purified viral protein VP1 using ultracentrifugation in Optiprep gradient. Then, we isolated four types of PsVs: control PsVs (BKPyV-I and BKPyV-IV) and mutant PsVs (BKPyV-IV-DEmut and BKPyV-IV-EFmut). PsVs based on BKPyV subtype I are shown in blue, and PsVs based on BKPyV subtype IV are in red. This scheme was created with Biorender.com.

4.1 The role of DE and EF loop of BKPyV VP1 in serological cross-reactivity

In this part of the project, we focused on defining the role of DE and EF loops of BKPyV VP1 in serological reactivity against BKPyV subtypes I and IV. Our goal was to analyze the capacity of mutant PsVs, BKPyV-IV-DEmut and BKPyV-IV-EFmut, to capture subtype-specific or cross-reactive antibodies, compared to control PsVs represented by naturally occurring BKPyV-I and BKPyV-IV subtypes. We hypothesised that mutant PsVs could be potentially better at eliminating cross-reactivity than control PsVs, and thus could serve as a good competing antigen in the antigen competition assay.

4.1.1 Plasmid isolation

We isolated four different plasmids harbouring different coding sequences for BKPyV VP1 protein under the control of EF1 promotor, and one of them (pBKV-I) also encodes genes for EGFP. Schematic representation of all four plasmids with their coding regions is shown in Figure 4.3. The first control plasmid, pBKPyV-I, encodes VP1 of the BKPyV-I subtype; and the second control plasmid, pBKPyV-IV, encodes VP1 of the BKPyV-IV subtype. Other plasmids, pBKPyV-IV-DEmut and pBKPyV-IV-EFmut, were previously created by site-directed mutagenesis of the original pBKPyV-IV (Tomanová, 2019). pBKPyV-IV-DEmut and pBKPyV-IV-EFmut carry specific mutations in the surface-exposed loops of VP1 protein in DE and EF loops, respectively. After the isolation of these plasmids, they were verified by digestion with restriction endonucleases and gel electrophoresis. Example verification of two plasmids (pBKPyV-IV-EFmut and pBKPyV-IV) is shown in Figure 4.4. All four plasmids were digested with three restriction endonucleases (EcoRI, EcoRV and BamHI) as expected.

4.1.2 Pseudovirions isolation

After we completed the isolation of four plasmids: pBKPyV-I, p-BKPyV-IV, pBKPyV-IV-DEmut and pBKPyV-IV-EFmut, we could proceed with the following step: PsVs isolation. The amount of PsVs obtained after isolation differs among the PsVs types, thus, for BKPyV-IV, several isolations were performed. However, BKPyV-IV-EFmut was isolated several times as it was the only antigen used for rabbit immunization (see section 4.1.4) for which a lot of material was needed. First of all, we transfected isolated plasmids into mammalian cell line 293TT. Two days post-transfection, we observed the signal of green-fluorescent protein in the case of pBKV-I as it was the only plasmid encoding control EGFP. In this case, we counted the number of transfected cells and calculated the transfection efficiency between 10 - 20 % (data not shown). Cells were harvested, and PsVs were purified from lysates using ultracentrifugation in an Optiprep gradient. After ultracentrifugation,

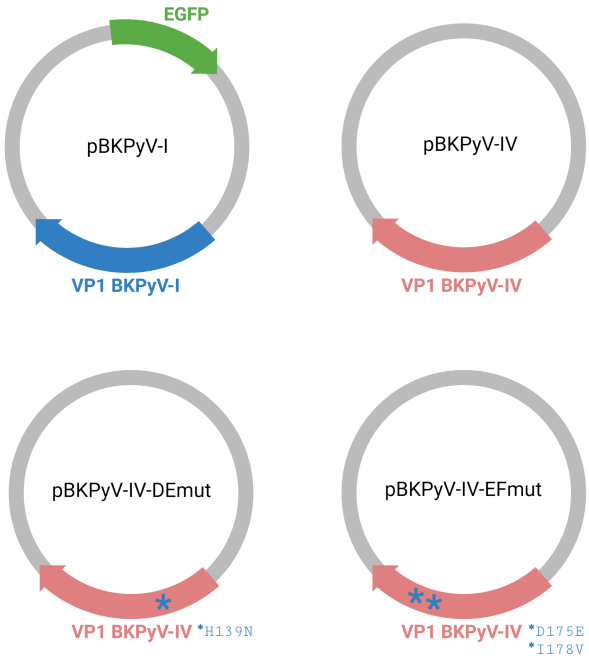

Figure 4.3: Schematic representation of plasmids used for cell transfection and subsequent isolation of PsVs. Arrows represent coding sequences of viral protein 1 (VP1) and enhanced green fluorescent protein (EGFP). Plasmids pBKPyV-IV-DEmut and pBKPyV-IV-EFmut are mutated in surface-exposed DE and EF loops resulting in the following amino acid substitutions: H139N and D175E, I178V.

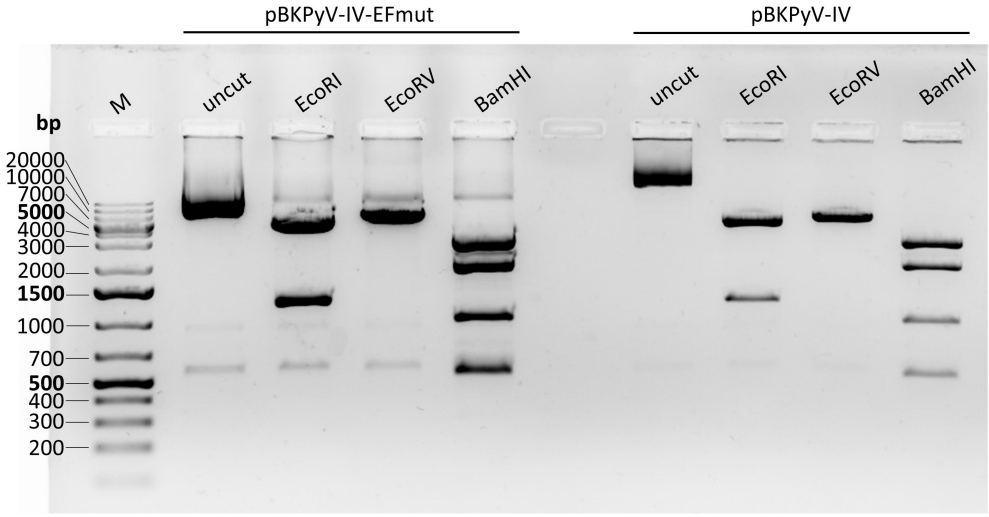

Figure 4.4: Restriction enzyme digestion of two plasmids (pBKPyV-IV-EFmut and pBKPyV-IV) shown after separation on 1% agarose gel. Plasmids were digested with three restriction endonucleases (EcoRI, EcoRV and BamHI). In both cases, EcoRI produced two bands of 5,210 and 1,217 bp; digestion with EcoRV resulted in the linearization of the plasmids, which produced a band of 6,427 bp representing the full plasmid size; and BamHI produced four bands 515; 986; 1,944 and 2,982 bp long. M - marker.

the gradient was separated into fractions (200 - 500 µL each).

Further, the presence and quality of PsVs in different fractions were verified in a three-step analysis. As a first step, the presence of VP1 protein was confirmed using immunodetection (dot blot) with polyclonal antibodies against SV40 VP1. These antibodies were previously shown to reliably detect BKPyV variants and mutants generated in our laboratory Sekavová (2017). Figure 4.5 shows that a strong positive signal was detected in each gradient (BKPyV-I, BKPyV-IV, BKPyV-IV-DEmut and BKPyV-IV-EFmut), which indicates that we managed to isolate VP1 protein successfully. However, as shown in Figure 4.5, the distribution of the VP1-rich fractions differed in the case of BKPyV-IV-DEmut and BKPyV-IV-EFmut. This result probably implies that the introduction of mutations in DE and EF loops changed the nature of epitopes recognized by antibodies against SV40 VP1 and that this antibody bound more preferably disassembled VP1 of mutant PsVs. Dot blot analysis was also performed with antibodies against BKPyV-I and BKPyV-IV VP1; however, this analysis was too sensitive as it detected signals in all fractions (data not shown). As a second step, SDS-PAGE and staining of polyacrylamide gels were performed to measure the molecular weight of the isolated protein, which corresponded to the molecular weight of VP1 - 42 kDa (Fig. 4.6). SDS-PAGE proved to be more accurate than dot blot analysis and helped us to reveal that fractions 1 - 4 usually contained the highest amounts of VP1. We found one exception in the first isolation of BKPyV-IV-EFmut. However, fractions of this isolation had approximately two times lower volume; therefore, VP1 was found in fractions 1 - 8. As a third step, the quality of VP1-rich fractions was checked on TEM. TEM images revealed assembled PsVs mostly in fractions 1 - 3 (Fig. 4.7), whereas fractions number 4 usually contained disassembled material (data not shown). In the case of the first isolation of BKPyV-IV-EFmut, we found assembled PsVs in fractions 1.2 - 1.7. Taken together, the three-step analysis identified fractions containing assembled PsVs, which could, thus, serve as a good antigen for serology testing. Table 4.1 provides detailed information about fractions and their protein concentration, which was measured using Bradford assay.

4.1.3 VLPs isolation

To isolate the second type of antigen necessary for serology testing (VLPs), we infected Sf9 cells with a viral inoculum containing baculovirus expressing BKPyV VP1 of two subtypes: BKPyV-I and BKPyV-IV. Cells were harvested three days post-infection and lysed using sonication. Samples were first ultracentrifuged through 10% sucrose for 3 hours 30 minutes and then in cesium chloride gradient for 20 hours.

After ultracentrifugation, the gradient was separated into fractions (0.5 mL each), and the presence of VLPs in fractions was verified using a three-step analysis. First, we performed a dot blot to detect fractions containing VP1 (Fig. 4.8). In both gradients (BKPyV-I and

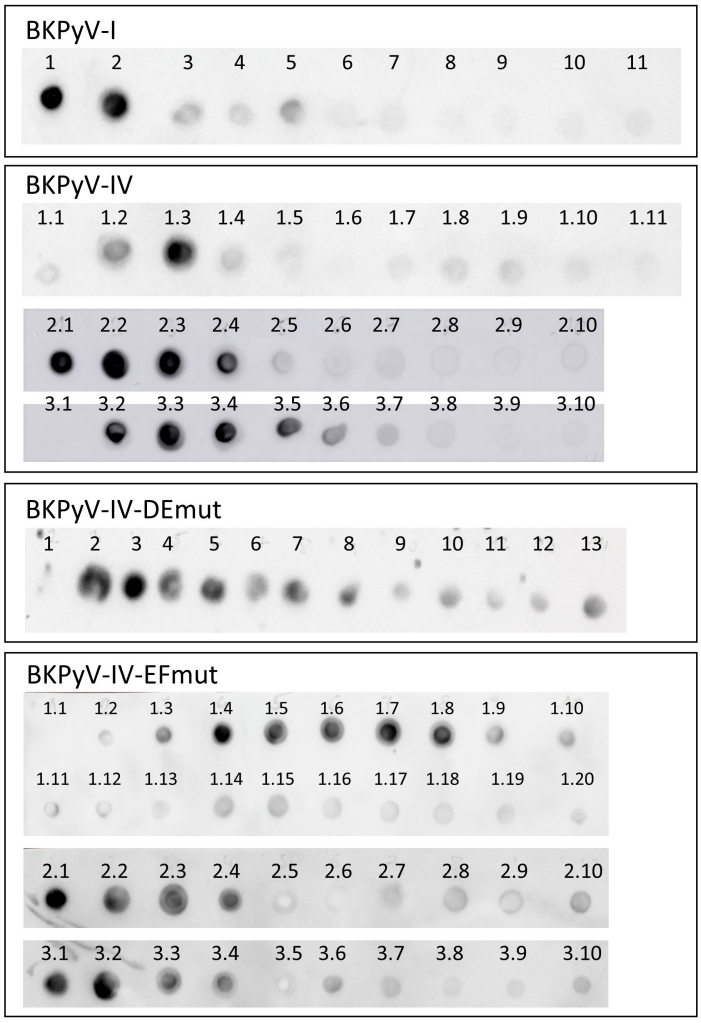

Figure 4.5: Immunodetection of VP1 protein (dot blot) after isolation in Optiprep gradient. The same amount of each fraction was loaded on the nitrocellulose membrane. The membrane was stained with primary antibody RbαSV40 followed by secondary antibody conjugated with horseradish peroxidase. Numbers correspond to numbers of fractions.

Table 4.1: PsVs fractions used for further analysis. Concentration was measured by Bradford assay.

Antigen type	BKPyV variant	Fraction	Concentration (µg/mL)
PsVs	BKPyV-I	fr. 1	1016
		fr. 2	648
		fr. 3	347
	BKPyV-IV	fr. 1.1	75
		fr. 1.2	275
		fr. 2.1	649
	BKPyV-IV-DEmut	fr. 2	664
	BKPyV-IV-EFmut	fr. 1.4	207
		fr. 1.5	791
		fr. 1.7	407
		fr. 2.1 + 3.1	174
		fr. 2.2	1289

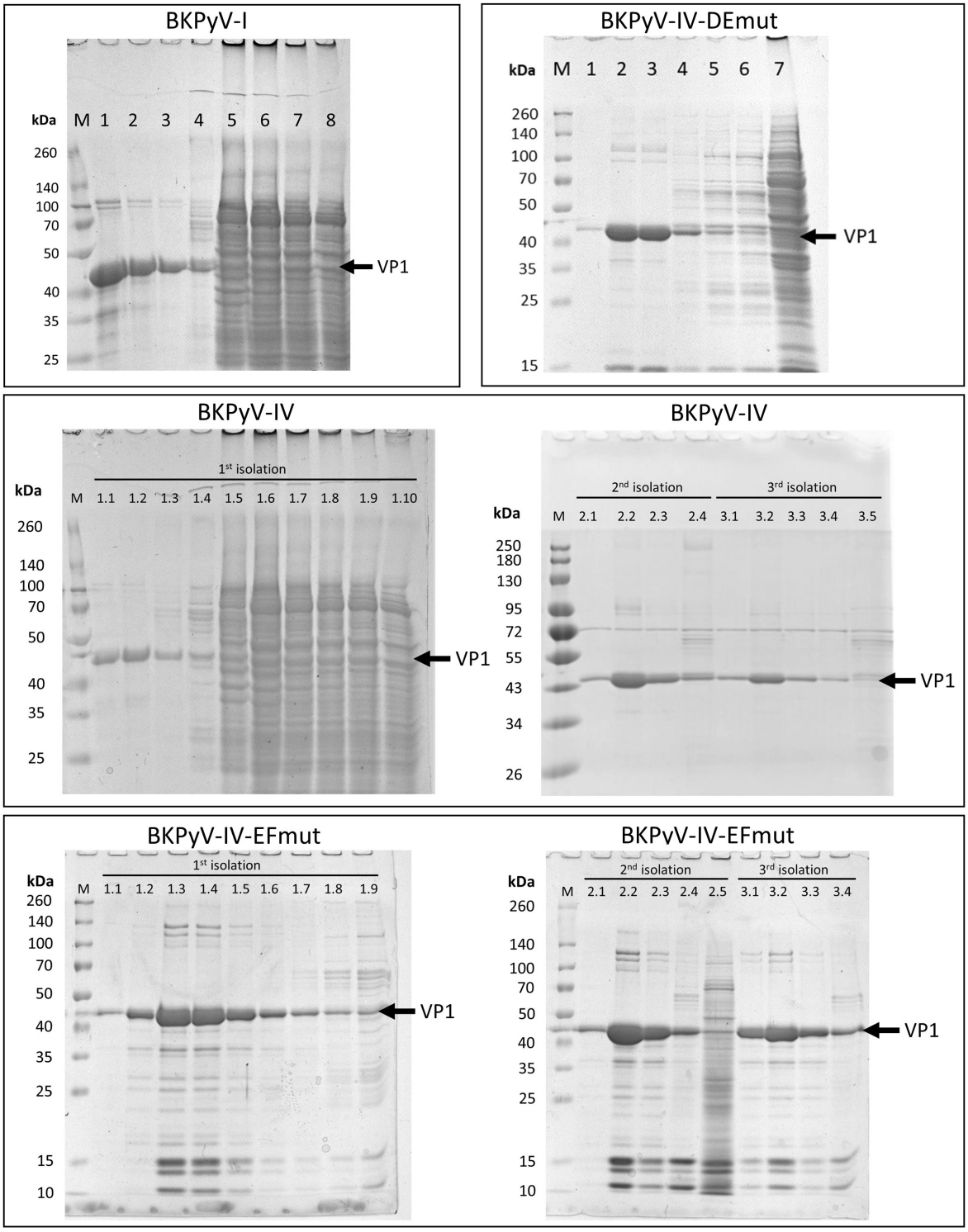

Figure 4.6: Representation of selected VP1 fractions after isolations of BKPyV-I, BKPyV-IV, BKPyV-IV-DEmut and BKPyV-IV-EFmut on polyacrylamid gels. The same amount of each fraction was loaded on the 10% gel. After electrophoresis, the proteins in the gel were stained with Imperial Protein Stain. Arrows indicate the presence of the 42-kDa VP1 protein. M - marker, 1 - fraction 1, 2 - fraction 2, etc.

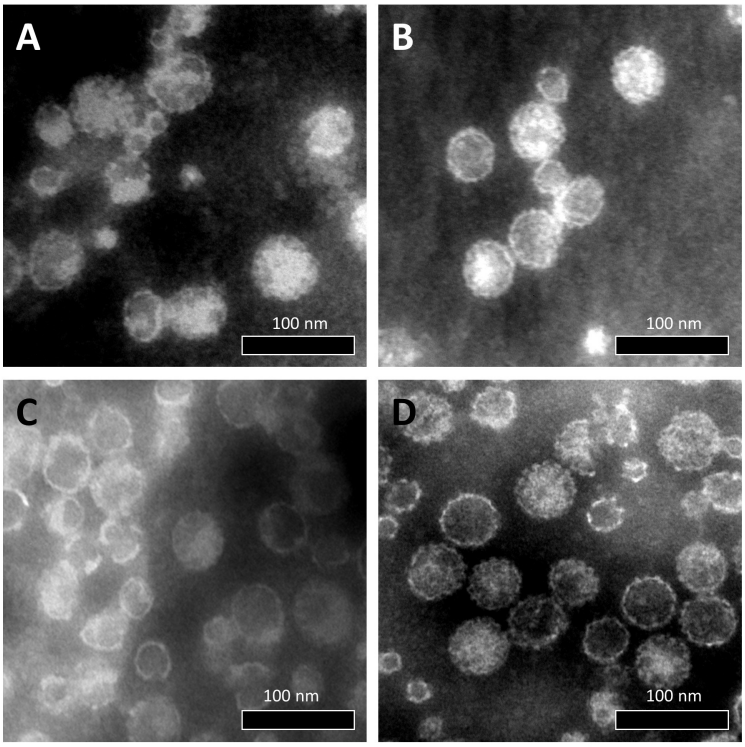

Figure 4.7: TEM images show selected VP1-rich fractions of A) BKPyV-I (fraction 2), B) BKPyV-IV (fraction 1.2), C) BKPyV-IV-DEmut (fraction 2), D) BKPyV-IV-EFmut (fraction 7). Samples were stained with PTA and visualized using electron microscopy.

BKPyV-IV), the strongest signal for VP1 was in the fractions 7 - 11. We also measured the refractive index in all fractions (Table 4.2). Based on the results from these two analyses, we combined selected fractions as shown in Table 4.2. These fractions were further dialyzed against buffer B. To confirm the presence of assembled VLPs in combined fractions, we visualized them using electron microscopy (Fig. 4.9) and measured protein concentration using Qubit Fluorometer in combined fractions (Table 4.3).

Figure 4.8: Immunodetection of VP1 protein (dot blot) after isolation in the gradient of cesium chloride. The same amount of each fraction was loaded on the nitrocellulose membrane. The membrane was stained with primary antibody RbαSV40 followed by secondary antibody conjugated with horseradish peroxidase. Numbers correspond to numbers of fractions.

Table 4.2: Refractive index was measured in all BKPyV-I and BKPyV-IV VLPs fractions. According to signals detected in dot blot analysis and refractive index values, fractions were combined, as shown in this table. Fr. - fraction. VLPs - virus-like particles.

Fr.	BKPyV-I VLPs refractive index	BKPyV-I VLPs combined fractions	BKPyV-IV VLPs refractive index	BKPyV-IV VLPs combined fractions
1	1,373	not combined	1,371	not combined
2	1,372		1,371	
3	1,369		1,368	
4	1,367	I	1,367	
5	1,365		1,365	I
6	1,364		1,364	
7	1,364	II	1,363	
8	1,363		1,363	
9	1,363	III	1,362	II
10	1,362		1,361	
11	1,360		1,360	III
12	1,359	IV	1,359	
13	1,358		1,357	

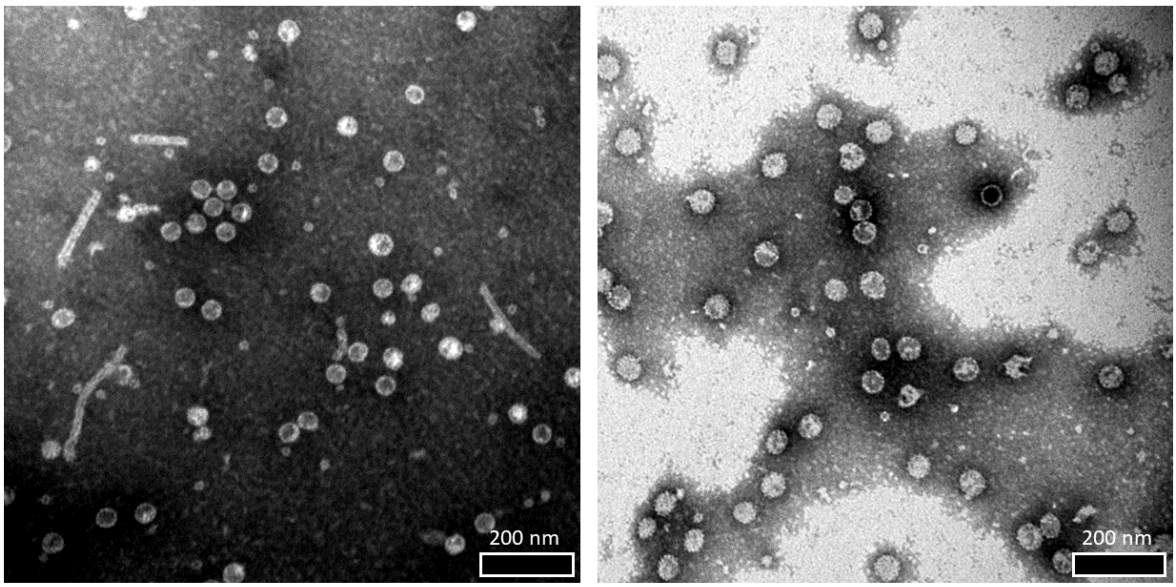

Figure 4.9: TEM images show combined fractions of BKPyV-I VLPs (left, fraction II) and BKPyV-IV VLPs (fraction II). Samples were stained with PTA and visualized using electron microscopy.

Table 4.3: Protein concentration of combined BKPyV-I and BKPyV-IV VLPs fractions. Protein concentration was measured using a Qubit fluorometer (Invitrogen).

Fraction	BKPyV-I VLPs concentration (µg/mL)	BKPyV-IV VLPs concentration (µg/mL)
I	104	74
II	98	91
III	159	108
IV	254	—

4.1.4 Rabbit immunization with PsVs BKPyV-IV-EFmut

Preliminary experiments conducted in our laboratory showed that one of the mutant PsVs (BKPyV-IV-EFmut) are almost non-reactive when tested on ELISA (Tomanová, 2019). Therefore, we hypothesised that mutation in the EF loop resulted in the decreased immunogenic potential of the BKPyV antigen. To investigate this hypothesis, we combined three BKPyV-IV-EFmut PsVs fractions 1.4, 1.5 and 2.2 (shown in Fig. 4.10) and used them for rabbit immunization (performed by HENAntibody, s.r.o.).

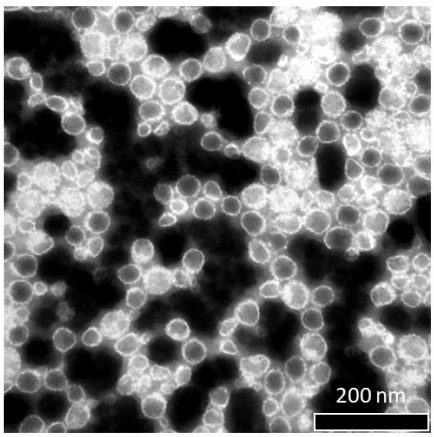

Figure 4.10: TEM image shows combined fractions 1.4, 1.5 and 2.2 containing PsVs BKPyV-IV-EFmut, which were used for rabbit immunization. The sample was stained with PTA and visualized using electron microscopy.

4.1.5 Titration of rabbit sera

First, serum RbαBKPyV-IV-EFmut was tested on ELISA to confirm that specific antibody response against BKPyV-IV-EFmut PsVs was stimulated. We tested the reactivity of serially diluted RbαBKPyV-IV-EFmut serum with mutant PsVs and control VLPs using ELISA (Fig. 4.11). Antibody titre was the highest against homologous antigen BKPyV-IV-EFmut followed by the other mutant PsVs BKPyV-IV-DEmut and control BKPyV-IV and BKPyV-I. This result shows that BKPyV-IV-EFmut was able to stimulate a strong antibody response and that mutations in the EF loop did not decrease its immunogenic potential.

In this experiment, we used VLPs as control particles, since the use of VLPs as antigens is a long-established system in our laboratory. Later, we also showed that VLPs and PsVs react similarly (see section 4.1.8), which implies that these two types of antigens consisting of VP1 can be used in ELISA settings interchangeably.

Second, we determined the titer of BKPyV antibodies using ELISA in two rabbit sera, RbαBKPyV-I and RbαBKPyV-IV (Fig. 4.12). We serially diluted both sera and added them to an ELISA plate coated with BKPyV-I and BKPyV-IV VLPs.

Our goal was to select a serum dilution in which cross-reactivity with the heterologous

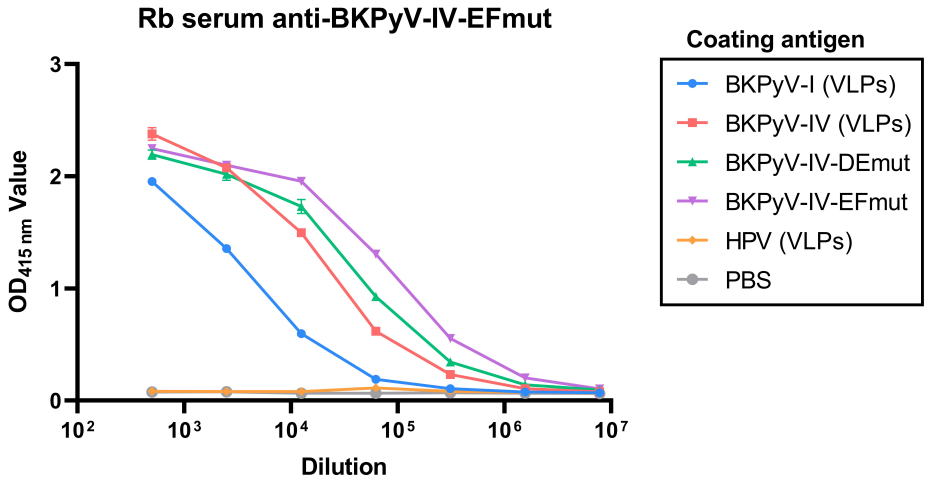

Figure 4.11: Titration of rabbit antiserum against BKPyV-IV-EFmut PsVs (tested on ELISA). Serum was added in serial dilution, and the reactivity with five antigens was tested. Coated PBS and VLPs of human papillomavirus (HPV) were used as a negative control. Experiments were conducted in duplicates. Reactivity is shown as mean absorbance ($OD_{415\ nm}$ value), and error bars represent SDs.

antigen would still be relatively high because the next experiment, antigen competition assay, aims to eliminate this cross-reactivity. Based on the results shown in Figure 4.12, we choose serum dilution 1:10,000 for both RbαBKPyV-I and RbαBKPyV-IV.

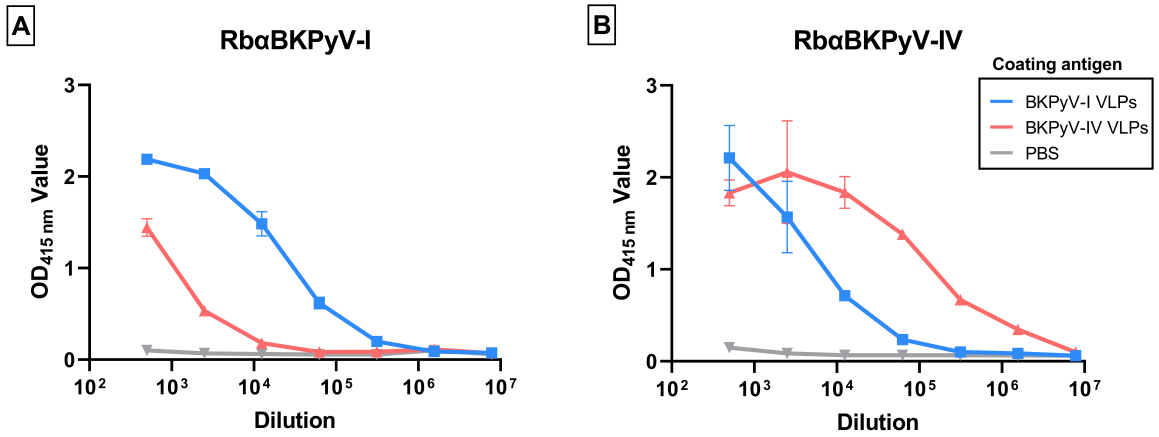

Figure 4.12: Reactivity of serially diluted rabbit serum samples with BKPyV VLPs was tested on ELISA. ELISA plate was coated with BKPyV-I VLPs, BKPyV-IV VLPs and PBS (negative control). Then, two rabbit sera, A) RbαBKPyV-I and B) RbαBKPyV-IV, were added to the plate in 5-fold serial dilutions. Experiments were conducted in duplicates. Reactivity is shown as mean $OD_{415\ nm}$ value, and error bars represent SDs.

4.1.6 Reactivity of rabbit sera with control and mutant PsVs

Previous experiments conducted by Tomanová (2019) tested the reactivity of both mutant and control PsVs with rabbit (RbαBKPyV-I and RbαBKPyV-IV) and human sera. BKPyV-

IV-DEmut reacted on ELISA slightly more than control BKPyV-IV PsVs. BKPyV-IV-EFmut PsVs, on the other hand, reacted much less than all other PsVs, with OD values being even below cut-off values (Tomanová, 2019). This result was unexpected, as BKPyV-IV-EFmut differs from BKPyV-IV only in two amino acids. Our goal was to repeat the same experiment to confirm the previously observed influence of mutated epitopes, DE and EF loop, on antibody response.

We tested three rabbit serum samples RbαBKPyV-I, RbαBKPyV-IV and RbαBKPyV-IV-EFmut on ELISA with coated PsVs. Figure 4.13.A,B,C shows that the reactivity of each serum was the highest with its cognate antigen; BKPyV-I, BKPyV-IV and BKPyV-IV-EFmut PsVs, respectively. What can be seen in Figure 4.13.A is that BKPyV-IV-DEmut binds more BKPyV-I subtype-specific antibodies than BKPyV-IV. This result is consistent with the previous study of Tomanová (2019) and supports our hypothesis that BKPyV-IV-DEmut could serve as a better competing antigen than BKPyV-IV itself. However, BKPyV-IV-EFmut PsVs that showed previously almost zero reactivity now reacted similarly to the original BKPyV-IV (Fig. 4.13.A,B,C). We believe that the previous lack of reactivity observed by Tomanová (2019) may be due to inaccuracies or contamination during the isolation protocol (e.g., DNA contamination). However, the exact causes are unknown, and we did not investigate them further.

Interestingly, in Figure 4.13.B we observed a lower level of cross-reactivity on PsVs-based antigens than was observed in Figure 4.12.B on VLPs-based antigens, even though the amount of coating antigens was the same. We decided to investigate this discrepancy further.

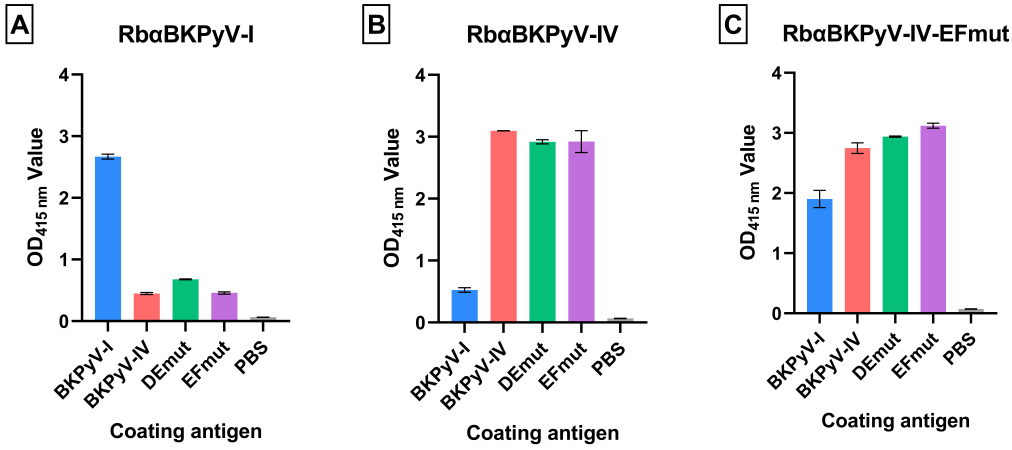

Figure 4.13: Reactivity of three rabbit serum samples A) RbαBKPyV-I, B) RbαBKPyV-IV and C) RbαBKPyV-IV-EFmut with BKPyV PsVs antigens. Sera were diluted 1:10,000 and reacted with four coated antigens: BKPyV-I, BKPyV-IV, BKPyV-IV-DEmut and BKPyV-IV-EFmut PsVs. PBS was coated as a negative control. Experiments were conducted in duplicates. Reactivity is shown as mean $OD_{415\ nm}$ value, and error bars represent SDs.

4.1.7 Reactivity of rabbit sera with PsVs and VLPs

For the titration in Figure 4.12, we used VLPs previously isolated in our laboratory. However, in the experiment shown in Figure 4.13, we used PsVs isolated as a part of this project. Therefore, we first examined whether using a different antigen (VLPs vs PsVs) could be responsible for the reduced cross-reactivity of RbαBKPyV-IV. This issue was also previously investigated in the work of Tomanová (2019) with the result that VLPs of both subtypes reacted on ELISA significantly more than PsVs. Data of Tomanová (2019) were supported by two experiments, one with rabbit sera and one with human IgG (Cytotect CP).

Our first goal was to repeat the same ELISA experiment as Tomanová (2019) with rabbit sera and two types of antigens: VLPs and PsVs. Figure 4.14.B showed that RbαBKPyV-IV reacted more with BKPyV-I VLPs than BKPyV-I PsVs. Apart from that, VLPs and PsVs seem to respond similarly (Figure 4.14.A,B). Although we observed higher reactivity of VLPs than PsVs, it happened only as an isolated event in the case of RbαBKPyV-IV experimental rabbit sera tested on BKPyV-I derived antigens.

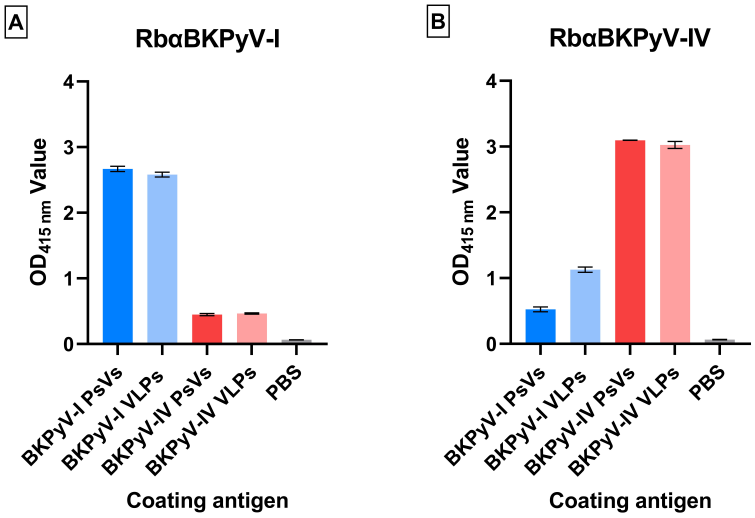

Figure 4.14: Reactivity of PsVs and VLPs with two rabbit serum samples A) RbαBKPyV-I and B) RbαBKPyV-IV was tested on ELISA with four antigens: BKPyV-I PsVs, BKPyV-I VLPs, BKPyV-IV PsVs and BKPyV-IV VLPs to compare the reactivity of PsVs and VLPs of both subtypes. This experiment runs in duplicates. Reactivity is shown as $OD_{415\ nm}$, and error bars represent SDs. PBS was coated as a negative control.

4.1.8 Reactivity of human sera with PsVs and VLPs

In the previous experiment with rabbit sera, we observed the discrepancy in reactivity of BKPyV-I PsVs and VLPs only when tested with RbαBKPyV-IV serum (Fig. 4.14). To further investigate the difference between the reactivity of these two types of antigens, we tested 21 human serum samples. Serum samples with absorbance values for either PsVs or VLPs,

which were below the cut-off value ($OD_{415\ nm}$ = 0.215), were not involved in the analysis. In the end, we got 19 serum samples and tested them on ELISA with coated BKPyV-I PsVs and VLPs. We measured $OD_{415\ nm}$ values and examined the relative difference in these OD values of PsVs and VLPs (with respect to PsVs values). Results show that PsVs and VLPs of BKPyV-I reacted similarly, with the median value being -1% (Fig. 4.15). Figure 4.15 shows that for all samples except for two outliers, the difference in reactivity was less than 10% and for eight samples, it was 2% or even less.

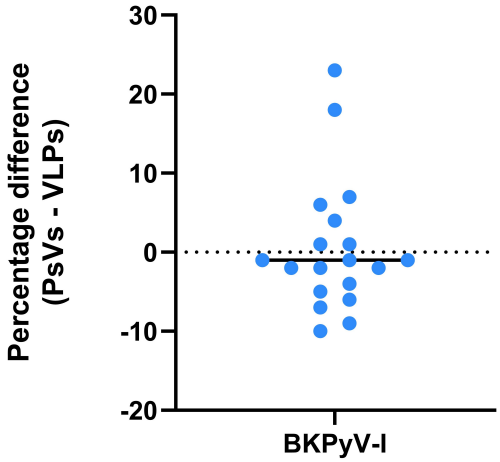

Figure 4.15: The relative difference in reactivity of PsVs and VLPs. We tested 19 human serum samples on ELISA with two antigens (BKPyV-I PsVs and BKPyV-I VLPs) to compare the reactivity of PsVs and VLPs of both subtypes. The black lines represent the median value (-1%).

We proved that PsVs and VLPs react on ELISA similarly with human sera, yet we did not elucidate previously observed differences in reactivity when tested with rabbit serum. Subsequently, we took a closer look at TEM images of tested batches of both BKPyV-I VLPs and PsVs and revealed that BKPyV-I VLPs contained not only assembled VLPs but also a lot of disassembled VP1 (Fig. 4.16). Therefore, we decided to analyze further the potential implications of a coated disassembled antigen for BKPyV diagnostics.

4.1.9 Serum reactivity with disassembled VLPs and PsVs

To answer the question if the quality of antigens in ELISA settings could be partly responsible for the serum cross-reactivity, we compared the reactivity of two VLPs fractions (Fig. 4.16). The first fraction contained a lot of disassembled VP1 (Fig. 4.16.A) and the second fraction contained mainly assembled VLPs (Fig. 4.16.B). On ELISA, we tested the reactivity of RbαBKPyV-IV serum with these two BKPyV-I VLPs fractions and one BKPyV-IV VLPs fraction (Fig. 4.17). From this data, we can see that the serum reacted more with BKPyV-I VLPs fraction A, which contained partly disassembled VP1 than with fraction B, which was composed of assembled VLPs.

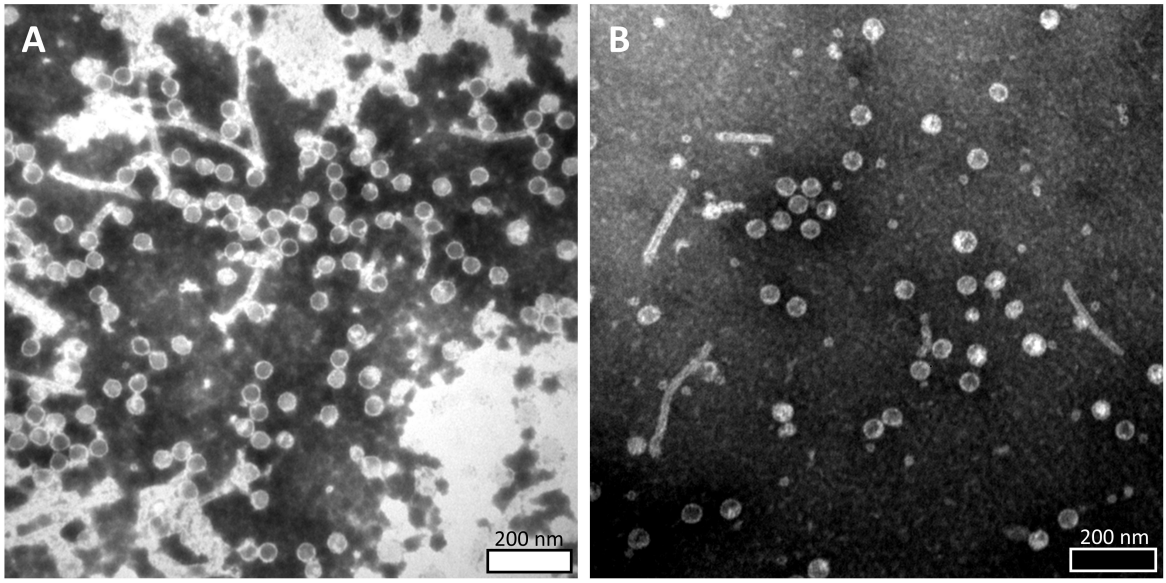

Figure 4.16: TEM images show selected fractions of BKPyV-I VLPs A) fraction II (previously isolated in our laboratory) and B) fraction II (isolated earlier in this project). Samples were stained with PTA and visualized using electron microscopy.

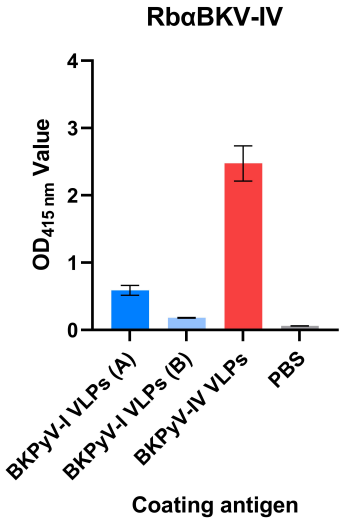

Figure 4.17: Reactivity of rabbit sera (RbαBKPyV-IV) with two BKPyV-I VLPs fractions was tested using ELISA. First, the ELISA plate was coated with BKPyV-I VLPs from fractions A and B (see Fig. 4.16), BKPyV-IV VLPs and PBS (coated as a negative control). Then, serum was added in standard dilution 1:10,000. This experiment ran in triplicates. Serum reactivity is shown as the mean absorbance ($OD_{415\ nm}$ value) of each sample. Error bars represent standard deviations (SDs).

To further evaluate the impact of disassembled antigen on the cross-reactivity of human sera, we disassembled BKPyV-I and BKPyV-IV PsVs and used them as coating antigens. We tested two rabbit (RbαBKPyV-I and RbαBKPyV-IV) and two human serum samples. One human serum sample reacted preferentially with BKPyV-I PsVs, the other with BKPyV-IV PsVs (Fig. 4.18).

Unexpectedly, a discrepancy between the reactivity of assembled and disassembled PsVs was evident in the case of RbαBKPyV-IV (Fig. 4.18.B), however, not in its human counterpart (Human serum sample 30, Fig. 4.18.D), which also reacted more with BKPyV-IV antigen. This result can be explained by the possibility that RbαBKPyV-IV originated from a rabbit immunization by a half-disassembled antigen. BKPyV-I and BKPyV-IV subtypes differ mainly in the surface-exposed loop, as was shown previously in VP1 alignment in Figure 1.3. Epitopes buried inside the capsid share more similarities; therefore exposure of buried BKPyV-I epitopes could cause increased reactivity with experimental RbαBKPyV-IV. Overall, a disassembled antigen only played a role in serum cross-reactivity in the experimental rabbit system.

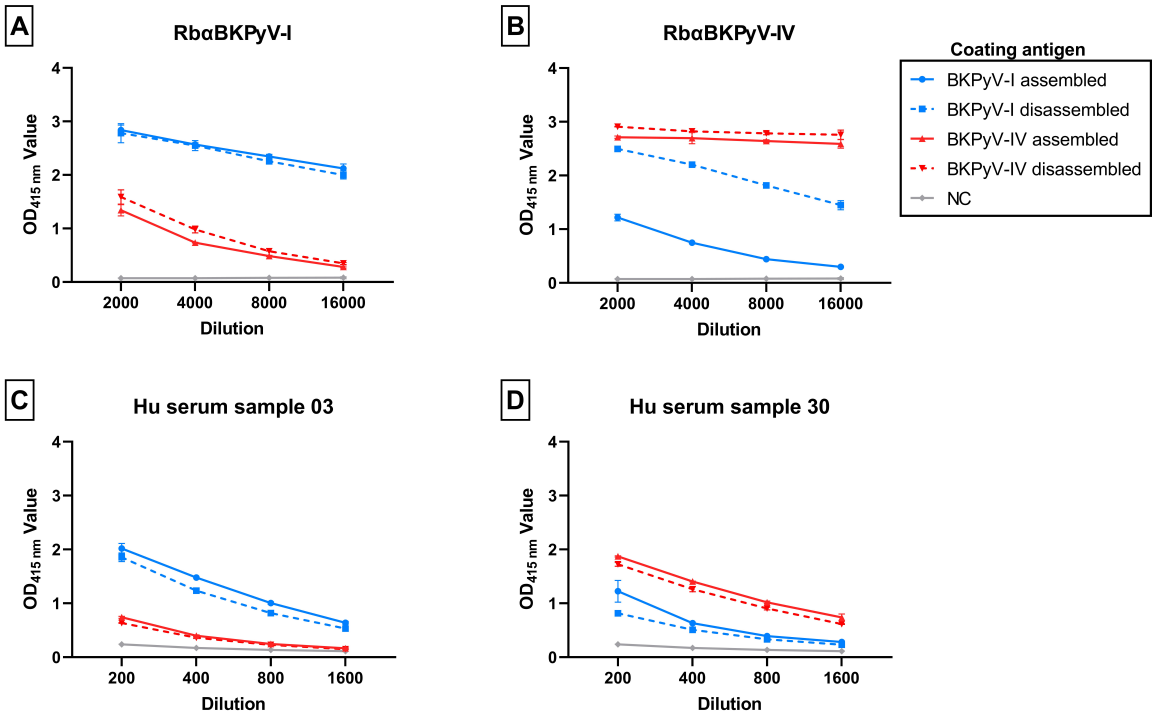

Figure 4.18: Reactivity of rabbit and human sera with compact (assembled) and disassembled PsVs. Reactivity of serum samples: A) RbαBKPyV-I, B) RbαBKPyV-IV, C) Human (Hu) serum sample 03 and D) Human serum sample 30 is shown as the mean absorbance ($OD_{415\ nm}$ value) of each sample. This experiment ran in duplicates. Error bars represent standard deviations (SDs). We added serum samples in serial dilution and used negative serum samples as a negative control (NC): RbαBcr-Abl in the case of rabbit sera and negative human serum sample from KTx patient for human sera.

4.1.10 Antigen competition assay with rabbit sera, control and mutant PsVs

The previous study from our laboratory showed that it is problematic to determine the BKPyV subtype-specific status using serological ELISA. Only a minority of the serum samples from KTx patients reacted on ELISA exclusively with one of the coated BKPyV-I or BKPyV-IV antigens, while most samples cross-reacted with both antigens (Hejtmánková et al., 2019). Hejtmánková et al. (2019) and Wunderink et al. (2019) used an antigen competition assay and showed its potential to overcome the cross-reactivity of BKPyV antibodies.

Antigen competition assay (ACA) is based on the saturation of serum sample antibodies with a soluble competing antigen. After saturation, the remaining antibodies are detected using a standard ELISA. If we saturate a serum sample with a homologous antigen, we eliminate the reactivity on both homologous and heterologous coating antigens. However, if we pre-incubate the serum sample with the heterologous antigen, the reactivity is eliminated only on the heterologous antigen. For instance, BKPyV-I subtype-specific serum sample is saturated only with BKPyV-I. In this case, BKPyV-I captures subtype-specific and cross-reactive antibodies, and BKPyV-IV, on the other hand, captures only cross-reactive antibodies.

In this part of this project, we performed ACA to determine the role of DE and EF loops in serological cross-reactivity caused by BKPyV subtypes I and IV. As a first step, we tested rabbit serum samples to optimize the concentration of a competing antigen (PsVs) which was sufficient to eliminate serum cross-reactivity. First, we pre-incubated rabbit serum samples (RbαBKPyV-I and RbαBKPyV-IV) with competing antigens (BKPyV-I, BKPyV-IV). Specifically, rabbit sera were diluted 1:1,000 and mixed with competing antigens in six different concentrations (1, 2.5, 5, 10, 25, 50 µg/mL). To determine if the saturation was successful, we then performed ELISA. We tested the reactivity of saturated rabbit sera (in final dilution 1:10,000) with two coating antigens (BKPyV-I and BKPyV-IV PsVs) and detected the level of remaining antibodies (Fig. 4.19).

When the concentration of competing antigens was 5 µg/mL, RbαBKPyV-I was saturated with 1) competing antigen BKPyV-I when tested with coating antigens BKPyV-I and BKPyV-IV (Fig. 4.19.A,B, black arrows) and with 2) competing BKPyV-IV when tested with coating BKPyV-IV (Fig. 4.19.B, black arrow). In comparison to RbαBKPyV-I, RbαBKPyV-IV was not saturated as efficiently. However, the reactivity of RbαBKPyV-IV dropped to relatively low values (Fig. 4.19.C,D, black arrows). Rabbit sera pre-incubated with coating antigens in concentrations 1 and 2.5 µg/mL were not saturated as successfully, and higher concentration of competing antigens (10, 25, 50 µg/mL) resulted only in a slight reduction of serum reactivity (data not shown). Human serum samples have a lower antibody titre than experimental rabbit sera. Thus, we expected the same antigen concentration (5 µg/mL) to be even more effective at eliminating the serum reactivity in that case.

In the same experiment, we saturated rabbit sera also with mutant PsVs as competing antigens. After saturation, the remaining antibodies were tested on standard ELISA (Fig. 4.19). Mutant PsVs, BKPyV-IV-DEmut and BKPyV-IV-EFmut, are almost identical to BKPyV-IV PsVs as they are both mutated in surface-exposed loops, DE and EF loop, respectively, with the mutations characteristic for BKPyV-I. Therefore, we expected mutant PsVs to have a better competing potential than the original BKPyV-IV when reacting with RbαBKPyV-I (Fig. 4.19.A,B). In Figure 4.19.A, we can see that saturation of RbαBKPyV-I with competing antigens BKPyV-IV and BKPyV-IV-EFmut did not decrease serum reactivity with coating BKPyV-I. However, saturation with competing BKPyV-IV-DEmut resulted in a slight drop in reactivity. This observation indicates that BKPyV-IV-DEmut could potentially capture more BKPyV-I-specific Abs than the original BKPyV-IV antigen. In Figure 4.19.B, we can see that saturation of RbαBKPyV-I with neither mutant PsVs eliminated the cross-reactivity better than BKPyV-I and BKPyV-IV did, meaning that mutants did not capture more cross-reactive Abs with BKPyV-I origin.

In the case of RbαBKPyV-IV, we expected competing mutant PsVs to saturate this serum better than competing BKPyV-IV when tested with coated BKPyV-I. This happened again just for BKPyV-IV-DEmut and indicates that BKPyV-IV-DEmut captures more cross-reactive Abs with BKPyV-IV origin than BKPyV-IV itself (Fig. 4.19.C). Next, we expected our mutants to saturate BKPyV-IV specific serum better than BKPyV-I antigen and slightly worse than BKPyV-IV antigen when tested on BKPyV-IV (Fig. 4.19.D). Saturation with BKPyV-IV eliminated the serum reactivity almost completely; however, the saturation with mutant PsVs had a little or negligible effect (Fig. 4.19.D). This result is surprising when we consider that BKPyV-IV-DEmut and BKPyV-IV-EFmut differ from the original BKPyV-IV only in one or two amino acids, respectively. These data confirm that we targeted epitopes crucial for binding most BKPyV-IV-specific antibodies in experimental hyperimmune rabbit serum. However, observed results needed to be confirmed further with a larger sample of human sera.

4.1.11 Pre-characterization of human sera using ELISA

Vidia s. r. o. kindly donated human serum samples from kidney transplant (KTx) patients. Previous testing of the blood and urine of these KTx patients revealed a specific BKPyV subtype present in some cases (Table 4.4). However, this initial screening does not provide information about previous infections possibly caused by different BKPyV subtypes. Therefore, we analysed antibody response using ACA and ELISA to elucidate the specificity of persistent BKPyV subtypes in individual patients.

As the initial step, we tested the reactivity of all 13 human serum samples (S) with coated BKPyV-I and BKPyV-IV using standard ELISA (Fig. 4.20). reveals a successful pre-

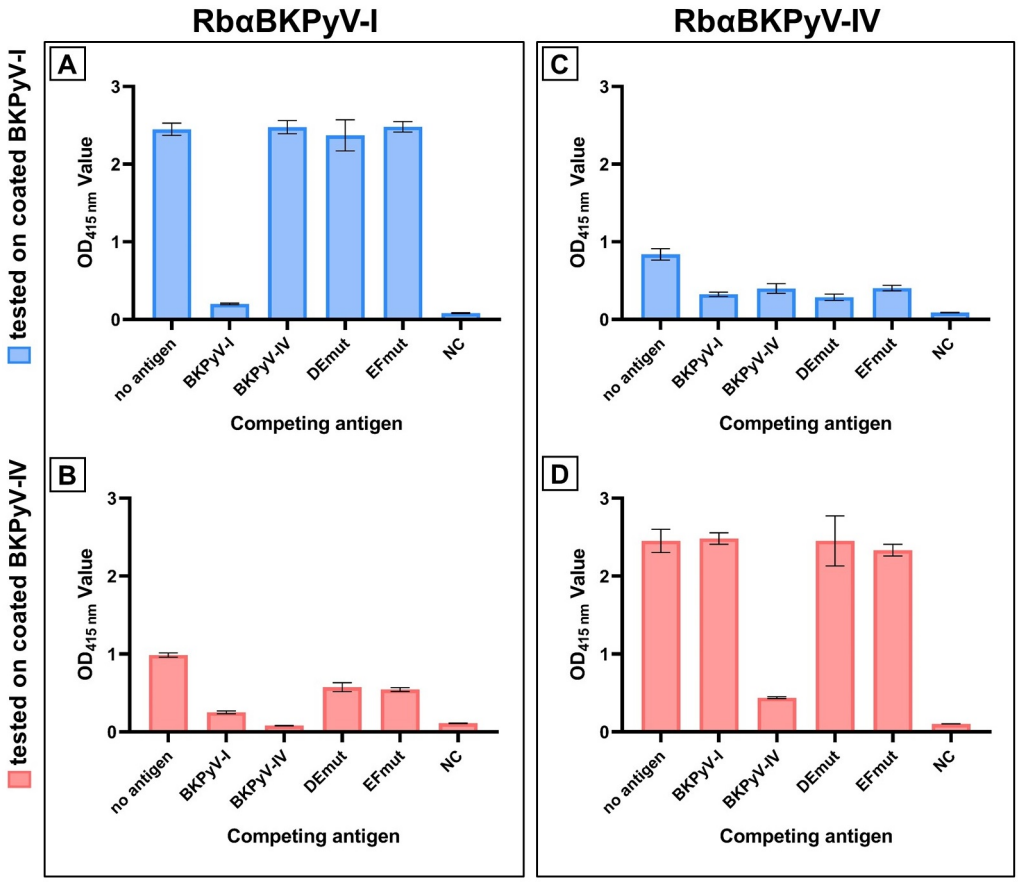

Figure 4.19: Reactivity after saturation of rabbit sera A, B) RbαBKPyV-I and C, D) RbαBKPyV-IV with competing antigens in concentration 5 µg/mL. First, rabbit sera were diluted 1:1,000 and mixed with competing PsVs antigens: BKPyV-I and BKPyV-IV, BKPyV-IV-DEmut (DEmut) and BKPyV-IV-EFmut (EFmut). Sera were then diluted to final dilution 1:10,000 and added to an ELISA plate, and reacted with coating antigens BKPyV-I and BKPyV-IV (shown in blue and red, respectively). Black arrows point to lowered reactivity caused by successful pre-incubation with homologous and heterologous antigens. Reactivity is shown as the mean absorbance ($OD_{415\ nm}$ value) of each sample. This experiment ran in quadruplicates, error bars represent SDs. NC shows reactivity of irrelevant Rb sera (RbαBcr-Abl).

Table 4.4: Screening of urine and blood samples from KTx recipients. Samples were donated by Vidia s. r. o. and analysed previously by Hejtmánková et al. (2019). DNA was isolated from urine and blood to confirm ongoing viruria and viremia, respectively, for specific BKPyV subtypes. The presence of BKPyV DNA was evaluated using quantitative real-time PCR, and genotype specification was based on the restriction fragment length polymorphism analysis of the BKPyV VP1 variable region as described previously by Hejtmánková et al. (2019).

Human serum sample	Viremia	Viruria
Sample 03	negative	negative
Sample 05	negative	positive (unknown)
Sample 07	negative	negative
Sample 17	negative	BKPyV-I
Sample 19	BKPyV-IV	BKPyV-IV
Sample 20	negative	BKPyV-I
Sample 22	negative	positive (unknown)
Sample 30	negative	BKPyV-IV
Sample 34	negative	BKPyV-I
Sample 35	negative	positive (unknown)
Sample 40	negative	positive (unknown)
Sample 45	positive (unknown)	BKPyV-I
Sample 46	negative	BKPyV-IV
Sample 49	negative	BKPyV-I

characterization of all human serum samples. According to our results (Fig. 4.20), the majority of the serum samples cross-reacted with both BKPyV-I and BKPyV-IV, which means that OD values for either BKPyV-I and BKPyV-IV coating antigens exceeded the cut-off value. S03 and S35 were the only samples strictly reacting with BKPyV-I and BKPyV-IV coating antigens, respectively, as we did not observe cross-reactivity in these two cases. However, the difference in reactivity with two coating antigens, BKPyV-I and BKPyV-IV, identified presumably the main target of antibody response in all cases except for three samples - S05, S45 and S49 (Fig. 4.20). For these samples, the reactivity with both BKPyV-I and BKPyV-IV coating antigens was equal (Fig. 4.20).

Combining the information from the previous screening (Table 4.4) and serum characterization using ELISA (Fig. 4.20), we divided serum samples into three groups. If we observed significantly higher reactivity with either BKPyV-I or BKPyV-IV, we put the sera in the respective group, BKPyV-I-reactive or BKPyV-IV-reactive. If we did not observe a significant difference in the reactivity, and the previous screening did not detect a specific BKPyV subtype (Table 4.4), we included the serum in the group called double-reactive. Altogether, results from pre-characterization by ELISA gave us an idea about the subtype-specificity of serum antibodies from individual patients. However, as we observed cross-reactivity in most cases, we needed to perform an ACA to confirm BKPyV subtype specificity.

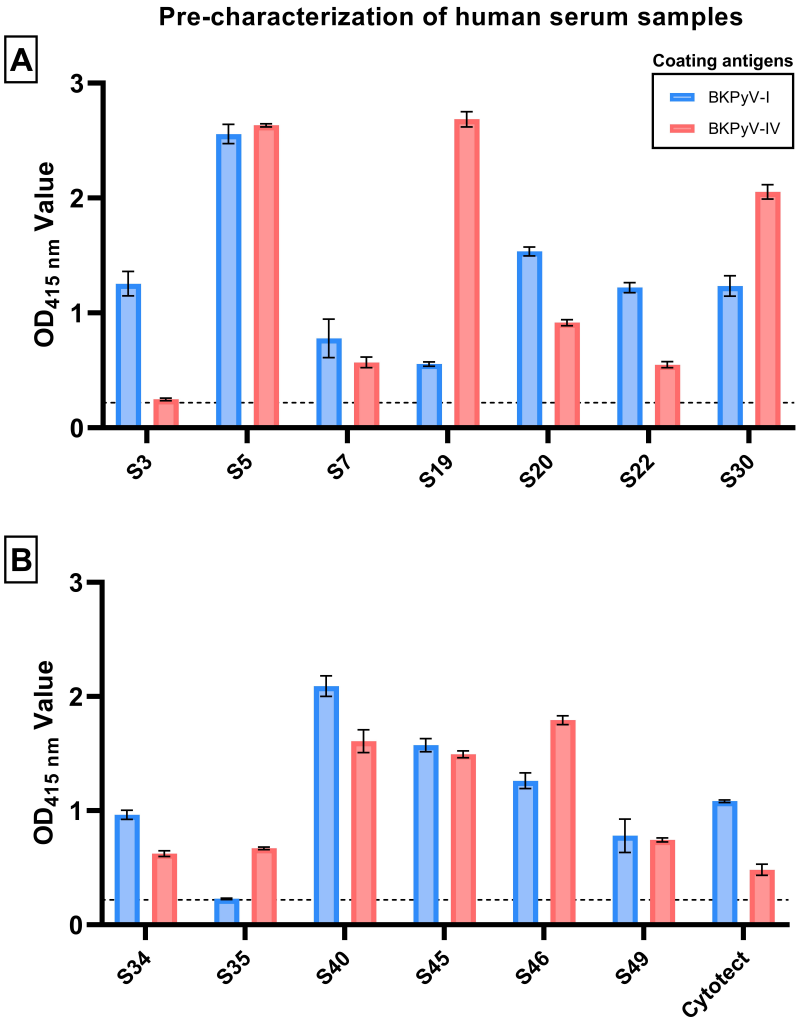

Figure 4.20: Pre-characterization of 13 human serum samples and Cytotect CP on ELISA. Serum samples were diluted 1:200 (Cytotect CP 1:2000) and added to an ELISA plate, and reacted with two coating antigens: BKPyV-I (blue) and BKPyV-IV (red) PsVs. Experiments were conducted in quadruplicates. The dotted line represents cut-off values calculated as the mean $OD_{415\ nm}$ value of six negative serum samples plus two standard deviations.

4.1.12 Antigen competition assay with human sera, control and mutant PsVs

The first goal of the next experiment, ACA with human serum samples, was to eliminate the cross-reactivity observed in 11 out of 13 pre-characterized human serum samples (Fig. 4.20) and thus provide information about the BKPyV subtype specificity of the antibody response. The second goal of these experiments was to explore the competing potential of mutant PsVs and thereby elucidate the importance of mutated epitopes in cross-reactivity against subtypes I and IV. BKPyV-IV-DEmut already proved to have the ability to capture more BKPyV-I-specific antibodies than the original BKPyV-IV (Fig. 4.19). However, the role of BKPyV-IV-EFmut was still unclear.

We first pre-incubated serum samples with four competing antigens (BKPyV-I, BKPyV-IV, BKPyV-IV-DEmut and BKPyV-IV-EFmut PsVs) and then tested the reactivity of saturated serum samples with two coating antigens, BKPyV-I and BKPyV-IV PsVs. As we divided sera into three groups based on DNA screening and specificity of antibody response: BKPyV-I-reactive, BKPyV-IV-reactive and double-reactive, we expected the reactivity of each serum in one group to drop similarly after pre-incubation with respective PsVs.

Group 1: BKPyV-I-reactive human serum samples

In the first group, we compared eight serum samples (S03, S07, S20, S22, S34, S40, S45 and S49) from which four samples (S17, S20, S34 and S45) were positive for BKPyV-I viruria (Table 4.4). In the previous pre-characterization using ELISA, all these serum samples reacted mostly with coated BKPyV-I except for two, S45 and S49, which reacted equally with coated BKPyV-I and BKPyV-IV antigens (Fig. 4.20). These two sera were also included in this group as S45 was positive for BKPyV-I viruria, and S49 later showed that its reactivity pattern corresponded to patterns of this group (Fig. 4.22). S03 was the only BKPyV-I-specific serum, as its reactivity with BKPyV-IV was below the cut-off value. Our goal was to eliminate cross-reactivity, thus confirming BKPyV-I specificity, and describe the behaviour of mutant PsVs. We were particularly interested in pre-incubation experiments with S03 as it was the only subtype-specific serum with a known origin of antibody response. Therefore, ACA with this sample could help us to elucidate the nature of antibodies recognized by our mutant PsVs.

To confirm the BKPyV-I specificity of selected sera, we focused on saturation with competing antigens BKPyV-I and BKPyV-IV. Competition with BKPyV-I PsVs eliminated the serum reactivity when tested with both BKPyV-I and BKPyV-IV coating antigens, as was expected for BKPyV-I positive sera (Fig. 4.21 and 4.22). However, there was one exception (S45), where we observed incomplete saturation with competing BKPyV-I when tested on coated BKPyV-I (Fig. 4.22.E). Sera saturation with BKPyV-IV did not result in the reduction of reactivity only in the case of S40 and S45 when tested on coated BKPyV-IV antigen (Fig.

4.22.D,F). This fact indicates that these two samples contain higher titers of cross-reacting Abs. Together these results confirmed the BKPyV-I specificity of six of eight serum samples: S03, S07, S20, S22, S34 and S49.

Then, we focused on serum saturation with mutant PsVs. In the majority of cases, saturation with all BKPyV-IV-derived antigens had none or just a very mild effect on the serum reactivity when tested on coated BKPyV-I (Fig. 4.21 and Fig. 4.22). However, the effect of competing BKPyV-IV-DEmut on the reduction of serum reactivity was substantially higher (than BKPyV-IV and BKPyV-IV-EFmut) in the cases of S34 and S40 (Fig. 4.22A,C). The most noticeable change after saturation with BKPyV-IV-DEmut is shown in Figure 4.22.C. This fact supports our hypothesis that the changed DE region binds BKPyV-I subtype-specific antibodies.

Interestingly, competing BKPyV-IV-DEmut captured the same or even higher amount of cross-reactive Abs (with BKPyV-I origin) than BKPyV-IV when tested on coated BKPyV-IV (Fig. 4.21.B,D,F,H and 4.22.B,D,F,H). The only one mutation in the DE loop characteristic for BKPyV-I caused the successful elimination of serological cross-reactivity in one serum sample (S40, Fig. 4.22.D). Serum saturation with BKPyV-IV-EFmut caused a slight drop in reactivity only when tested on BKPyV-IV (Fig. 4.21.D,F,H and Fig. 4.22B,F,H). However, there was one exception - S45. This serum reacted differently than the other seven BKPyV-I-reactive samples as it was the only serum saturated with BKPyV-IV-EFmut more than with BKPyV-IV and BKPyV-IV-DEmut when tested on both coating antigens (Fig. 4.22.E,F). Apart from this sample, BKPyV-IV and BKPyV-IV-DEmut as competing antigens were always more efficient in capturing BKPyV-I specific and cross-reactive antibodies than mutated BKPyV-IV-EFmut.

Group 2: BKPyV-IV-reactive human serum samples

In the second group, we compared four serum samples (S19, S30, S35 and S46). In the case of S19, the BKPyV-IV subtype was detected in blood and urine, whereas in the cases of S30 and S46, the presence of the BKPyV-IV subtype was confirmed only in urine (Table 4.4). Pre-characterization using ELISA showed that the samples in this group reacted preferentially with coated BKPyV-IV than with coated BKPyV-I (Fig. 4.20).

If antibodies in S19, S30, S35 and S46 are truly BKPyV-IV specific, we expected the reactivity to be eliminated by sera saturation with competing BKPyV-IV when tested on coated BKPyV-I and BKPyV-IV. Our expectations were confirmed only for two samples, S19 and S35 (Fig. 4.23.A,B,E,F), as S30 was not saturated by competing BKPyV-IV when tested on coated BKPyV-I (Fig. 4.23. C) and S46 was not saturated by competing BKPyV-IV when tested on coated BKPyV-IV (Fig. 4.23.H).

Furthermore, when we pre-incubate BKPyV-IV specific serum with competing BKPyV-I,

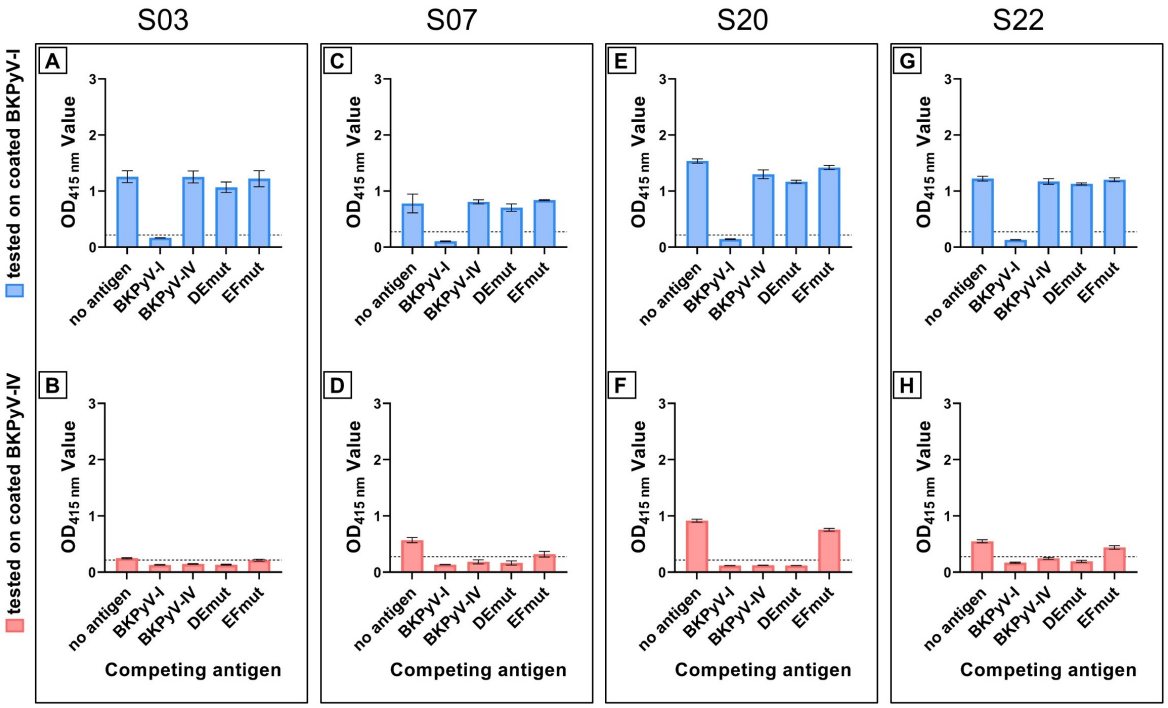

Figure 4.21: Reactivity of four BKPyV-I-reactive human serum samples (S03, S07, S20 and S22) after antigen competition assay. Serum samples diluted 1:100 were pre-incubated with competing antigens: BKPyV-I, BKPyV-IV, BKPyV-IV-DEmut (DEmut) and BKPyV-IV-EFmut (EFmut); and subsequently tested in final dilution 1:200 on coating antigens BKPyV-I (shown in blue) and BKPyV-IV (shown in red) using ELISA. The concentration of competing antigen was 5 µg/mL. Experiments were carried out in quadruplicates. The dotted line in each graph represents a cut-off value calculated as the mean $OD_{415\ nm}$ value of 6 unreactive serum samples plus two standard deviations. For details of the statistical analysis, see Appendix (Table A.1).

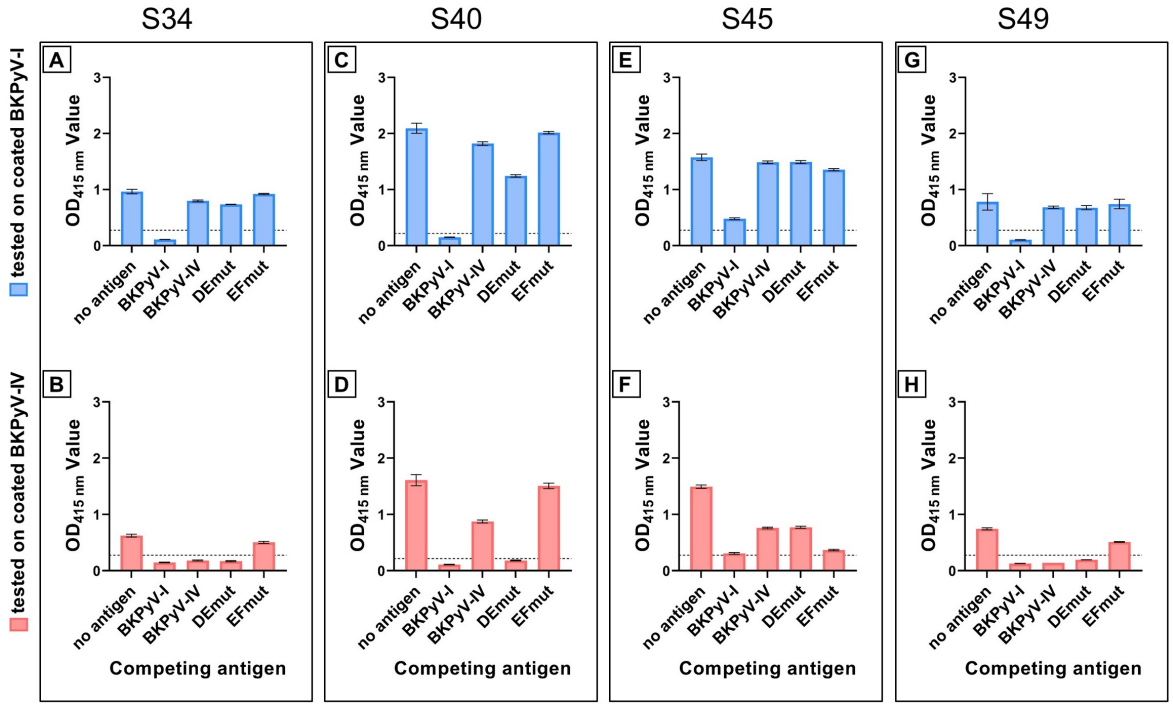

Figure 4.22: Reactivity of four BKPyV-I-reactive human serum samples (S34, S40, S45 and S49) after antigen competition assay. Serum samples diluted 1:100 were pre-incubated with competing antigens: BKPyV-I, BKPyV-IV, BKPyV-IV-DEmut (DEmut) and BKPyV-IV-EFmut (EFmut); and subsequently tested in final dilution 1:200 on coating antigens BKPyV-I (shown in blue) and BKPyV-IV (shown in red) using ELISA. The concentration of competing antigen was 5 µg/mL. Experiments were carried out in quadruplicates. The dotted line in each graph represents a cut-off value calculated as the mean $OD_{415\ nm}$ value of 6 unreactive serum samples plus two standard deviations. For details of the statistical analysis, see Appendix (Table A.1).

we expect the reactivity to be eliminated on coated BKPyV-I. However, this did not happen in the case of S19 and S46 (Fig. 4.23.A,G). Altogether, we had difficulties confirming the BKPyV-IV specificity of selected samples using ACA with competing BKPyV-I and BKPyV-IV. Only one serum sample (S35) was saturated, as expected. However, this sample is problematic when we take into account its generally very low antibody titre.

Next, we focused on saturation with mutant PsVs. According to results obtained earlier from ACA with rabbit sera (Fig. 4.19), we expected BKPyV-IV-DEmut to pre-incubate BKPyV-IV-reactive sera better than original BKPyV-IV when tested on coated BKPyV-I. For S19 and S35, we did not observe such a trend as the reactivity of these sera was generally too low, and so was the reactivity after pre-incubation (Fig. 4.23.A,E). In the case of S30 and S46, we observed the exact opposite as the original BKPyV-IV antigen was more efficient in capturing cross-reactive antibodies (with BKPyV-IV origin) than BKPyV-IV-DEmut (Fig. 4.22.C,G). However, BKPyV-IV-DEmut captured substantially more antibodies than BKPyV-IV-EFmut in all cases where was the serum reactivity above the cut-off value (Fig. 4.23.B,C,D,G,H), which is consistent with the result obtained with BKPyV-I-reactive sera.

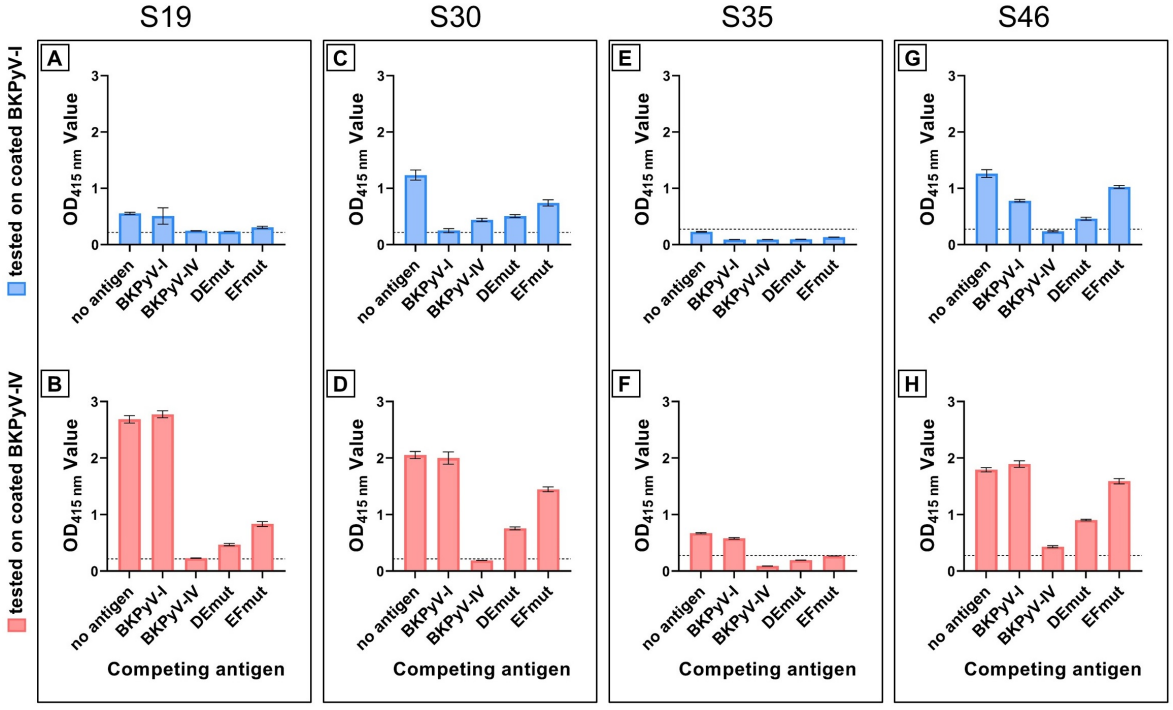

Figure 4.23: Reactivity of four BKPyV-IV-reactive human serum samples (S19, S30, S35 and S46) after antigen competition assay. Serum samples diluted 1:100 were pre-incubated with competing antigens: BKPyV-I, BKPyV-IV, BKPyV-IV-DEmut (DEmut) and BKPyV-IV-EFmut (EFmut); and subsequently tested in final dilution 1:200 on coating antigens BKPyV-I (shown in blue) and BKPyV-IV (shown in red) using ELISA. The concentration of competing antigen was 5 µg/mL. Experiments were carried out in quadruplicates. The dotted line in each graph represents a cut-off value calculated as the mean $OD_{415\ nm}$ value of 6 unreactive serum samples plus two standard deviations. See Appendix (Table A.1) for details of the statistical analysis.

Group 3: Double-reactive human serum samples

There was only one serum sample in this group: S05. The previous screening revealed the presence of BKPyV in urine, however, a specific subtype of this BKPyV isolate was not determined (Table 4.4). Pre-characterization using ELISA showed very high and equal antibody titres against both BKPyV subtypes I and IV.

For this sample, we first performed ACA and subsequent ELISA to confirm or exclude the previous infection caused by multiple BKPyV subtypes. In that case, we expected serum saturation not to be effective in the elimination of serum reactivity. We first performed ACA in standard serum dilution 1:100 and then tested the reactivity of this sample in final dilution 1:200 (Fig. 4.24.A,B). Pre-incubation of this serum with competing BKPyV-I resulted in almost 3-fold lower reactivity when tested with both coating antigens. After pre-incubation with BKPyV-IV PsVs, the reactivity did not change when tested with coated BKPyV-I. Altogether, these data indicate that mainly BKPyV-I subtype-specific antibodies were present, however, due to high titres of serum antibodies, this sample was not saturated completely with the standard concentration of competing antigens.

To confirm the BKPyV-I specificity of S05, we pre-incubated this sample in higher dilution with coating antigens in standard concentration (5 µg/mL) and expected the reactivity after saturation with BKPyV-I to drop below the cut-off value. In Figure 4.24.C,D, we can see the reactivity of S05 saturated in dilution 1:1,000 and tested in final dilution 1:2,000. As expected, after saturation of 1:1,000 diluted serum, its reactivity decreased below the cut-off value. The whole reactivity pattern of this sample now resembles that of other BKPyV-I specific serum samples as 1) saturation with competing BKPyV-I eliminated reactivity when tested on coated BKPyV-I and BKPyV-IV, and 2) saturation with competing BKPyV-IV eliminated reactivity on coated BKPyV-IV.

Serum saturation with mutant PsVs also caused a similar effect as we observed previously for BKPyV-I-specific serum samples. Namely, saturation with competing BKPyV-IV-DEmut was more successful than saturation with competing BKPyV-IV when tested on coated BKPyV-I and BKPyV-IV (Fig. 4.24.C,D). And saturation with competing BKPyV-IV-EFmut had no effect on serum reactivity when tested on BKPyV-I and only a very mild effect when tested on BKPyV-IV (Fig. 4.24.C,D).

Another sample (Cytotect CP) was tested using ACA to confirm previously observed serum reactivity patterns after saturation with mutant PsVs. Cytotect CP is commercially produced from serum samples of healthy donors. This product contains polyclonal immunoglobulins (IgG) neutralizing Human Cytomegalovirus (HCMV), and it is recommended as prophylactic for KTx recipients. However, Randhawa et al. (2015) showed that different IVIG prevent not only HCMV infection but also BKPyV as the authors of this study detected neutralizing antibodies against major BKPyV subtypes (Ia, Ib2, Ic, II, III, and IV).

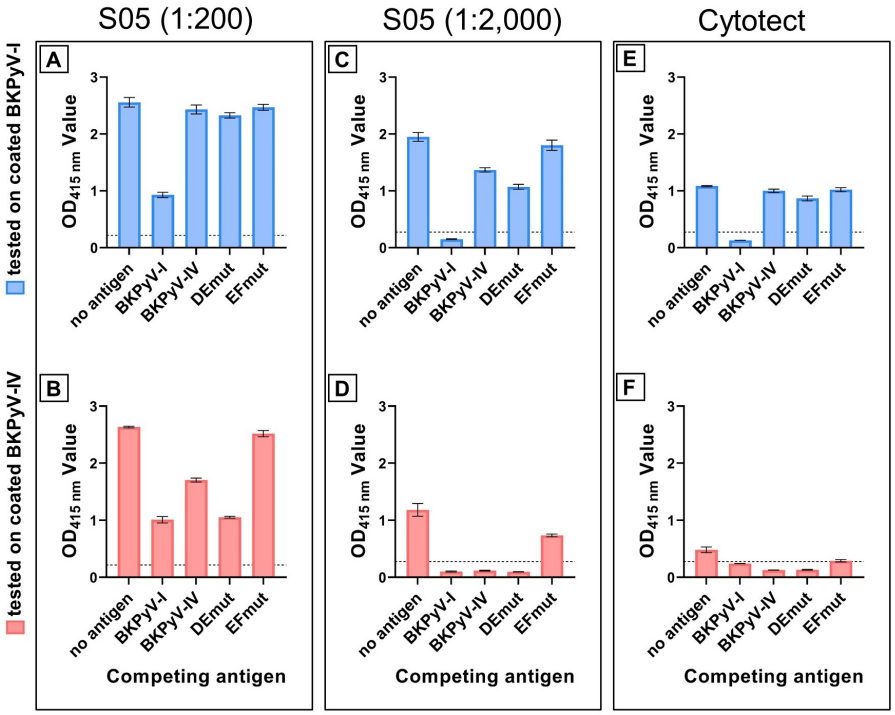

Figure 4.24: Reactivity of double-reactive human serum sample S05 after antigen competition assay. Serum sample S05 was diluted 1:100 and 1:1,000, pre-incubated with competing antigens: BKPyV-I, BKPyV-IV, BKPyV-IV-DEmut (DEmut) and BKPyV-IV-EFmut (EFmut); and subsequently tested in final dilution 1:200 (A, B) and 1:2,000 on coating antigens BKPyV-I (shown in blue) and BKPyV-IV (shown in red) using ELISA. The concentration of competing antigen was 5 µg/mL. Experiments were carried out in quadruplicates. The dotted line in each graph represents a cut-off value calculated as the mean $OD_{415\ nm}$ value of 6 unreactive serum samples plus two standard deviations. See Appendix (Table A.1) for details of the statistical analysis.

The distribution of subtype-specific antibodies in Cytotect CP should, therefore, mirror the distribution of these antibodies in the general population. Thus, experiments with Cytotect CP were used in this thesis as a positive control and provided strong evidence which supported previously obtained data.

We first diluted Cytotect CP 1:1,000, incubate it with respective competing antigens and tested the reactivity on ELISA (Fig. 4.24). Cytotect CP was completely saturated with competing BKPyV-I when tested with both coating antigens (Fig. 4.24.E,F). However, saturation with competing BKPyV-IV reduced Cytotect CP reactivity only when tested with coated BKPyV-I (Fig. 4.24.F). Together these results support the fact that the frequency of the BKPyV-I subtype predominates over BKPyV-IV in the human population.

Furthermore, results obtained from ACA and ELISA with Cytotect CP confirmed previously observed trends after saturation with mutant PsVs. First, saturation with competing BKPyV-IV-DEmut resulted in significantly lowered Cytotect CP reactivity when tested with coated BKPyV-I (Fig. 4.24.E). And second, saturation with competing BKPyV-IV-EFmut did not affect Cytotect CP reactivity when tested on coated BKPyV-I (Fig. 4.24.F).

These data show that we successfully used ACA to determine serum-specificity in 8 of 13 serum samples. Experiments based on sera saturation with homologous and heterologous antigens confirmed BKPyV-I specificity of S03, S05, S07, S20, S22, S34 and S49; and BKPyV-IV specificity of S35. The situation in the remaining cases (S40, S45, S19, S30, S46) remains elusive.

Saturation of specific human serum samples with mutant PsVs helped to elucidate the importance of targeted epitopes in serological cross-reactivity between two BKPyV subtypes (I and IV). First, we proved that changes introduced in the two surface-exposed loops of BKPyV VP1, DE and EF, play an essential role in binding antibodies in general. Sera saturation with BKPyV-IV-DEmut reduced the reactivity of some BKPyV-I-reactive samples substantially more than the original BKPyV-IV antigen when tested on coated BKPyV-I. Furthermore, in two BKPyV-I-reactive serum samples (S40 and S05), BKPyV-IV-DEmut showed a better capacity to capture antibodies than BKPyV-IV when tested on coated BKPyV-IV. Thus, we assumed that the context of the DE loop could be responsible for binding BKPyV-I-specific antibodies.

Interestingly, BKPyV-IV-EFmut had the lowest ability of all antigens to saturate sera. Although the saturation with this antigen (BKPyV-IV-EFmut) decreased substantially the reactivity of all BKPyV-IV-reactive serum samples when tested on coated BKPyV-IV, it was never as efficient as saturation with BKPyV-IV and BKPyV-IV-DEmut. However, in the majority of BKPyV-I-reactive serum samples, the reactivity after saturation with BKPyV-IV-EFmut remained unchanged (when tested on coated BKPyV-I) and the original BKPyV-IV proved a better capacity to capture anti-BKPyV-I antibodies (except for one sample S45).

4.2 Effect of DE and EF loops mutations on BKPyV biology

The next goal of this thesis was to characterize the effect of the introduced mutations in DE and EF loops on the biology of BKPyV. We analysed VP1 sequences of BKPyV obtained from online sources and created a database with the final size of 643 sequences (for more details, see section 4.3.1). None of these sequences was identical to the VP1 sequence of mutant PsVs, BKPyV-IV-DEmut and BKPyV-IV-EFmut, as mutations in the DE and EF loops are always accompanied by the different amino acid composition of the BC loop. We wanted to exclude the possibility that mutations in amino acid positions we targeted have a critical effect on the virus biology, e.g. bringing selective disadvantage to the virus. Specifically, we aimed to elucidate if these mutations influence virus entry into the cells. For that purpose, we first planned to prepare PsVs containing minor capsid proteins and a reporter gene for cell transduction. Second, we aimed to repeat transduction experiments in the presence of human sera from KTx recipients and thus determine the potential of mutant PsVs to escape from neutralizing antibodies.

4.2.1 Plasmid isolation

Plasmids encoding BKPyV structural proteins (VP1, VP2 and VP3) and luciferase were needed to co-transfect cells and subsequently isolate PsVs with the transduction ability. The plasmids with the gene for VP1 were already prepared (see section 4.1.1). Plasmids with the genes for VP2 and VP3 protein were isolated (pwB2b and pwB3b) as well as the plasmid with the gene encoding luciferase (pGL3-Control) and verified using restriction digestion (data not shown).

4.2.2 Isolation and characterization of PsVs composed of VP1, VP2 and VP3 proteins

Firstly, we transfected cells to check that all proteins were expressed. Cells were transfected with each plasmid separately and co-transfected with four plasmids in different combinations. Two days post-transfection, the cells were lysed, and protein expression in cells was verified by specific antibodies using SDS-PAGE and Western blot analysis (Fig. 4.25). The presence of viral protein VP1 was detected in all lysates, whereas a stronger signal was observed when the cells were transfected with one plasmid compared to co-transfection with four plasmids (Fig. 4.25.A). Minor proteins, VP2 and VP3, were stained with the same antibody (against VP2/3, Fig. 4.25.B). VP2 signal was very strong when the cells were transfected with ph2b only. On the contrary, after co-transfection with four plasmids, the production of VP2 was relatively low. In the case of BKPyV-IV-EFmut co-transfection, we detected no VP2 signal at all. For VP3, we observed strong bands for transfection with one plasmid

as well as for co-transfections. Surprisingly, the bend for VP3 was also visible in the case of transfection with ph2b (Fig. 4.25.B - VP2 column), where it probably represents VP2 after partial degradation. These results were sufficient to confirm VP2 expression in the majority of samples, and we proceeded with PsVs production, while the BKPyV-IV-EFmut sample required further optimization of the transfection condition.

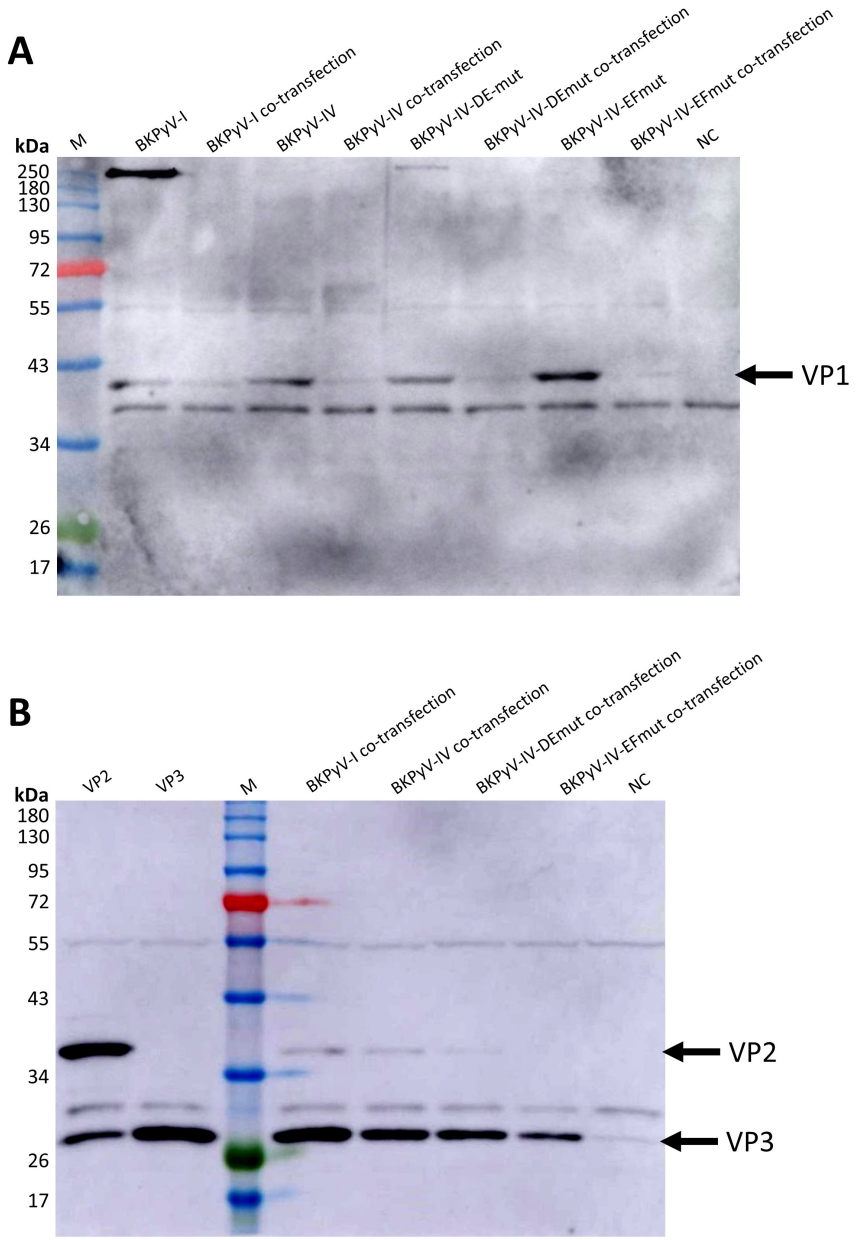

Figure 4.25: Western blot of control co-transfections. Cell lysates were separated by SDS-PAGE, and transferred into nitrocellulose membranes and proteins were stained with A) primary antibody against VP1 and B) primary antibody against VP2/VP3. On membrane A, every two samples which contained identical VP1 protein were loaded next to each other: BKPyV-I (transfection with pBKPyV-I) and BKPyV-I co-transfection (co-transfection of pBKPyV-I, ph2b, ph3b and pGL3-Control) etc. On membrane B, there were samples VP2 (cell transfected only with ph2b), VP3 (cell transfected only with ph3b) and then each co-transfection. Arrows indicate the expected size of VP1, VP2 and VP3. M - molecular weight marker.

For PsVs production, we co-transfected cells with four plasmids to get four types of PsVs: two control (BKPyV-I and BKPyV-IV) and two mutant (BKPyV-IV-DEmut and BKPyV-IV-EFmut). PsVs were isolated from lysates using ultracentrifugation in an Optiprep gradient. Several fractions from the gradients were collected and the presence of VP1 in fractions was verified by two primary antibodies (Fig. 4.26). We detected a positive signal in all isolations. The first antibody (specific to SV40 VP1), which previously proved effective in detecting PsVs of all variants (Fig. 4.5), now bound better mutant than control PsVs (Fig. 4.26.A). VP1 seemed to be present mainly in fractions 1 - 4. The second antibody specific to BKPyV VP1 showed higher sensitivity and indicated the presence of VP1 through the whole gradient (Fig. 4.26.B).

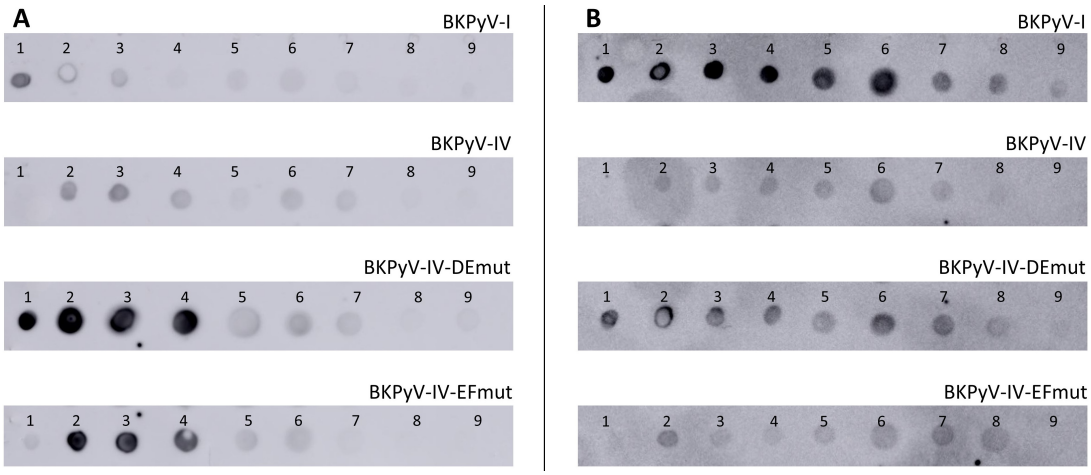

Figure 4.26: Immunodetection of VP1 protein (dot blot analysis). The same amount of each fraction was loaded on the membrane. The membrane was stained with primary antibody A) against VP1 SV40 or B) against VP1 BKPyV followed by a secondary antibody conjugated with horseradish peroxidase. Numbers correspond to numbers of fractions.

To further characterize isolated fractions, we performed SDS-PAGE (Fig. 4.27) and Western blot analysis (Fig. 4.28) for BKPyV-I and BKPyV-IV co-transfections. According to the previous results obtained from dot blot analysis (Fig. 4.26.A), we expected fractions 1 - 4 to be pure with a strong bend for VP1. However, Figure 4.27 shows that all fractions contained a lot of unpurified material; therefore, we could not observe a clear band for VP1/2/3. Western blot analysis (Fig. 4.28) revealed only a weak signal for VP1 protein in the case of BKPyV-I co-transfection (in fractions 1 - 3) and no signal in the case of BKPyV-IV co-transfection (Fig. 4.28.A). When staining with anti VP2/3 antibody, we observed strong signals for both VP2 and VP3 in the case of BKPyV-I co-transfection (fraction 2); however, only a weak signal for VP3 in the case of BKPyV-IV co-transfection (fraction 5). Further visualization of selected fractions (fraction 2) using TEM showed that compact viral particles were present only rarely and were therefore not purified in sufficient amounts to proceed with the next analysis (Fig. 4.29).

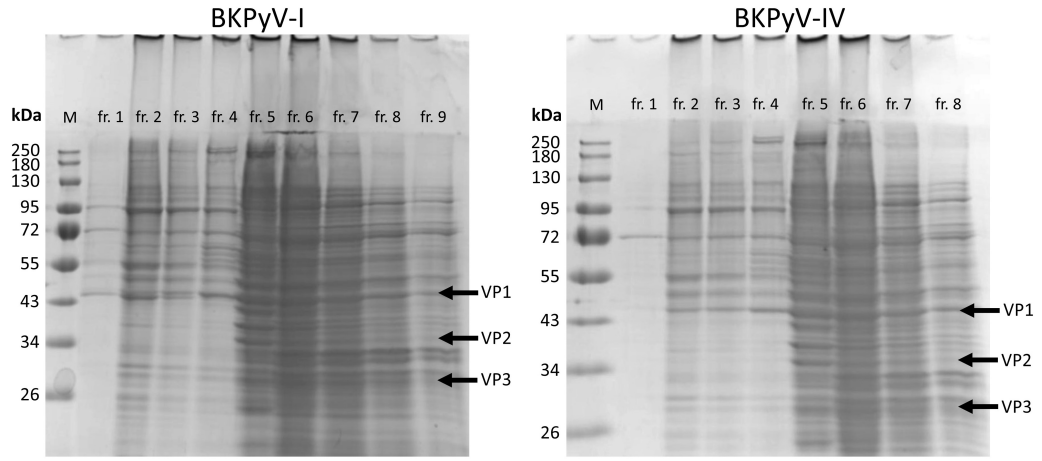

Figure 4.27: Representation of selected VP1 fractions after isolations of PsVs composed of VP1/2/3 on polyacrylamide gels. The same amount of each fraction was loaded on the 10% gel. After electrophoresis, the proteins in the gel were stained with Imperial Protein Stain. Arrows indicate the expected size of VP1, VP2 and VP3. M - molecular weight marker, fr. 1 - fraction 1, fr. 2 - fraction 2, etc.

4.2.3 In-Fusion cloning

As co-transfection with four plasmids appeared problematic, we decided to eliminate the number of plasmids used for cell transfection. The idea was to combine two regions carried by two plasmids into one plasmid. Later, we could co-transfect cells with three plasmids instead of four: the first one with the sequence of VP1 (pBKPyV-I, pBKPyV-IV, pBKPyV-IV-DEmut or pBKPyV-IV-EFmut), the second one with both VP2 and VP3 coding sequence (pwB2b/3b), and the third one with a luciferase reporter gene (pGL3-Control).

To clone a vector carrying both VP2 and VP3, we used In-Fusion cloning system. The plasmid with the VP3 gene was used as a vector (pwB3b), and the plasmid pwB2b as a donor of the VP2 gene. First, we designed primers using an online tool (In-Fusion Cloning Primer Design Tool). The first set of primers (pwB3b-Fw and pwB3b-Rv) was used to amplify the linearized vector without a redundant region coding VP1 protein. The second set of primers (BKPyV-VP2-Fw and BKPyV-VP2-Rv) was designed to amplify our insert (VP2 gene) from plasmid pwB2b. The latter pair of primers had 15 bp extensions homologous to the ends of the linearized vector. Combining vector and insert with homologous ends in In-Fusion reaction results in shortening 3′ ends on both sequences. Consequently, homologous sequences can join and anneal in the right direction.

After a few PCR condition optimizations, both VP2 insert and VP3 vector sequences were successfully amplified (Fig. 4.30 and Fig. 4.31). Separated PCR products were extracted from the gel and used for In-Fusion reaction followed by Stellar Competent Cells transformation. After selection using plates containing appropriate antibiotics, the colonies were screened for desired cloned vector using restriction digestion and colony PCR. We did not

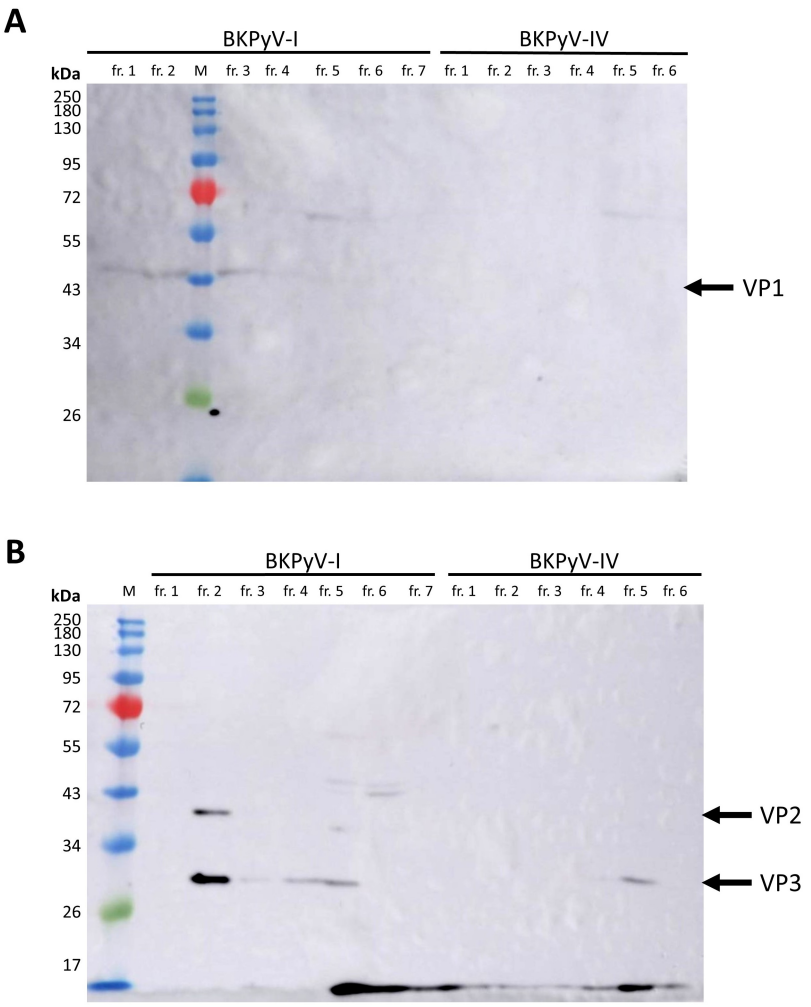

Figure 4.28: Western blot of two PsVs isolations. Purified protein fractions were run on SDS-PAGE, transferred onto nitrocellulose membrane and stained with A) primary antibody against VP1 and B) primary antibody against VP2/VP3 followed by incubation with secondary antibody conjugated with horseradish peroxidase. Arrows indicate the expected size of VP1, VP2 and VP3. M - molecular weight marker, fr. 1 - fraction 1, fr. 2 - fraction 2, etc.

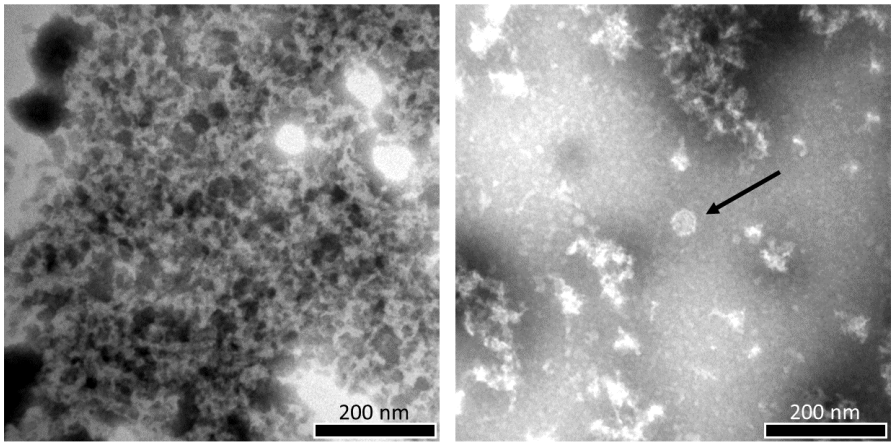

Figure 4.29: TEM images show selected fractions of BKPyV-I PsVs (fraction 2, left) and BKPyV-IV PsVs (fraction 2, right) after isolations of PsVs composed of VP1/2/3. Samples were stained with PTA and visualized using electron microscopy. Black arrow points to assembled PsVs.

obtain the desired plasmid as neither method revealed any positive clone. As we saw that our attempts were unsuccessful, we stopped optimizing the isolation protocol for PsVs with minor proteins, mainly because the time spent in the laboratory was limited. Consequently, we did not have the necessary material to proceed with the next step to determine the potential of mutant PsVs to escape from neutralizing antibodies present in human sera from KTx. However, we devised an alternative plan to study the impact of BKPyV VP1 mutations using bioinformatics tools.

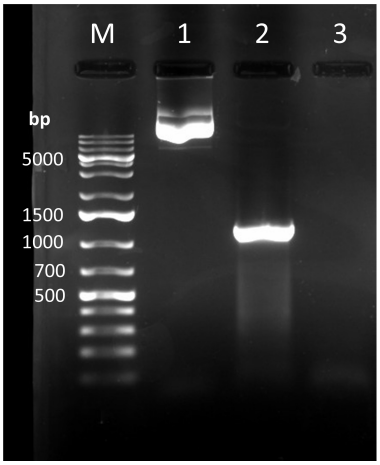

Figure 4.30: Electrophoretic separation of PCR reaction on 1% agarose gel. As a template, pwB2b plasmid was used, and the VP2 PCR insert was amplified by Vent polymerase. M - marker, 1 - original pwB2b plasmid with VP2 gene (6,746 bp), 2 - amplified VP2 gene (insert, 1,056 bp), 3 - negative control.

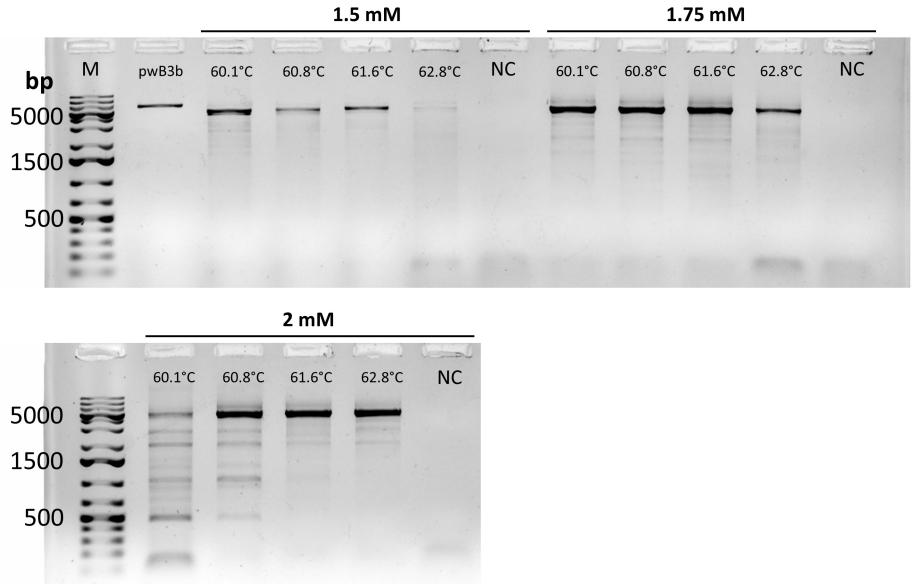

Figure 4.31: Electrophoretic separation of PCR reaction on 1% agarose gel. As a template, pwB3b plasmid was used, and the VP3 vector was amplified by HiFi polymerase using increasing concentrations of $MgCl_2$ (1.5, 1.75 and 2 mM) and increasing temperatures for primer annealing (60.1, 60.8, 61.6 and 62.8°C).

4.3 Analysis of BKPyV VP1 sequences

Previous research findings investigating the impact of different BKPyV genotypes on virus pathology have been inconsistent and contradictory (Nukuzuma et al., 2006; Tremolada et al., 2010a; Korth et al., 2019). We, therefore, decided to perform a bioinformatic analysis (Aim 3), collected so far published BKPyV VP1 sequences available in online databases, connected them with the patient's clinical condition and subsequently determined if some specific BKPyV genotypes (or specific mutations) are associated with pathology. The schematic workflow of our analysis is shown in Figure 4.32. Collected BKPyV VP1 sequences were divided into groups based on the patient's clinical condition and subjected to phylogenetic and selection analysis.

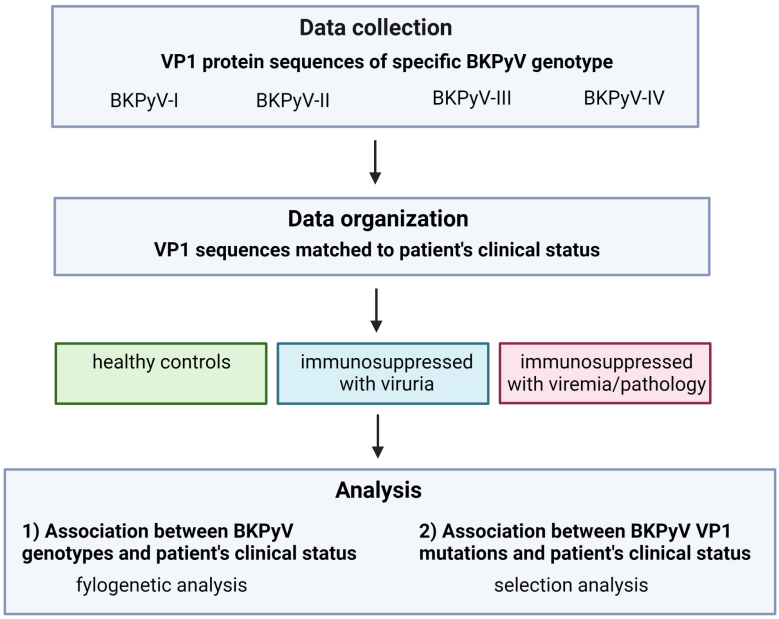

Figure 4.32: Simplified scheme of the steps performed to research Aim 3. We first collected and organized protein sequences of BKPyV VP1, which were isolated from patients with different clinical statuses, and used them for several analyses. This scheme was created with Biorender.com.

4.3.1 Collection and organization of BKPyV VP1 sequences

We collected 643 nucleotide sequences of 1086 bp long coding sequence for VP1 protein. Each sequence was freely accessible in the NCBI database. We first visualized the distribution of amino acid in all VP1 sequences using the online tool WebLogo (Schneider and Stephens, 1990; Crooks et al., 2004). This analysis (shown in Fig. 4.32) revealed the most variable sites located in the BC loop (aa 54 - 90).

Then, we divided sequences into groups based on the patient's clinical status. The majority of the sequences were already analysed and published previously, and thus the information about the clinical status of the patient from which they were isolated was obtained from

the relevant publication. In the minority of cases, such information was obtained straightforwardly from the sequence description in NCBI. Overall, all sequences were successfully linked to the patient's clinical status and, based on that, subsequently sorted into three groups:

1. healthy controls with viruria (171 sequences)
2. immunosuppressed patients with viruria (229 sequences)
3. immunosuppressed patients with viremia/BKPyV-associated pathology (115 seq.).

The origin of the remaining 128 sequences was unknown, and these sequences were, therefore, not assigned to either group. However, they were used in one of the following analyses (section 4.3.3).

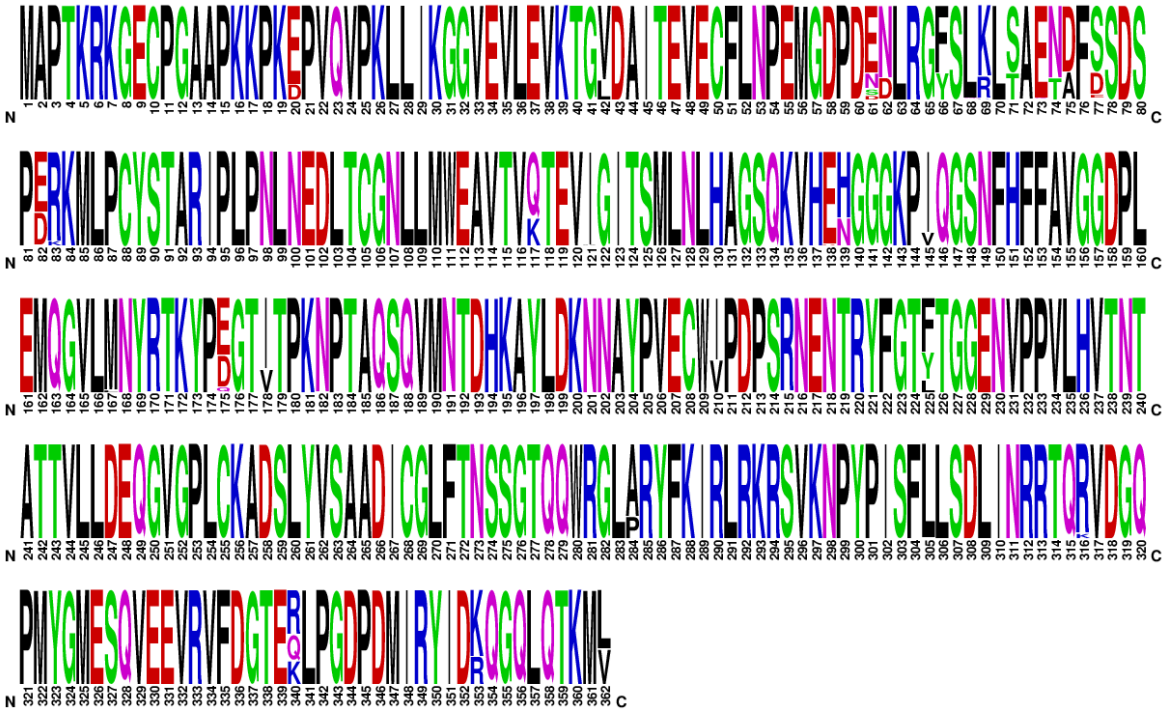

Figure 4.33: Graphical representation of the amino acid alignment of BKPyV VP1 sequences. All downloaded sequences were subjected to analysis using WebLogo, which showed percentage aa distribution (y-axis) at specific positions in 362 aa long BKPyV VP1 protein. Four surface-exposed loops are distributed as follows: BC loop (aa 54 - 90), DE loop (aa 128 - 148), EF loop (aa 157 - 219), and HI loop (aa 269 - 279).

4.3.2 Association between BKPyV genotypes and patient's clinical status

One of our goals was to test the hypothesis that specific BKPyV genotypes are preferably associated with BKPyV pathology. We first needed to assign each nucleotide sequence of BKPyV VP1 to the corresponding genotype. For that purpose, we aligned sequences from all three patient groups and used them to construct a rooted phylogenetic tree (Fig. 4.34). It showed the evolutionary relationships of individual BKPyV VP1 nucleotide sequences and their distribution into four BKPyV genotypes. Further, the assignment of each sequence to

the corresponding genotype was verified using an online tool based on VP1 genotyping - BKTyper tool (Martí-Carreras et al., 2020).

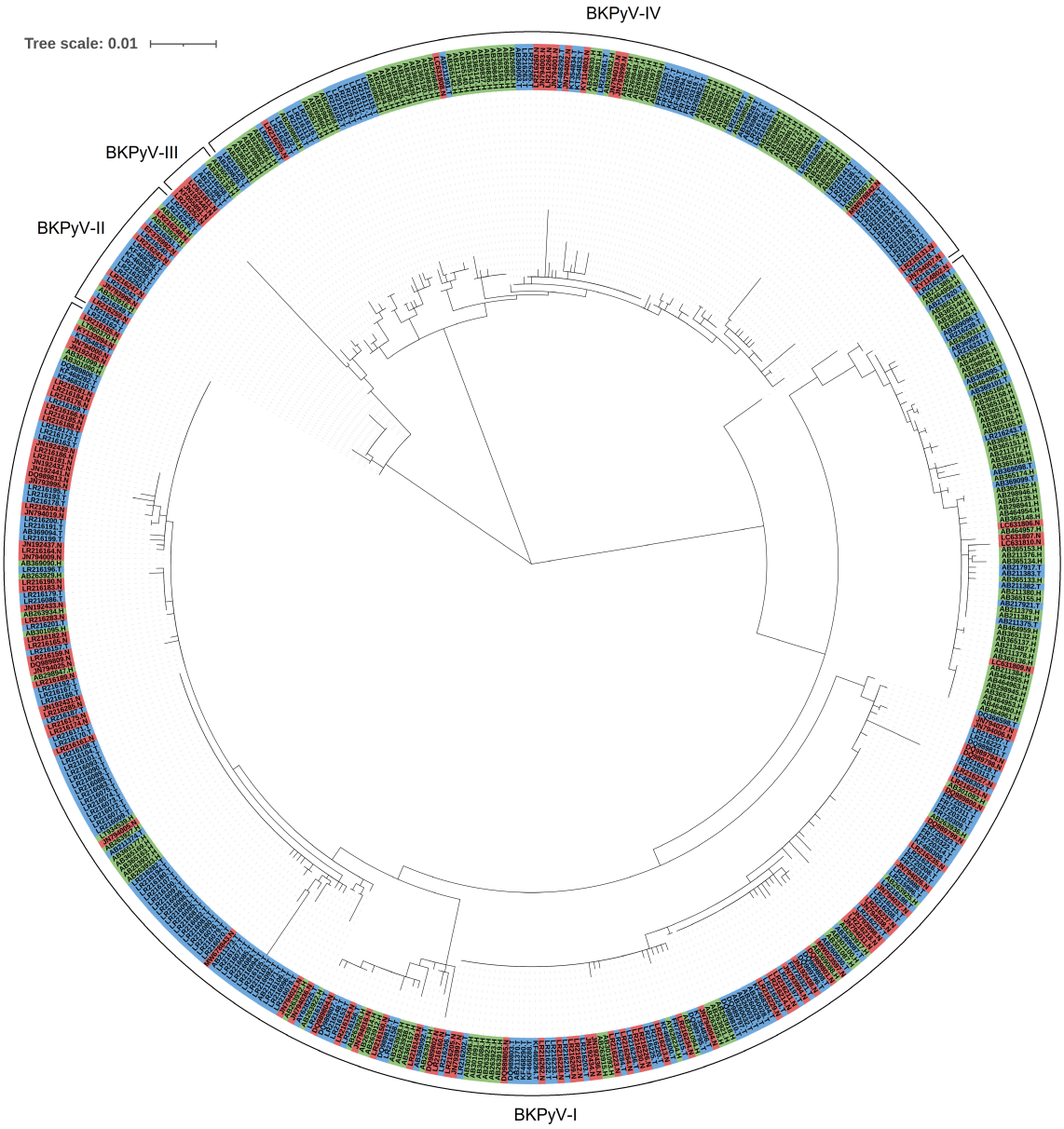

Figure 4.34: The phylogenetic tree of analysed sequences. The tree was visualized using an online tool iTol v6. Sequences are named according to their GenBank accession numbers. Sequences originating from individual groups of patients are distinguished by different colours: green - healthy controls with viruria, blue - immunosuppressed patients with viruria, and red - immunosuppressed patients with viremia/pathology.

The percentage distribution of BKPyV genotypes in patient groups is shown in Figure 4.35, where we can see that the distribution differed. Specifically, we can observe that the BKPyV-IV infected more healthy patients (48%) than BKPyV-I and BKPyV-II/III (28% and 18%), and fewer patients with BKPyV pathology (10%) that the other genotypes (27% and 30%). We also created a contingency table (Table 4.5) showing the numbers of sequences of

different genotypes found in the individual patient groups.

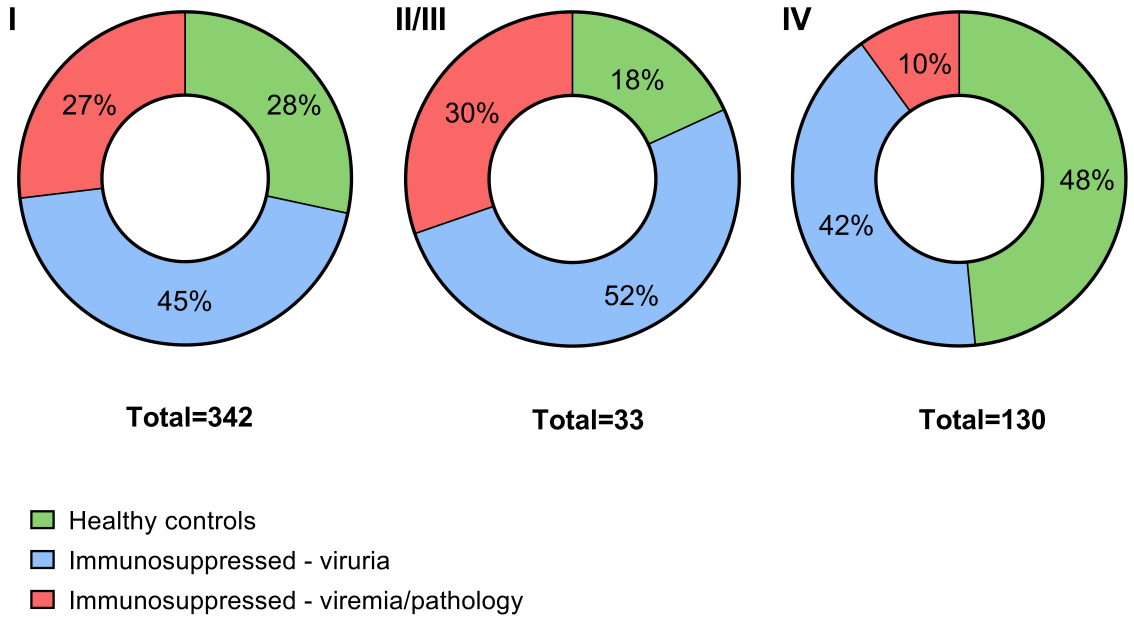

Figure 4.35: Distribution of genotypes (I, II/III, IV) in patient's groups.

Table 4.5: Overview of the distribution of genotypes and patient groups.

	I	**II/III**	**IV**	**In total**
Healthy controls	97	6	63	166
Immunosuppressed - viruria	153	17	54	224
Immunosuppressed - viremia/pathology	92	10	13	115
In total	342	33	130	**505**

A closer look at aligned sequences with determined genotype-specificity enabled us to investigate the amino acid distribution in more detail. We did not find any sequence identical to VP1 of mutant BKPyV-IV-DEmut and BKPyV-IV-EFmut. This means that BKPyV-IV genotype-specific differences in the BC loop were always accompanied by certain amino acids found in DE and EF regions. Furthermore, we found that the BC loop of BKPyV-I appeared in the same sequence together with the composition of DE loop characteristic for BKPyV-IV (139N) only in three cases, whereas the sequence of the EF loop (at positions 175 and 178) showed higher diversity. Specifically, at position 175, we frequently found either D or E. However, 175D was never accompanied by 178V, as typically found in VP1 of BKPyV-IV (data not shown).

4.3.3 Selection analysis of BKPyV VP1 sequences

Further, we were interested in identifying amino acids in the VP1 protein that are affected by positive selection and whether these amino acids preferentially occur in the group c) immunosuppressed patients with viremia/pathology, and so they could potentially contribute

to the pathogenesis caused by BKPyV. We hypothesised that we might be able to detect such amino acids in the surface loops, not only BC but also DE or EF.

We performed selection analysis using the HyPhy tool integrated into the Datamonkey interface (https://www.datamonkey.org/), specifically the FEL (Fixed Effects Likelihood) approach (described in section 3.2.6.3), and we analysed all sequences available (n = 643). The analysis showed that seven amino acids of 362 amino acids long VP1 protein were under positive selection (shown in red in Fig. 4.36). These amino acids were at positions 42, 60, 62, 73, 77, 305 and 362; four of which (at positions 60, 62, 73 and 77) are part of the surface-exposed BC loop and the other two (at positions 305 and 362) are buried inside the protein structure (probably not forming an epitope). However, none of them was part of the DE and EF loop, which are of particular interest in this thesis. We used Fisher's exact test to examine the significance of the association of positively selected amino acids and a specific group of patients. Two-tailed p-value was not smaller than 0.05 in any case, so we did not prove that positively selected mutations are present in any of the patient's groups with higher probability.

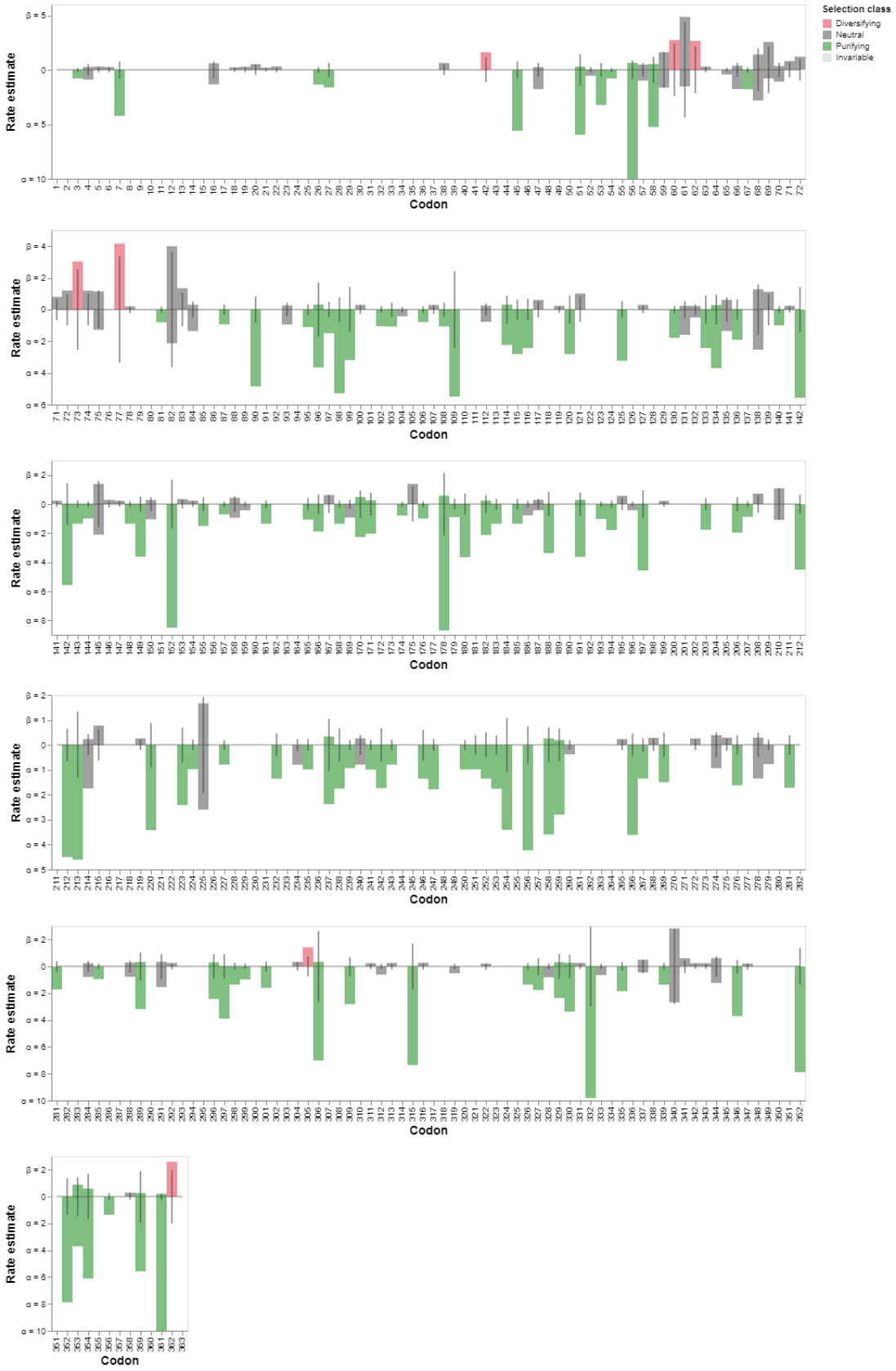

Figure 4.36: Detailed selection analysis of BKPyV VP1. The graph shows the estimate of synonymous (α) and non-synonymous (β) substitution rates, which indicate the rate of selection acting on individual protein residues ($\alpha < \beta$ - positive/diversifying selection, $\alpha > \beta$ - negative/conserving selection, $\alpha \sim \beta$ - neutral evolution) on a total of 362 codons encoding the VP1 protein. Estimates values exceeding 10 are not shown.

5. Discussion

BKPyV is an almost omnipresent pathogen in the human population. After primary infection, BKPyV replication is controlled by the immune system, so this virus persists in the kidneys in a state of clinical latency. However, when the immune surveillance fails, this pathogen can reactivate and cause severe pathology, mainly in KTx and stem cell recipients. In the European population, there are predominantly two subtypes of BK polyomavirus, BKPyV-I and BKPyV-IV. These subtypes behave as different serotypes as they differ in the sequence of the major structural protein VP1. Previously, it was shown that BKPyV serotyping of donors and recipients could identify patients at high risk of developing BKPyV-associated pathology. However, as subtype-specific antibodies cross-react on ELISA, there is so far no easy serological test to distinguish between BKPyV subtypes. Therefore, this work aimed to identify epitopes on VP1, which would bind subtype-specific antibodies. Identification of such epitopes could potentially lead to the improvement of BKPyV subtype-specific diagnostics.

Improvement of BKPyV diagnostics is of long-term focus of our laboratory. Sekavová (2017) attempted to create antigens with the potential to capture solely subtype-specific antibodies. These antigens consisted of VP1 of MPyV, since antibodies against this virus do not occur in the human population, and carried one surface-exposed loop (BC loop) specific for either BKPyV-I or BKPyV-IV as subtype differences cluster within the BC loop. After the isolation, Sekavová (2017) observed mainly disassembled material as the changes in protein structure were probably too extensive. Therefore, Tomanová (2019) later refocused on neighbouring surface-exposed loops of VP1, which contain a lower number of subtype differences, but might be part of the conformational epitope binding subtype-specific antibodies. Tomanová (2019) prepared two antigens. Both antigens consisted of VP1 assembled into PsVs. Specifically, the first antigen, BKPyV-IV-DEmut, was mutated in the DE loop, so the only one amino acid difference between BKPyV-I and IV exposed on the surface (aa 139), was exchanged for the amino acid, which is specific for BKPyV-I subtype. In EF loop region of VP1, there are 5 aa differences between subtypes I and IV. However, two of them (aa 158 and 215) are buried inside the viral capsid, and the other one (aa 171) is exposed on the capsid surface only partly. Therefore, the remaining aa (aa 175 and 178) were exchanged for aa typical for BKPyV-I in the case of the other mutated antigen BKPyV-IV-EFmut. Two mutant PsVs were created to analyse the binding of antibodies on these antigens.

In this thesis, our first aim was to identify the role of DE and EF loop in serological cross-reactivity using mutant antigens previously designed by Tomanová (2019) and control antigens identical to naturally occurring subtypes I and IV. We purified VP1 of all types of antigens (PsVs) together with control VLPs as most of the previous serology testing con-

ducted in our laboratory was performed with VLPs as a coating antigen (Sekavová, 2017; Hejtmánková et al., 2019; Tomanová, 2019). It is important to note that PsVs are viral particles that contain also a reporter gene. However, for the purposes of this thesis, we use the term "PsVs" and "VLPs" for antigens produced using mammalian and insect expression systems, respectively. PsVs were isolated using ultracentrifugation through an Optiprep gradient previously described by Buck et al. (2004), and VLPs were isolated using ultracentrifugation in CsCl gradient as described by Forstová et al. (1993). After purification of both PsVs and VLPs, we analyzed protein fractions in a multi-step procedure, including dot blot analysis, SDS-PAGE, measurement of protein concentration and visualization using electron microscopy. This analysis helped to identify several protein fractions which contained assembled particles and were, therefore, suitable for further serology testing. Then, we compared the reactivity of coated PsVs and VLPs of BKPyV subtype I with 19 human serum samples as it might be influenced by the fact that particles were obtained using different expression systems as some types of N-glycans produced in insect cell lines can be highly immunogenic to humans (reviewed in Betenbaugh et al., 2004). This comparison showed that both PsVs and VLPs react similarly (Fig. 4.15), and their reactivity is, therefore, not influenced by any post-translation modification unique to the mode of expression system used.

Then, we tested the reactivity of rabbit serum samples of known subtype specificity on ELISA with purified PsVs and VLPs. Interestingly, RbαBKPyV-IV cross-reacted with BKPyV-I VLPs substantially more than with BKPyV-I PsVs (Fig. 4.14). We suggested that this discrepancy was caused by the fact that the used fraction of VLPs contained a lot of disassembled material. To further prove that disassembled VP1 caused increased cross-reactivity of rabbit serum, we disassembled a fraction of PsVs, and we again observed higher reactivity of RbαBKPyV-IV with disassembled BKPyV-I antigen (Fig. 4.18). To define the impact of disassembled antigens on the reactivity of human sera, we tested several human serum samples with assembled and disassembled PsVs and observed slightly lower reactivity in the case of disassembled antigens (Fig. 4.18). This result is consistent with published literature showing that capsid disruption leads to a decrease in seroreactivity with human serum samples (Viscidi et al., 2003; Bodaghi et al., 2009) and indicates that antigens used for serology testing should contain compact particles. Data obtained from experiments with rabbit sera suggests that RbαBKPyV-IV originated from immunization by a partly disassembled fraction of VLPs and implies that the quality of antigen should be carefully checked before rabbit immunizations to get an experimental model that accurately resembles BKPyV infection in humans. For example, in the study of Pastrana et al. (2012), they observed a higher level of cross-reactivity after rabbit immunization with BKPyV-I and BKPyV-IV VLPs than observed in this study. However, they do not provide any information about the qual-

ity of the fraction used for either immunization or coating and we can only speculate about the potential role of disassembled antigens in serum cross-reactivity in that case.

In healthy donors, BKPyV remains clinically latent, and the virus replication occurs only occasionally. Most of the time, it is not possible to detect viral DNA from urine or blood. Under these circumstances, serology-based testing is the only option to obtain information about the BKPyV subtype in a given persistently infected individual. Antigen competition assay is one of the approaches used for the determination of BKPyV subtype-specificity; however, it was so far used only in two studies (Hejtmánková et al., 2019; Wunderink et al., 2019). Both of these studies concluded that this approach could be beneficial; however, it still needs further improvements.

For ACA, it is critical to use a sufficient amount of a competing antigen and test the sera in proper dilution. Thus, we first conducted a series of experiments with different concentrations of competing antigen saturating rabbit sera. We showed that the concentration of competing antigen 5 µg/mL was sufficient to eliminate cross-reactivity of highly immunogenic RbαBKPyV-I sera (Fig. 4.19). RbαBKPyV-IV was apparently containing even higher antibody titers. Despite this difference, we used 5 µg/mL as a concentration of competing antigen for further experiments with human sera as they usually have lower antibody titres (in standard dilution 1:200) than experimental rabbit sera (in standard dilution 1:10,000). Later, we showed that one human serum sample with an antibody titer exceeding OD value 2.5 was not saturated with this standard concentration of competing antigen (Fig. 4.24). However, if we first diluted the sample (1:1,000) so that its reactivity reached approximately OD value 2, this serum was then saturated with a standard concentration of competing antigen, and we were able to determine its subtype-specificity (Fig. 4.24). Authors of other studies who also performed competing experiments used different concentrations of competing antigens. For the ELISA setting, concentrations were much lower: 1 µg/mL (Hejtmánková et al., 2019) or 250 ng/mL (Kardas et al., 2015). On the contrary, for Luminex technology, the authors used even 2 mg/mL (Kamminga et al., 2018; Wunderink et al., 2019). Also, serum dilution differs in different studies. Most of the experiments are performed on serially diluted serum samples. However, this approach does not seem practical for routine use in diagnostics. The study of Kardas et al. (2015) tested different sera dilutions for optimized sensitivity and specificity of VLPs-based ELISA assay (testing both BKPyV and JCPyV seropositivity) with the result that sera in dilution 1:200 appeared to be optimal, as used in this study.

Using ACA assay with human serum samples and control PsVs, we determined subtype specificity in 8 of 13 serum samples. The fact that this assay is valuable as a confirmation test only for some of the sera tested was consistent with the data obtained earlier from our laboratory by Hejtmánková et al. (2019), which showed complete elimination of serum reactivity in 2 of 3 sera tested. Also, in the study of Wunderink et al. (2019), they pointed to the limi-

tations of ACA. The authors of this study used Luminex technology and higher diversity of coating and competing antigens (VP1 monomer fused with GST) derived from six BKPyV subtypes (Ib1, Ib2, Ic, II, III and IV). They first tested serum samples with coated antigens and then used ACA as a confirmation test for observed results. They confirmed that antibody response against BKPyV-I and BKPyV-IV was genuine; however, specific BKPyV-I subgroups (Ib1, Ib2 and Ic) were detected only in one of three cases. Additionally, antibody response against BKPyV-II and BKPyV-III was eliminated by saturation with all types of antigen, and therefore, it still remains unclear whether this approach is able to detect these rare BKPyV subtypes II and III. Accumulation of mutation in VP1, which are frequent in KTx (McIlroy et al., 2020), can also reduce the effectiveness of this method, as was also shown in this work. Each mutation can change the conformational epitopes on the capsid surface, which may result in neutralization escape (McIlroy et al., 2020) and probably also in the ineffective binding of laboratory-produced competing antigens. This fact, together with our data, implies that standard antigen competition assay is problematic and that BKPyV serotyping using this method may not be possible.

We performed ACA with human sera and mutant PsVs to determine the role of DE and EF loops in serological cross-reactivity. In some cases, we observed that the competing potential of mutant PsVs was better compared to control BKPyV-IV PsVs. Specifically, when testing BKPyV-I-reactive serum samples, BKPyV-IV-DEmut showed an increased ability to capture serum antibodies compared to BKPyV-IV when tested on coated BKPyV-I. Although this trend was significant only in the case of one sample (S40), it was apparent in the majority of BKPyV-I-reactive serum samples (Fig. 4.21 and 4.22) as well as in Cytotect CP (Fig. 4.24). When tested with coated BKPyV-IV, saturation with competing BKPyV-IV-DEmut was the same or even more efficient than saturation with BKPyV-IV in the case of two sera (S05 and S40, Fig 4.24 and Fig. 4.22, respectively). In the case of S40, we observed a complete elimination of reactivity after saturation with BKPyV-IV-DEmut when tested on BKPyV-IV. This result indicates that the surface-exposed DE loop in the BKPyV-I arrangement was an important part of an epitope targeted by antibodies in this particular serum sample.

The other mutant antigen, BKPyV-IV-EFmut, did not attract antibodies targeted to VP1 of BKPyV-I in contrast to BKPyV-IV-DEmut as was proved on the panel of BKPyV-I-reactive human serum samples (Fig. 4.21 and Fig. 4.22). However, there was one exception - S45 (Fig. 4.22.E,F). We suggest that in this particular case, cross-reactive antibodies may not bind conformational but linear epitopes in EF loop. This suggestion is supported by the study of Randhawa et al. (2009) in which the authors first produced monoclonal antibodies to VLPs of three polyomaviruses (BKPyV, JCPyV and SV40) and then found that most of the antibodies bound conformational antibodies. However, there were a few antibodies which bound linear epitopes buried inside the capsid or exposed on the surface.

When tested with BKPyV-IV-specific sera, saturation with BKPyV-IV-EFmut was more effective than saturation with BKPyV-I as expected (Fig. 4.23). However, BKPyV-IV-EFmut was not better at competing than the original BKPyV-IV in any case. Overall, this antigen (BKPyV-IV-EFmut) showed worse competing abilities than the original BKPyV-IV in the case of both BKPyV-I and BKPyV-IV-reactive serum samples (Fig. 4.21, 4.22 and 4.23) and this trend was also further confirmed with ACA conducted with Cytotect CP (Fig. 4.24). Taken together, the introduction of two point mutations into EF loop resulted in abrupt antibody biding potential in general. This finding corresponds to the results obtained by Lindner et al. (2019), which identified specific aa sites involved in the interaction of polyreactive antibodies neutralizing all BKPyV subtypes (I, II, III and IV). This antibody bound quaternary epitope of two adjacent pentamers, named, for example, A and B. Binding site on pentamer A involved four aa in BC loop and 9 aa in EF loop; and the binding site on pentamer B involved 5 aa in the C-terminus of VP1. Interestingly, the binding site in EF loop also involved one of the targeted mutations of BKPyV-IV-EFmut (at position 175). Despite the fact that the EF loop is located on the pentamer side, it is probably involved in binding not only cross-reactive but also subtype-specific antibodies.

Interestingly, when we compared the outcomes of ACA performed with rabbit and human sera, we observed some consistent results but also some unexpected differences. The consistency was found when we tested BKPyV-I-reactive samples with coated BKPyV-I antigen: the reactivity patterns of human sera after saturation with mutant PsVs was identical to the pattern of rabbit sera (RbαBKPyV-I), which were saturated with the same PsVs (Fig. 4.21. and 4.22 vs Fig. 4.19.A). Namely, that saturation with BKPyV-IV-DEmut caused a slight decline of serum reactivity (however, usually not significant) and saturation with BKPyV-IV-EFmut had no effect. On the other hand, the difference in reactivity patterns was observed in the case of BKPyV-IV-reactive sera when tested on coated BKPyV-IV antigen. Specifically, a saturation of human BKPyV-IV-reactive sera with mutant PsVs caused a drop in serum reactivity (Fig. 4.23), which reached statistical significance in two (S30, S35) out of four cases (Appendix, Table A.1). However, a saturation of RbαBKPyV-IV with mutant PsVs had almost no effect on the reactivity (Fig. 4.19.D). In other words, the introduction of mutations into both DE and EF regions of VP1 protein prevented the binding of antibodies produced after experimental rabbit immunization to a higher extent than it prevented the binding of human antibodies.

We observed the difference in reactivity not only between rabbit and human sera but also between several human sera, which reacted preferentially with the same antigen. Novel virus exposure induces the production of antibodies that bound multiple molecularly distinct epitopes (Guthmiller et al., 2020). Subsequently, the development program of B cells is accompanied by stochastic changes (e.g., recombination of gene segments and somatic

hypermutation), which indicates that antibody repertoire is unique for a given individual. Furthermore, it is generally believed that the affinity of antibodies increases during the B cell maturation as well as the specificity (Wedemayer et al., 1997). Antibody response in rabbit sera was induced upon experimental immunization with VLPs derived from either BKPyV-I or BKPyV-IV. However, during infection in humans, BKPyV evolves rapidly (Domingo-Calap et al., 2018), and mutations in antigenic sites are probably accompanied by the changes of immunodominant epitope as was shown for other viruses (Sato et al., 2004; Greaney et al., 2022). Taken together, this points to the uniqueness of antibody response when comparing rabbit vs human, but also human vs other human sera and further support the previous suggestion that the determination of sera subtype-specificity using ACA may not be possible.

In conclusion, saturation experiments with mutant antigens provided valuable information about subtype-specific and cross-reactive epitopes on the surface of the BKPyV capsid. The first antigen, BKPyV-IV-DEmut bound serum antibodies preferentially targeted to BKPyV-I VLPs as efficiently as BKPyV-I in the case of two human serum samples when tested on coated BKPyV-IV (S05 and S40, Fig 4.24 and Fig. 4.22, respectively). This finding implies that the introduction of a mutation into the DE region (H139N) resulted in increased potential to bind anti-BKPyV-I antibodies. Furthermore, our bioinformatic analysis revealed that subtype-specific sites in BC loop of VP1 are accompanied by the specific amino acid composition in the neighbouring DE loop at position 139 (asparagine for BKPyV-IV and histidine for BKPyV-I). This was confirmed for all sequences of BKPyV-IV VP1 and for all sequences of BKPyV-IV VP1 except for three (out of 342). These results imply that the combination of BC and DE loop is worth further study in order to contribute to the development of an assay with increased subtype-specificity.

Furthermore, we aimed to experimentally analyze the transduction potential of the mutant PsVs (BKPyV-IV-DEmut and BKPyV-IV-EFmut) as well as the potential to escape from neutralization antibodies. However, due to the obstacles in the production of transduction-competent PsVs, we had to change the strategy. Consequently, we investigated the impact of the variation of VP1 by using bioinformatic tools.

A number of studies have postulated the hypothesis that specific BKPyV genotypes might be associated with an increased risk of BKPyV-associated pathology. We, therefore, decided to test this hypothesis using bioinformatic analysis. First, we collected 643 nucleotide sequences of BKPyV VP1 freely accessible in the NCBI database, which were previously obtained by PCR and sequencing from different patient groups. The first group contained healthy controls with BKPyV viruria, the second group involved immunosuppressed patients with viruria, and the third group involved immunosuppressed patients

with viruria and/or pathology (BKPyVAN). Then, we constructed a phylogenetic tree to sort all sequences into four BKPyV subtypes. Subsequently, we found that genotype IV infected a higher percentage of healthy patients and fewer patients with viremia and/or BKPyVAN than the other genotypes (I and II/III; Fig. 4.35). However, it needs to be pointed out that collected BKPyV VP1 sequences were previously obtained by researchers from different geographical areas, and thus the distribution of BKPyV genotypes in this work did not mirror the distribution in the general human population. Furthermore, the occurrence of multiple BKPyV genotypes within one individual seems to be common, as it was detected by Luo et al. (2012) in 12 out of 25 patients. However, for the analysis performed in this thesis, only one sequence from each patient was available, and it remains unclear whether this sequence represents the dominant virus variant in a given individual. Despite these limitations, the suggestion that BKPyV-IV is less likely associated with pathology is consistent with the outcome of a functional study of Nukuzuma et al. (2006), which showed that genotype BKPyV-IV replicates less efficiently than BKPyV-I in the human culture of kidney cells. However, other studies researching the same topic had different outcomes. As Solis et al. (2018) highlighted the importance of high antibody titres against donor's BKPyV strain, Korth et al. (2019) postulated that rare BKPyV genotypes (II and IV) are more likely associated with pathology due to low prevalence and lack of antibody protection against these subtypes in the general human population. The question about the potential association of certain BKPyV subtypes with a higher risk of BKPyVAN would be better answered in a longitudinal study. Careful examination of predominant BKPyV genotypes, as well as disease outcomes, would enable to confirm or exclude the presence of a particular BKPyV genotype as a factor that increases or decreases the likelihood of developing BKPyVAN.

BKPyV has the highest mutation rate amongst other double-stranded DNA viruses, as was shown in the work of Domingo-Calap et al. (2018). Recent studies examined the diversity of BKPyV on the individual level (Luo et al., 2012; Peretti et al., 2018; Wunderink et al., 2019). One of them, the work of Luo et al. (2012), studied BKPyV quasispecies within 25 individuals from different patient groups and showed that the selection pressure acting on VP1 was higher in viremia/nephropathy subjects compared to transplanted-viruria and healthy-viruria groups. Similarly, we aimed to explore the evolution of the BKPyV VP1 region to investigate the impact of VP1 mutations on BKPyVAN, however, at the population level. We performed a selection analysis with previously collected BKPyV VP1 sequences and revealed seven amino acids under positive selection (Fig. 4.36). Four of these amino acids were located in the surface-exposed BC loop, which is responsible for the interaction with the cell receptor. Therefore, the selection pressure in this loop is most likely driven by more efficient virus entry into the cell. The remaining three amino acids experiencing positive selection are not located on the capsid surface. However, also amino acid positions in

VP1 which do not form receptor or antibody binding sites participate in processes essential for the polyomavirus replication cycle, e.g. disulfide and calcium ion binding sites (which influence disassembly and capsid shape; Ishizu et al., 2001), VP1 nuclear localization signal site (Moreland and Garcea, 1991), and epitopes recognized by T-lymphocytes (Krymskaya et al., 2005). After the identification of positively selected mutations, we used statistical analysis and showed that these mutations are equally distributed in all three patient groups and, thus, probably do not increase virus pathological potentials. Therefore, the results of our analysis imply that BKPyV VP1 evolution does not contribute to BKPyVAN at the population level. As some of the collected BKPyV sequences include all genomic data, there is still an open possibility to research variability of the other BKPyV regions, e.g. NCCR, which is in literature often associated with a higher rate of BKPyV replication and thus with a worse course of BKPyV infection.

Conclusion

The primary aim of this project was to identify the role of DE and EF loops of BKPyV VP1 in serological cross-reactivity between BKV subtypes I and IV. We used mammalian and insect expression systems to produce viral particles consisting of VP1 suitable as antigens for serology testing. First, we isolated four types of pseudovirions produced in mammalian cell line 293TT: control PsVs identical to two BKPyV subtypes I and IV (BKPyV-I and BKPyV-IV), and mutant PsVs identical to BKPyV-IV but carrying mutations in the surface-exposed loops of VP1 (DE and EF loop) characteristic for BKPyV-I, named BKPyV-IV-DEmut and BKPyV-IV-EFmut. Second, we isolated virus-like particles (BKPyV-I and BKPyV-IV) produced in insect cell line Sf9, which served (unlike PsVs) as laboratory standards for ELISA testing. We tested the reactivity of PsVs and VLPs with a panel of human sera and provided evidence that their reactivity was comparable. We also investigated the impact of disassembled antigen on the reactivity of both rabbit and human serum with the result that one rabbit serum sample (RbαBKPyV-IV) reacted more with disassembled BKPyV-I PsVs. Human serum samples, on the other hand, reacted with disassembled PsVs slightly less.

Antigen competition assay was performed to study the effect of introduced mutations on antibody binding. We first set up optimal conditions for ACA assay, including the concentration of competing antigens and sera dilution, while testing experimental rabbit sera. Then, we pre-characterized the panel of human serum samples using standard ELISA and showed their preferential reactivity with either BKPyV-I, BKPyV-IV or equal reactivity with both antigens. We confirmed subtype-specific seropositivity of 8 out of 13 serum samples using control PsVs (BKPyV-I and BKPyV-IV) as competing antigens in ACA. Then, we performed ACA with mutant PsVs with the following observation:

- Competing potential of BKPyV-IV-DEmut was the same or even more effective than the original BKPyV-IV in the case of BKPyV-I-reactive serum samples when tested on coated BKPyV-I. Furthermore, BKPyV-IV-DEmut saturated two serum samples which reacted preferentially with coated BKPyV-I as efficiently as the original BKPyV-I. We, therefore, assumed that the DE loop might serve as the target of BKPyV-I-specific antibodies in some serum samples.
- Competing potential of BKPyV-IV-EFmut was generally worse than the competing potentials of all other PsVs. These results indicate that the region of the EF loop is essential for binding cross-reactive and subtype-specific antibodies.

The secondary aim of this project was to characterize the effect of mutations in the DE and EF loop of BKPyV VP1 on the virus biology. However, the initial task to prepare PsVs containing minor proteins VP2 and VP3 and a reporter gene was not completed, as isolated proteins did not assemble into PsVs and were, therefore, unsuitable for further experiments.

The tertiary aim was to identify VP1 mutations as a risk factor for BKPyV-associated pathology. We collected BKPyV VP1 sequences from an online database (NCBI) and connected each sequence with a patient's clinical status: healthy controls with BKPyV viruria, immunosuppressed with viruria and immunosuppressed with viremia or BKPyV-associated pathology. Then, we constructed a phylogenetic tree and assigned to each VP1 sequence its genotype (I, II/III, IV). Data analysis revealed that patients with genotype IV contained a higher percentage of healthy controls and fewer patients with BKPyVAN. The selection analysis identified amino acids under purifying selection; however, they were equally distributed in all three patient groups and, therefore, probably do not participate in BKPyVAN at the population level. In the future, we are planning to extend our database of BKPyV sequences and evaluate the potential impact of NCCR rearrangements on virus pathology.

Bibliography

Abend, J. R., Joseph, A. E., Das, D., Campbell-Cecen, D. B., and Imperiale, M. J. (2009). A truncated T antigen expressed from an alternatively spliced BK virus early mRNA. *The Journal of general virology*, 90(Pt 5):1238.

Andrews, C., Daniel, R., and Shah, K. (1983). Serologic studies of papovavirus infections in pregnant women and renal transplant recipients. *Progress in clinical and biological research*, 105:133–141.

Arthur, R. R., Shah, K. V., Baust, S. J., Santos, G. W., and Saral, R. (1986). Association of BK viruria with hemorrhagic cystitis in recipients of bone marrow transplants. *http://dx.doi.org/10.1056/NEJM198607243150405*, 315:230–234.

Bauer, P. H., Bronson, R. T., Fung, S. C., Freund, R., Stehle, T., Harrison, S. C., and Benjamin, T. L. (1995). Genetic and structural analysis of a virulence determinant in polyomavirus VP1. *Journal of Virology*, 69:7925–7931.

Berger, G., Durand, S., Fargier, G., Nguyen, X.-N., Cordeil, S., Bouaziz, S., Muriaux, D., Darlix, J.-L., and Cimarelli, A. (2011). APOBEC3A is a specific inhibitor of the early phases of HIV-1 infection in myeloid cells. *PLoS pathogens*, 7(9):e1002221.

*Betenbaugh, M. J., Tomiya, N., Narang, S., Hsu, J. T., and Lee, Y. C. (2004). Biosynthesis of human-type N-glycans in heterologous systems. *Current Opinion in Structural Biology*, 14:601–606.

Black, P. H., Rowe, W. P., Turner, H. C., and Huebner, R. J. (1963). A specific complement-fixing antigen present in SV40 tumor and transformed cells. *Proceedings of the National Academy of Sciences of the United States of America*, 50(6):1148.

*Blackard, J. T., Davies, S. M., and Laskin, B. L. (2020). Bk polyomavirus diversity—why viral variation matters. *Reviews in medical virology*, 30(4):e2102.

Bodaghi, S., Comoli, P., Bösch, R., Azzi, A., Gosert, R., Leuenberger, D., Ginevri, F., and Hirsch, H. H. (2009). Antibody responses to recombinant polyomavirus BK large T and VP1 proteins in young kidney transplant patients. *Journal of Clinical Microbiology*, 47:2577–2585.

Boldorini, R., Veggiani, C., Barco, D., and Monga, G. (2005). Kidney and urinary tract polyomavirus infection and distribution: molecular biology investigation of 10 consecutive autopsies. *Archives of pathology & laboratory medicine*, 129:69–73.

Bressollette-Bodin, C., Coste-Burel, M., Hourmant, M., Sebille, V., Andre-Garnier, E., and Imbert-Marcille, B. (2005). A prospective longitudinal study of BK virus infection in 104 renal transplant recipients. *American Journal of Transplantation*, 5(8):1926–1933.

Buck, C. B., Pastrana, D. V., Lowy, D. R., and Schiller, J. T. (2004). Efficient intracellular assembly of papillomaviral vectors. *Journal of Virology*, 78:751–757.

Carter, J. J., Paulson, K. G., Wipf, G. C., Miranda, D., Madeleine, M. M., Johnson, L. G., Lemos, B. D., Lee, S., Warcola, A. H., Iyer, J. G., Nghiem, P., and Galloway, D. A. (2009). Association of Merkel cell polyomavirus-specific antibodies with Merkel cell carcinoma. *Journal of the National Cancer Institute*, 101:1510–1522.

Chesters, P. M., Heritage, J., and McCance, D. J. (1983). Persistence of DNA sequences of BK virus and JC virus in normal human tissues and in diseased tissues. *The Journal of Infectious Diseases*, 147:676–684.

Chong, S., Antoni, M., Macdonald, A., Reeves, M., Harber, M., and Magee, C. N. (2019). BK virus: Current understanding of pathogenicity and clinical disease in transplantation. *Reviews in Medical Virology*, 29:e2044.

Corallini, A., Mazzoni, E., Taronna, A., Manfrini, M., Carandina, G., Guerra, G., Guaschino, R., Vaniglia, F., Magnani, C., Casali, F., Dolcetti, R., Palmonari, C., Rezza, G., Martini, F., Barbanti-Brodano, G., and Tognon, M. G. (2012). Specific antibodies reacting with simian virus 40 capsid protein mimotopes in serum samples from healthy blood donors. *Human Immunology*, 73:502–510.

Crooks, G. E., Hon, G., Chandonia, J.-M., and Brenner, S. E. (2004). WebLogo: a sequence logo generator. *Genome research*, 14(6):1188–1190.

Daniels, R., Rusan, N. M., Wadsworth, P., and Hebert, D. N. (2006a). SV40 VP2 and VP3 insertion into ER membranes is controlled by the capsid protein VP1: implications for DNA translocation out of the ER. *Molecular cell*, 24(6):955–966.

Daniels, R., Rusan, N. M., Wilbuer, A.-K., Norkin, L. C., Wadsworth, P., and Hebert, D. N. (2006b). Simian virus 40 late proteins possess lytic properties that render them capable of permeabilizing cellular membranes. *Journal of virology*, 80(13):6575–6587.

De Gascun, C. F. and Carr, M. J. (2013). Human polyomavirus reactivation: disease pathogenesis and treatment approaches. *Clinical and Developmental Immunology*, 2013.

Doehle, B. P., Schäfer, A., and Cullen, B. R. (2005). Human APOBEC3B is a potent inhibitor of HIV-1 infectivity and is resistant to HIV-1 Vif. *Virology*, 339(2):281–288.

Domingo-Calap, P., Schubert, B., Joly, M., Solis, M., Untrau, M., Carapito, R., Georgel, P., Caillard, S., Fafi-Kremer, S., Paul, N., Kohlbacher, O., González-Candelas, F., and Bahram, S. (2018). An unusually high substitution rate in transplant-associated BK polyomavirus in vivo is further concentrated in HLA-C-bound viral peptides. *PLoS Pathogens*, 14.

Dugan, A. S., Eash, S., and Atwood, W. J. (2005). An N-linked glycoprotein with alfa(2,3)-linked sialic acid is a receptor for BK virus. *Journal of virology*, 79(22):14442–14445.

Egli, A., Infanti, L., Dumoulin, A., Buser, A., Samaridis, J., Stebler, C., Gosert, R., and Hirsch, H. H. (2009). Prevalence of polyomavirus BK and JC infection and replication in 400 healthy blood donors. *The Journal of infectious diseases*, 199(6):837–846.

Erickson, K. D., Bouchet-Marquis, C., Heiser, K., Szomolanyi-Tsuda, E., Mishra, R., Lamothe, B., Hoenger, A., and Garcea, R. L. (2012). Virion assembly factories in the nucleus of polyomavirus-infected cells. *PLoS pathogens*, 8(4):e1002630.

Fareed, G. C. and Davoli, D. (1977). Molecular biology of papovaviruses. *Annual review of biochemistry*, 46(1):471–522.

Forstová, J., Krauzewicz, N., Wallace, S., Street, A., Dilworth, S., Beard, S., and Griffin, B. (1993). Cooperation of structural proteins during late events in the life cycle of polyomavirus. *Journal of virology*, 67(3):1405–1413.

Gardner, S. D., Field, A. M., Coleman, D. V., and Hulme, B. (1971). New human papovavirus (BK) isolated from urine after renal transplantation. *The Lancet*, 297(7712):1253–1257.

Geoghegan, E. M., Pastrana, D. V., Schowalter, R. M., Ray, U., Gao, W., Ho, M., Pauly, G. T., Sigano, D. M., Kaynor, C., Cahir-McFarland, E., Combaluzier, B., Grimm, J., and Buck, C. B. (2017). Infectious entry and neutralization of pathogenic JC polyomaviruses. *Cell reports*, 21:1169.

*Gerits, N. and Moens, U. (2012). Agnoprotein of mammalian polyomaviruses. *Virology*, 432(2):316–326.

Gorelik, L., Reid, C., Testa, M., Brickelmaier, M., Bossolasco, S., Pazzi, A., Bestetti, A., Carmillo, P., Wilson, E., McAuliffe, M., Tonkin, C., Carulli, J. P., Lugovskoy, A., Lazzarin, A., Sunyaev, S., Simon, K., and Cinque, P. (2011). Progressive multifocal leukoencephalopathy (PML) development is associated with mutations in JC virus capsid protein VP1 that change its receptor specificity. *Journal of Infectious Diseases*, 204:103–114.

Gosert, R., Rinaldo, C. H., Funk, G. A., Egli, A., Ramos, E., Drachenberg, C. B., and Hirsch, H. H. (2008). Polyomavirus BK with rearranged noncoding control region emerge in vivo in renal transplant patients and increase viral replication and cytopathology. *Journal of Experimental Medicine*, 205:841–852.

Greaney, A. J., Starr, T. N., Eguia, R. T., Loes, A. N., Khan, K., Karim, F., Cele, S., Bowen, J. E., Logue, J. K., Corti, D., et al. (2022). A SARS-CoV-2 variant elicits an antibody response with a shifted immunodominance hierarchy. *PLoS pathogens*, 18(2):e1010248.

Guthmiller, J. J., Lan, L. Y. L., Fernández-Quintero, M. L., Han, J., Utset, H. A., Bitar, D. J., Hamel, N. J., Stovicek, O., Li, L., Tepora, M., Henry, C., Neu, K. E., Dugan, H. L., Borowska, M. T., Chen, Y. Q., Liu, S. T., Stamper, C. T., Zheng, N. Y., Huang, M., Palm, A. K. E., García-Sastre, A., Nachbagauer, R., Palese, P., Coughlan, L., Krammer, F., Ward, A. B., Liedl, K. R., and Wilson, P. C. (2020). Polyreactive broadly neutralizing B cells are selected to provide defense against pandemic threat influenza viruses. *Immunity*, 53:1230.

Haines, H. L., Laskin, B. L., Goebel, J., Davies, S. M., Yin, H. J., Lawrence, J., Mehta, P. A., Bleesing, J. J., Filipovich, A. H., Marsh, R. A., and Jodele, S. (2011). Blood, and not urine, BK viral load predicts renal outcome in children with hemorrhagic cystitis following hematopoietic stem cell transplantation. *Biology of Blood and Marrow Transplantation*, 17:1512–1519.

*Han, S. B., Cho, B., and Kang, J. H. (2014). BK virus-associated hemorrhagic cystitis after pediatric stem cell transplantation. *Korean Journal of Pediatrics*, 57:514.

Handala, L., Blanchard, E., Raynal, P.-I., Roingeard, P., Morel, V., Descamps, V., Castelain, S., Francois, C., Duverlie, G., Brochot, E., and Helle, F. (2020). BK polyomavirus hijacks extracellular vesicles for en bloc transmission. *Journal of Virology*, 94.

Hejtmánková, A., Roubalová, K., Forejtová, A., Žáčková Suchanová, J., Forstová, J., Viklickỳ, O., and Španielová, H. (2019). Prevalence of antibodies against BKPyV subtype i and iv in kidney transplant recipients and in the general Czech population. *Journal of medical virology*, 91(5):856–864.

Henry, M., Guétard, D., Suspène, R., Rusniok, C., Wain-Hobson, S., and Vartanian, J.-P. (2009). Genetic editing of HBV DNA by monodomain human APOBEC3 cytidine deaminases and the recombinant nature of APOBEC3G. *Plos one*, 4(1):e4277.

*Horníková, Bruštíková, K., Huérfano, S., and Forstová, J. (2022). Nuclear cytoskeleton in virus infection. *International Journal of Molecular Sciences*, 23(1):578.

Huérfano, S., Ryabchenko, B., Španielová, H., and Forstová, J. (2017). Hydrophobic domains of mouse polyomavirus minor capsid proteins promote membrane association and virus exit from the ER. *The FEBS Journal*, 284(6):883–902.

Hurdiss, D. L., Frank, M., Snowden, J. S., Macdonald, A., and Ranson, N. A. (2018). The structure of an infectious human polyomavirus and its interactions with cellular receptors. *Structure*, 26(6):839–847.

Hurdiss, D. L., Morgan, E. L., Thompson, R. F., Prescott, E. L., Panou, M. M., Macdonald, A., and Ranson, N. A. (2016). New structural insights into the genome and minor capsid proteins of BK polyomavirus using cryo-electron microscopy. *Structure*, 24(4):528–536.

Iida, T., Kitamura, T., Guo, J., Taguchi, F., Aso, Y., Nagashima, K., and Yogo, Y. (1993). Origin of JC polyomavirus variants associated with progressive multifocal. *Source: Proceedings of the National Academy of Sciences of the United States of America*, 90:5062–5065.

Ikegaya, H., Saukko, P. J., Tertti, R., Metsärinne, K. P., Carr, M. J., Crowley, B., Sakurada, K., Zheng, H. Y., Kitamura, T., and Yogo, Y. (2006). Identification of a genomic subgroup of BK polyomavirus spread in european populations. *Journal of General Virology*, 87:3201–3208.

Ishizu, K.-I., Watanabe, H., Han, S.-I., Kanesashi, S.-N., Hoque, M., Yajima, H., Kataoka, K., and Handa, H. (2001). Roles of disulfide linkage and calcium ion-mediated interactions in assembly and disassembly of virus-like particles composed of simian virus 40 VP1 capsid protein. *Journal of virology*, 75:61–72.

Jin, L. (1993). Rapid genomic typing of BK virus directly from clinical specimens. *Molecular and Cellular Probes*, 7:331–334.

Kamminga, S., Meijden, E. V. D., Wunderink, H. F., Touzé, A., Zaaijer, H. L., and Feltkamp, M. C. (2018). Development and evaluation of a broad bead-based multiplex immunoassay to measure IgG seroreactivity against human polyomaviruses. *Journal of Clinical Microbiology*, 56.

Kantola, K., Sadeghi, M., Ewald, M. J., Weissbrich, B., Allander, T., Lindau, C., Andreasson, K., Lahtinen, A., Kumar, A., Norja, P., Jartti, T., Lehtinen, P., Auvinen, E., Ruuskanen, O., Söderlund-Venermo, M., and Hedman, K. (2010). Expression and serological characterization of polyomavirus WUPyV and KIPyV structural proteins. *https://home.liebertpub.com/vim*, 23:385–393.

Kapusinszky, B., Chen, S. F., Sahoo, M. K., Lefterova, M. I., Kjelson, L., Grimm, P. C., Kambham, N., Concepcion, W., and Pinsky, B. A. (2013). BK polyomavirus subtype III in a pediatric renal transplant patient with nephropathy. *Journal of Clinical Microbiology*, 51:4255–4258.

Kardas, P., Leboeuf, C., and Hirsch, H. H. (2015). Optimizing JC and BK polyomavirus IgG testing for seroepidemiology and patient counseling. *Journal of Clinical Virology*, 71:28–33.

Kling, C. L., Wright, A. T., Katz, S. E., Mcclure, G. B., Gardner, J. S., Williams, J. T., Meinerz, N. M., Garcea, R. L., and Vanchiere, J. A. (2012). Dynamics of urinary polyomavirus shedding in healthy adult women. *Journal of Medical Virology*, 84:1459–1463.

*Knipe, D. M. and Howley, P., editors (2013). *Fields virology, 6th ed.* Lippincott Williams & Wilkins, Philadelphia.

Knowles, W. A., Gibson, P. E., and Gardner, S. D. (1989). Serological typing scheme for BK-like isolates of human polyomavirus. *Journal of Medical Virology*, 28:118–123.

Kojzarová, M. (2011). Construction of mouse polyomavirus chimeric VLPs bearing melanoma epitopes. Master's thesis, Charles University.

Korth, J., Anastasiou, O. E., Bräsen, J. H., Brinkhoff, A., Lehmann, U., Kribben, A., Dittmer, U., Verheyen, J., Wilde, B., Ciesek, S., Witzke, O., and Widera, M. (2019). The detection of BKPyV genotypes II and IV after renal transplantation as a simple tool for risk assessment for PyVAN and transplant outcome already at early stages of BKPyV reactivation. *Journal of Clinical Virology*, 113:14–19.

Kosakovsky Pond, S. L. and Frost, S. D. (2005). Not so different after all: a comparison of methods for detecting amino acid sites under selection. *Molecular biology and evolution*, 22(5):1208–1222.

Krautkrämer, E., Klein, T. M., Sommerer, C., Schnitzler, P., and Zeier, M. (2009). Mutations in the BC-loop of the BKV VP1 region do not influence viral load in renal transplant patients. *Journal of Medical Virology*, 81:75–81.

Krymskaya, L., Sharma, M. C., Martinez, J., Haq, W., Huang, E. C., Limaye, A. P., Diamond, D. J., and Lacey, S. F. (2005). Cross-reactivity of T lymphocytes recognizing a human cytotoxic T-lymphocyte epitope within BK and JC virus VP1 polypeptides. *Journal of virology*, 79(17):11170–11178.

*Kuypers, D. R. (2012). Management of polyomavirus-associated nephropathy in renal transplant recipients. *Nature Reviews Nephrology*, 8(7):390.

Lagatie, O., Loy, T. V., Tritsmans, L., and Stuyver, L. J. (2014). Antibodies reacting with JCPyV-VP2 167-15mer as a novel serological marker for JC polyomavirus infection. *Virology Journal*, 11:1–10.

Lindner, J. M., Cornacchione, V., Sathe, A., Be, C., Srinivas, H., Riquet, E., Leber, X. C., Hein, A., Wrobel, M. B., Scharenberg, M., Pietzonka, T., Wiesmann, C., Abend, J., and Traggiai, E. (2019). Human memory B cells harbor diverse cross-neutralizing antibodies against BK and JC polyomaviruses. *Immunity*, 50:668–676.e5.

Luo, C., Hirsch, H. H., Kant, J., and Randhawa, P. (2012). VP-1 quasispecies in human infection with polyomavirus BK. *Journal of Medical Virology*, 84:152–161.

Martí-Carreras, J., Mineeva-Sangwo, O., Topalis, D., Snoeck, R., Andrei, G., and Maes, P. (2020). Bktyper: free online tool for polyoma BK virus VP1 and NCCR typing. *Viruses*, 12(8):837.

*Mayberry, C. L. and Maginnis, M. S. (2020). Taking the scenic route: polyomaviruses utilize multiple pathways to reach the same destination. *Viruses*, 12(10):1168.

Mcclure, G. B., Gardner, J. S., Williams, J. T., Copeland, C. M., Sylvester, S. K., Garcea, R. L., Meinerz, N. M., Groome, L. J., and Vanchiere, J. A. (2012). Dynamics of pregnancy-associated polyomavirus urinary excretion: A prospective longitudinal study. *Journal of Medical Virology*, 84:1312–1322.

McIlroy, D., Hönemann, M., Nguyen, N.-K., Barbier, P., Peltier, C., Rodallec, A., Halary, F., Przyrowski, E., Liebert, U., Hourmant, M., et al. (2020). Persistent BK polyomavirus viruria is associated with accumulation of VP1 mutations and neutralization escape. *Viruses*, 12(8):824.

*McIlroy, D., Halary, F., and Bressollette-Bodin, C. (2019). Intra-patient viral evolution in polyomavirus-related diseases. *Philosophical Transactions of the Royal Society B: Biological Sciences*, 374.

Moreland, R. B. and Garcea, R. L. (1991). Characterization of a nuclear localization sequence in the polyomavirus capsid protein VP1. *Virology*, 185(1):513–518.

Morris-Love, J., Gee, G. V., O'Hara, B. A., Assetta, B., Atkinson, A. L., Dugan, A. S., Haley, S. A., and Atwood, W. J. (2019). JC polyomavirus uses extracellular vesicles to infect target cells. *mBio*, 10.

Mrkáček, M. (2018). Major structural protein of polyomaviruses: Interactions with host cell structures. Master's thesis, Charles University.

Murata, H., Teferedegne, B., Sheng, L., Lewis Jr, A. M., and Peden, K. (2008). Identification of a neutralization epitope in the VP1 capsid protein of SV40. *Virology*, 381(1):116–122.

Narvaiza, I., Linfesty, D. C., Greener, B. N., Hakata, Y., Pintel, D. J., Logue, E., Landau, N. R., and Weitzman, M. D. (2009). Deaminase-independent inhibition of parvoviruses by the APOBEC3A cytidine deaminase. *PLoS pathogens*, 5(5):e1000439.

Neu, U., Allen, S.-a. A., Blaum, B. S., Liu, Y., Frank, M., Palma, A. S., Ströh, L. J., Feizi, T., Peters, T., Atwood, W. J., et al. (2013). A structure-guided mutation in the major capsid protein retargets BK polyomavirus. *PLoS pathogens*, 9(10):e1003688.

Neu, U., Wang, J., Macejak, D., Garcea, R. L., and Stehle, T. (2011). Structures of the major capsid proteins of the human Karolinska Institutet and Washington University polyomaviruses. *Journal of Virology*, 85:7384–7392.

*Nickeleit, V., Hirsch, H. H., Zeiler, M., Gudat, F., Prince, O., Thiel, G., and Mihatsch, M. J. (2000). Bk-virus nephropathy in renal transplants—tubular necrosis, MHC-class II expression and rejection in a puzzling game. *Nephrology Dialysis Transplantation*, 15:324–332.

Nishimoto, Y., Zheng, H.-Y., Zhong, S., Ikegaya, H., Chen, Q., Sugimoto, C., Kitamura, T., and Yogo, Y. (2007). An asian origin for subtype IV BK virus based on phylogenetic analysis. *Journal of molecular evolution*, 65(1):103–111.

Nukuzuma, S., Takasaka, T., Zheng, H.-Y., Zhong, S., Chen, Q., Kitamura, T., and Yogo, Y. (2006). Subtype I BK polyomavirus strains grow more efficiently in human renal epithelial cells than subtype IV strains. *Journal of general virology*, 87(7):1893–1901.

Olsen, G. H., Andresen, P. A., Hilmarsen, H. T., Bjørang, O., Scott, H., Midtvedt, K., and Rinaldo, C. H. (2006). Genetic variability in BK virus regulatory regions in urine and kidney biopsies from renal-transplant patients. *Journal of Medical Virology*, 78:384–393.

Olsen, G. H., Hirsch, H. H., and Rinaldo, C. H. (2009). Functional analysis of polyomavirus BK non-coding control region quasispecies from kidney transplant recipients. *Journal of Medical Virology*, 81:1959–1967.

Pallas, D. C., Shahrik, L. K., Martin, B. L., Jaspers, S., Miller, T. B., Brautigan, D. L., and Roberts, T. M. (1990). Polyoma small and middle T antigens and SV40 small t antigen form stable complexes with protein phosphatase 2A. *Cell*, 60(1):167–176.

Pastrana, D. V., Brennan, D. C., Çuburu, N., Storch, G. A., Viscidi, R. P., Randhawa, P. S., and Buck, C. B. (2012). Neutralization serotyping of BK polyomavirus infection in kidney transplant recipients. *PLoS Pathog*, 8(4):e1002650.

Pastrana, D. V., Ray, U., Magaldi, T. G., Schowalter, R. M., Çuburu, N., and Buck, C. B. (2013). BK polyomavirus genotypes represent distinct serotypes with distinct entry tropism. *Journal of virology*, 87(18):10105–10113.

Peretti, A., Geoghegan, E. M., Pastrana, D. V., Smola, S., Feld, P., Sauter, M., Lohse, S., Ramesh, M., Lim, E. S., Wang, D., Borgogna, C., FitzGerald, P. C., Bliskovsky, V., Starrett, G. J., Law, E. K., Harris, R. S., Killian, J. K., Zhu, J., Pineda, M., Meltzer, P. S., Boldorini, R., Gariglio, M., and Buck, C. B. (2018). Characterization of BK polyomaviruses from kidney transplant recipients suggests a role for APOBEC3 in driving in-host virus evolution. *Cell Host and Microbe*, 23:628–635.e7.

Purchio, A. F. and Fareed, G. C. (1979). Transformation of human embryonic kidney cells by human papovarirus BK. *Journal of Virology*, 29:763–769.

Randhawa, P., Pastrana, D. V., Zeng, G., Huang, Y., Shapiro, R., Sood, P., Puttarajappa, C., Berger, M., Hariharan, S., and Buck, C. B. (2015). Commercially available immunoglobulins contain virus neutralizing antibodies against all major genotypes of polyomavirus BK. *American journal of transplantation : official journal of the American Society of Transplantation and the American Society of Transplant Surgeons*, 15:1014.

Randhawa, P., Viscidi, R., Carter, J. J., Galloway, D. A., Culp, T. D., Huang, C., Ramaswami, B., and Christensen, N. D. (2009). Identification of species-specific and cross-reactive epitopes in human polyomavirus capsids using monoclonal antibodies. *The Journal of general virology*, 90(Pt 3):634.

Randhawa, P. S., Finkelstein, S., Scantlebury, V., Shapiro, R., Vivas, C., Jordan, M., Picken, M. M., and Demetris, A. J. (1999). Human polyomavirus-associated interstitial nephritis in the allograft kidney. *Transplantation*, 67(1):103–109.

Randhawa, P. S., Khaleel-Ur-Rehman, K., Swalsky, P. A., Vats, A., Scantlebury, V., Shapiro, R., and Finkelstein, S. (2002). Dna sequencing of viral capsid protein VP-1 region in patients with BK virus interstitial nephritis. *Transplantation*, 73:1090–1094.

Rubinstein, R., Schoonakker, B. C. A., and Harley, E. H. (1991). Recurring theme of changes in the transcriptional control region of BK virus during adaptation to cell culture. *Journal of Virology*, 65:1600.

Salunke, D. M., Caspar, D. L., and Garcea, R. L. (1989). Polymorphism in the assembly of polyomavirus capsid protein VP1. *Biophysical Journal*, 56:887.

Sato, K., Morishita, T., Nobusawa, E., Tonegawa, K., Sakae, K., Nakajima, S., and Nakajima, K. (2004). Amino-acid change on the antigenic region B1 of H3 haemagglutinin may be a trigger for the emergence of drift strain of influenza a virus. *Epidemiology & Infection*, 132(3):399–406.

Sawinski, D., Forde, K. A., Trofe-Clark, J., Patel, P., Olivera, B., Goral, S., and Bloom, R. D. (2015). Persistent BK viremia does not increase intermediate-term graft loss but is associated with de novo donor-specific antibodies. *Journal of the American Society of Nephrology*, 26(4):966–975.

Schaub, S., Hirsch, H., Dickenmann, M., Steiger, J., Mihatsch, M., Hopfer, H., and Mayr, M. (2010). Reducing immunosuppression preserves allograft function in presumptive and definitive polyomavirus-associated nephropathy. *American journal of transplantation*, 10(12):2615–2623.

Schmitt, C., Raggub, L., Linnenweber-Held, S., Adams, O., Schwarz, A., and Heim, A. (2014). Donor origin of BKV replication after kidney transplantation. *Journal of Clinical Virology*, 59:120–125.

Schneider, T. D. and Stephens, R. M. (1990). Sequence logos: a new way to display consensus sequences. *Nucleic Acids Research*, 18:6097–6100.

Seifert, M. E., Gunasekaran, M., Horwedel, T. A., Daloul, R., Storch, G. A., Mohanakumar, T., and Brennan, D. C. (2017). Polyomavirus reactivation and immune responses to kidney-specific self-antigens in transplantation. *Journal of the American Society of Nephrology*, 28(4):1314–1325.

Sekavová, A. (2017). Preparation of polyomaviral nanostructures for diagnostics of BK virus infections. Master's thesis, Charles University.

Shah, K. V. (2000). Human polyomavirus BKV and renal disease. *Nephrology Dialysis Transplantation*, 15(6):754–755.

Soldatova, I., Prilepskaja, T., Abrahamyan, L., Forstová, J., and Huérfano, S. (2018). Interaction of the mouse polyomavirus capsid proteins with importins is required for efficient import of viral DNA into the cell nucleus. *Viruses*, 10(4):165.

Solis, M., Velay, A., Porcher, R., Domingo-Calap, P., Soulier, E., Joly, M., Meddeb, M., Kack-Kack, W., Moulin, B., Bahram, S., et al. (2018). Neutralizing antibody-mediated response and risk of BK virus-associated nephropathy. *Journal of the American Society of Nephrology*, 29(1):326–334.

Šroller, V., Hamšíková, E., Ludvíková, V., Vochozková, P., Kojzarová, M., Fraiberk, M., Saláková, M., Morávková, A., Forstová, J., and Němečková, Š. (2014). Seroprevalence rates of BKV, JCV, and MCPyV polyomaviruses in the general Czech Republic population. *Journal of medical virology*, 86(9):1560–1568.

Stehle, T., Gamblin, S. J., Yan, Y., and Harrison, S. C. (1996). The structure of simian virus 40 refined at 3.1 å resolution. *Structure*, 4(2):165–182.

Stolt, A., Sasnauskas, K., Koskela, P., Lehtinen, M., and Dillner, J. (2003). Seroepidemiology of the human polyomaviruses. *Journal of General Virology*, 84(6):1499–1504.

Stoner, G. L. and Ryschkewitsch, C. F. (1995). Capsid protein VP1 deletions in JC virus from two AIDS patients with progressive multifocal leukoencephalopathy. *Journal of neurovirology*, 1:189–194.

Ströh, L. J., Gee, G. V., Blaum, B. S., Dugan, A. S., Feltkamp, M. C., Atwood, W. J., and Stehle, T. (2015). Trichodysplasia spinulosa-associated polyomavirus uses a displaced binding site on VP1 to engage sialylated glycolipids. *PLoS Pathogens*, 11.

Suspene, R., Aynaud, M.-M., Koch, S., Pasdeloup, D., Labetoulle, M., Gaertner, B., Vartanian, J.-P., Meyerhans, A., and Wain-Hobson, S. (2011). Genetic editing of herpes simplex virus 1 and Epstein-Barr herpesvirus genomes by human APOBEC3 cytidine deaminases in culture and in vivo. *Journal of virology*, 85(15):7594–7602.

Takasaka, T., Goya, N., Tokumoto, T., Tanabe, K., Toma, H., Ogawa, Y., Hokama, S., Momose, A., Funyu, T., Fujioka, T., et al. (2004). Subtypes of BK virus prevalent in japan and variation in their transcriptional control region. *Journal of General Virology*, 85(10):2821–2827.

Tomanová, T. (2019). Analysis of antibody response during BK virus infection. Master's thesis, Charles University.

Tremolada, S., Akan, S., Otte, J., Khalili, K., Ferrante, P., Chaudhury, P. R., Woodle, E. S., Trofe-Clark, J., White, M. K., and Gordon, J. (2010a). Rare subtypes of BK virus are viable and frequently detected in renal transplant recipients with BK virus-associated nephropathy. *Virology*, 404:312–318.

Tremolada, S., Delbue, S., Castagnoli, L., Allegrini, S., Miglio, U., Boldorini, R., Elia, F., Gordon, J., and Ferrante, P. (2010b). Mutations in the external loops of BK virus VP1 and urine viral load in renal transplant recipients. *Journal of Cellular Physiology*, 222:195–199.

Tremolada, S., Delbue, S., Larocca, S., Carloni, C., Elia, F., Khalili, K., Gordon, J., and Ferrante, P. (2010c). Polymorphisms of the BK virus subtypes and their influence on viral in vitro growth efficiency. *Virus Research*, 149:190–196.

Vartanian, J.-P., Guétard, D., Henry, M., and Wain-Hobson, S. (2008). Evidence for editing of human papillomavirus DNA by APOBEC3 in benign and precancerous lesions. *Science*, 320(5873):230–233.

Vinšová, B. (2017). Minor structural proteins of polyomaviruses: attributes and interactions with cellular structures. Master's thesis, Charles University.

Viscidi, R. P. and Clayman, B. (2006). Serological cross-reactivity between polyomavirus capsids. *Polyomaviruses and human diseases*, pages 73–84.

Viscidi, R. P., Rollison, D. E., Viscidi, E., Clayman, B., Rubalcaba, E., Daniel, R., Major, E. O., and Shah, K. V. (2003). Serological cross-reactivities between antibodies to simian virus 40, BK virus, and JC virus assessed by virus-like-particle-based enzyme immunoassays. *Clinical and Diagnostic Laboratory Immunology*, 10:278.

Wedemayer, G. J., Patten, P. A., Wang, L. H., Schultz, P. G., and Stevens, R. C. (1997). Structural insights into the evolution of an antibody combining site. *Science*, 276(5319):1665–1669.

Wunderink, H. F., de Brouwer, C. S., van der Meijden, E., Pastrana, D. V., Kroes, A. C., Buck, C. B., and Feltkamp, M. C. (2019). Development and evaluation of a BK polyomavirus serotyping assay using Luminex technology. *Journal of Clinical Virology*, 110:22–28.

Wunderink, H. F., van der Meijden, E., van der Blij-de Brouwer, C. S., Mallat, M. J., Haasnoot, G. W., van Zwet, E. W., Claas, E. C., de Fijter, J. W., Kroes, A. C., Arnold, F., Touzé, A., Claas, F. H., Rotmans, J. I., and Feltkamp, M. C. (2017). Pretransplantation donor–recipient pair seroreactivity against BK polyomavirus predicts viremia and nephropathy after kidney transplantation. *American Journal of Transplantation*, 17:161–172.

Zheng, H. Y., Ikegaya, H., Takasaka, T., Matsushima-Ohno, T., Sakurai, M., Kanazawa, I., Kishida, S., Nagashima, K., Kitamura, T., and Yogo, Y. (2005a). Characterization of the VP1 loop mutations widespread among JC polyomavirus isolates associated with progressive multifocal leukoencephalopathy. *Biochemical and Biophysical Research Communications*, 333:996–1002.

Zheng, H. Y., Nishimoto, Y., Chen, Q., Hasegawa, M., Zhong, S., Ikegaya, H., Ohno, N., Sugimoto, C., Takasaka, T., Kitamura, T., and Yogo, Y. (2007). Relationships between BK virus lineages and human populations. *Microbes and Infection*, 9:204–213.

Zheng, H.-Y., Takasaka, T., Noda, K., Kanazawa, A., Mori, H., Kabuki, T., Joh, K., Oh-Ishi, T., Ikegaya, H., Nagashima, K., et al. (2005b). New sequence polymorphisms in the outer loops of the JC polyomavirus major capsid protein (VP1) possibly associated with progressive multifocal leukoencephalopathy. *Journal of General Virology*, 86(7):2035–2045.

Zhong, S., Randhawa, P. S., Ikegaya, H., Chen, Q., Zheng, H.-Y., Suzuki, M., Takeuchi, T., Shibuya, A., Kitamura, T., and Yogo, Y. (2009). Distribution patterns of bk polyomavirus (BKV) subtypes and subgroups in american, european and asian populations suggest co-migration of BKV and the human race. *Journal of General Virology*, 90(1):144–152.

Zhong, S., Zheng, H.-Y., Suzuki, M., Chen, Q., Ikegaya, H., Aoki, N., Usuku, S., Kobayashi, N., Nukuzuma, S., Yasuda, Y., et al. (2007). Age-related urinary excretion of BK polyomavirus by nonimmunocompromised individuals. *Journal of clinical microbiology*, 45(1):193–198.

***review**

A. Appendix

Table A.1: Statistical analysis for $OD_{415\ nm}$ measurement after pre-incubation with BKPyV-I, BKPyV-IV, BKPyV-IV-DEmut (DE) or BKPyV-IV-EFmut (EF) antigens tested on BKPyV-I antigen. The one-way ANOVA with Welch and Brown and Forsythe test with Tamhane's T2 multiple comparisons test was performed for samples that passed the normality test by Shapiro-Wilk test (S/W), or Dunn's post hoc test was performed after Kruskal-Wallis (K/W) analysis in other samples. Asterisks indicate statistical significance (*p<0.05; **<0.01; ***<0.001; ****<0.0001) in pairwise comparisons as indicated in the tables heading. Comparisons with p-value > 0.05 are described as non-significant (ns).

Tested on coated BKPyV-I antigen												
Sample	S/W	K/W	No antigen vs.				BKPyV-I vs.			BKPyV-IV vs.		DE vs.
			I	IV	DE	EF	IV	DE	EF	DE	EF	EF
S03	yes	-	**	ns	ns	ns	**	**	**	ns	ns	ns
S05	yes	-	****	ns	ns	ns	****	****	****	ns	ns	ns
S07	no	**	*	ns	ns	ns	ns	ns	*	ns	ns	ns
S17	yes	-	ns	**	ns	ns	***	*	ns	ns	ns	ns
S19	yes	-	ns	***	***	****	ns	ns	ns	*	ns	*
S20	yes	-	****	*	***	*	***	****	****	ns	ns	***
S22	yes	-	***	ns	ns	ns	***	****	****	ns	ns	ns
S30	no	**	**	*	ns	ns	ns	ns	*	ns	ns	ns
S34	yes	-	***	*	*	ns	****	****	****	*	**	****
S35	no	**	**	*	ns	ns	ns	ns	ns	ns	ns	ns
S40	yes	-	***	ns	**	ns	****	****	****	****	**	****
S45	yes	-	***	ns	ns	*	****	****	****	ns	**	**
S46	yes	-	**	***	***	*	****	****	****	***	****	****
S49	yes	-	*	ns	ns	ns	****	***	**	ns	ns	ns
Cytotect	yes	-	****	*	*	ns	****	***	***	ns	ns	*

Tested on coated BKPyV-IV antigen												
Sample	S/W	K/W	No antigen vs.				BKPyV-I vs.			BKPyV-IV vs.		DE vs.
			I	IV	DE	EF	IV	DE	EF	DE	EF	EF
S03	yes	-	***	***	****	ns	ns	ns	**	ns	*	**
S05	no	**	**	ns	*	ns	ns	ns	ns	ns	ns	ns
S07	yes	-	**	***	***	**	ns	ns	ns	ns	ns	*
S17	yes	-	*	ns	*	**	ns	ns	**	*	***	***
S19	no	**	ns	*	ns	ns	**	ns	ns	ns	ns	ns
S20	yes	-	****	****	****	**	ns	ns	***	ns	***	***
S22	yes	-	***	****	****	*	**	ns	**	*	**	***
S30	yes	-	ns	***	****	***	***	**	**	***	***	****
S34	yes	-	***	****	****	**	*	ns	***	ns	****	****
S35	yes	-	***	****	****	****	****	****	***	****	****	****
S40	yes	-	***	**	***	ns	****	****	****	****	****	****
S45	yes	-	****	****	****	****	****	****	**	ns	****	****
S46	no	**	ns	*	ns	ns	**	*	ns	ns	ns	ns
S49	yes	-	****	****	****	***	ns	****	****	****	****	****
Cytotect	no	*	ns	**	*	ns	ns	ns	ns	ns	ns	ns

B. Supplementary Material

Attachment B.1 - Throughout the work on this thesis, we prepared a manuscript which partly corresponds to Aim 1 of this thesis (Hejtmánková et al., 2022). This research paper has already been reviewed and accepted for publication by Virus Research. For the pre-proof version, please see the Supplementary Material attached to this thesis.

Hejtmánková, A., Caisová, H., Tomanová, T., Španielová, H. (2022). The role of the DE and EF loop of BKPyV VP1 in the serological cross-reactivity between subtypes. *Virus Research*. 10.1016/j.virusres.2022.199031.